Characterization of Regulatory Mechanisms in Mucosal Immunity by Systems Immunology

Nuria Tubau Juni

Dissertation submitted to the faculty of the Virginia Polytechnic Institute and State University in partial fulfillment of the requirements for the degree of

Doctor of Philosophy
In
Genetics, Bioinformatics, and Computational Biology

Josep Bassaganya-Riera, Chair
Raquel Hontecillas-Magarzo, Co-Chair
Vida Abedi
David R. Bevan

November 18th, 2019
Blacksburg, VA

Keywords: Immunology, enteric infections, *Helicobacter pylori*, *Clostridium difficile*, immunoregulatory mechanisms

Characterization of Regulatory Mechanisms in Mucosal Immunity by Systems Immunology

Nuria Tubau Juni

ABSTRACT

The mucosal immunity of the gastrointestinal (GI) tract is constituted by a complex, highly specialized and dynamic system of immune components that aim to protect the gut from external threats. The sustained exposure of the mucosal immune system of the GI tract to an enormous number of lumen antigens, requires the constant upkeep of a highly regulated balance between initiation of immune responses against harmful agents and the generation of immune tolerance towards innocuous antigens. Therefore, the regulatory component is key to preserve tissue homeostasis and a normal functioning of the system. Indeed, defective regulatory responses lead to the development of pathological conditions, including unresolved infections, and inflammatory diseases. In this study, we aim to elucidate novel mechanisms involved in host-pathogen interactions during *Helicobacter pylori* and *Clostridium difficile* infections. Indeed, this work integrates preclinical *in vivo* and *in vitro* experimental approaches together with a bioinformatics pipeline to identify and characterize novel regulatory mechanisms and molecular targets of the mucosal immune system during enteric infections. Firstly, we identified a novel regulatory mechanism during *H. pylori* infection mediated by a specific subset of IL10-producing tissue resident macrophages. Secondly, we employed an *ex vivo H. pylori* co-culture with bone marrow derived macrophages, that together with a global transcriptomic analysis and a bioinformatics pipeline, lead to the discovery of promising regulatory genes based on expression kinetics. Lastly, we characterized the innate inflammatory responses induced during the course of *C. difficile* infection and identified IL-1ß, and its subsequent induction of neutrophil recruitment, as a key mediator of *C. difficile*-induced effectors responses. The characterized regulatory mechanisms in this work show promise to lead the generation of new host-centered therapeutics through the modulation of the immune response as promising alternative treatments for infectious diseases.

Characterization of Regulatory Mechanisms in Mucosal Immunity by Systems Immunology

Nuria Tubau Juni

GENERAL AUDIENCE ABSTRACT

The immune system is responsible for protecting the human body from external threats. To achieve this goal, it must differentiate between harmless and harmful agents to only fight the latter. To combat these dangerous agents, the immune system induces highly controlled, inflammatory processes that aim to eliminate the external threat while minimizing the damage of human tissues and organs. The gastrointestinal tract is exposed to an enormous number of molecules, mostly harmless molecules from both the ingested food and the beneficial bacteria inhabiting the gut, but also from harmful bacteria and agents, only separated from the internal body structures by a thin layer called the epithelial barrier of the gut. The immune system responsible for the protection of the gastrointestinal tract includes an important regulatory component critical to maintain a proper gut function. This regulatory component regulates the generation of inflammatory processes to fight the dangerous agents, while blocking the responses against the inoffensive agents and preventing excessive tissue damage to maintain the integrity of the epithelial barrier. Indeed, a failure in the regulatory component results in severe consequences for the body's health, such as the inability to resolve infections. In this study, we aim to investigate the interaction between the human body and the enteric bacteria *Helicobacter pylori* and *Clostridium difficile*, to bring new insights in the regulatory component of the immune system of the gut. Moreover, the new mechanisms discovered in the regulatory system, might allow the development of new treatments for infectious diseases.

Acknowledgements

Neither this dissertation nor the accomplishments achieved to date would have been possible without the contribution and support of many others I am truly grateful to.
First, I would like to express my gratitude and appreciation to the members of my committee. I would like to thank my advisors, Dr. Josep Bassaganya-Riera and Dr. Raquel Hontecillas, for their guidance and support, and also for encouraging me to grow, both professionally and as the person I am today. I thank Josep for giving me the opportunity to start my career at NIMML, to teach me to think bigger and to not give up until you achieve your goals. I thank Raquel for the patience she had with me, for sharing her research knowledge and teaching me countless lab techniques, and always having her door open for me. I thank Dr. Vida Abedi, for always being supportive and positive, and introducing me to the data analytics tools and techniques. I also thank Dr. Bevan, for his input and feedback in my research projects as well as for being a great program director.

I would also like to thank the current and former members of the NIMML team. First, to the NIMML students preceding me. To Cassy and Monica, thank you for your help during my first months in Blacksburg and in the lab, for all the lab trainings and being examples of success. To Andrew, thank you for always being the person there, to help with a lab experiment or mouse project, to find solutions to failed methods or hypothesis, to just have a random conversation or laugh about anything to keep us going, and for listening to my mental breakdowns. To Noah, thanks for always caring about everybody in the lab and for being an example of how a great lab manager should be. To Meghna, thanks for helping with the computational analysis as well as your willingness to learn and help with the experimental projects, and specially with the colony work, always that an extra hand was needed. To my friend Victoria, for being my partner in crime both in and outside the lab during these years. For always being willing to help, no matter how long it would take, for our long nights in the lab and walks early in the morning, and for being a true support in Blacksburg, I thank you. To all current and former undergraduates, thank you for all your contributions in the research projects, keeping the colony tight and helping out with the lab. To all of you, I wish you the best in the next stages of your career.

I also would like to thank the GBCB program, including Dr. Chris Lawrence and Dennie Munson, for their continuous support to the students and willingness to help in any situation or issue. To all BI people that with their daily work facilitate the research of graduate students like me, including, Amy, Barbara, Annette, Shelanna, Ben, Andrew, amongst others, I thank you.

And finally, I would like to thank my family and friends. To my friends in Blacksburg and the US, thanks for keeping me going during these four years, to help me celebrate the successes but also to forget the sorrows. To my friends in Catalunya, thanks for your long-distance support, for the long skype calls, and always willing to adapt your schedules to make sure we see each other every visit home. And lastly to my family. I want to thank my parents for teaching me that the only path to achieve your goals is the hard work, for always being supportive with my decisions and encouraging me to follow

my path. To my dad, for always believing in me, to my mom, for her unconditional support no matter what, to my sister Roser, for making me smile in any situation and make me feel in every visit home that I never left, for all this, moltes gràcies!

Attributions

This work has been possible through the collaborative effort of several team members. This section aims to give credit to all the authors that contributed significantly in each chapter of this dissertation.

Chapter 1

Josep Bassaganya-Riera (Virginia Tech, Nutritional Immunology and Molecular Medicine Laboratory), and Raquel Hontecillas (Virginia Tech, Nutritional Immunology and Molecular Medicine Laboratory) contributed in the design and revision of this chapter.

Chapter 2

Josep Bassaganya-Riera and Raquel Hontecillas contributed to conceiving the design and writing of the manuscript. Andrew Leber (Virginia Tech, Nutritional Immunology and Molecular Medicine Laboratory), Victoria Zoccoli-Rodriguez (Virginia Tech, Nutritional Immunology and Molecular Medicine Laboratory), Monica Viladomiu (Virginia Tech, Nutritional Immunology and Molecular Medicine Laboratory), Barbara Kronsteiner (Virginia Tech, Nutritional Immunology and Molecular Medicine Laboratory) and Casandra W. Philipson (Virginia Tech, Nutritional Immunology and Molecular Medicine Laboratory) contributed in the generation of experimental data.

Chapter 3

Josep Bassaganya-Riera and Raquel Hontecillas contributed to conceiving the design and writing of the manuscript. Andrew Leber contributed in the bioinformatics analysis and the generation of experimental data. Victoria Zoccoli-Rodriguez, Barbara Kronsteiner and Monica Viladomiu contributed in the generation of experimental data. Vida Abedi (Virginia Tech, Nutritional Immunology and Molecular Medicine Laboratory) contributed in the bioinformatics analysis.

Chapter 4

Josep Bassaganya-Riera and Raquel Hontecillas contributed to conceiving the design and writing of the manuscript. Meghna Verma (Virginia Tech, Nutritional Immunology and Molecular Medicine Laboratory) contributed in the literature review and data analysis.

Chapter 5

Josep Bassaganya-Riera and Raquel Hontecillas contributed in the design and revision of this chapter.

Table of Contents

List of figures

List of tables

Chapter 1

Introduction: Mucosal Immunity of the Gastrointestinal Tract and Enteric Infections

Nuria Tubau Juni, Raquel Hontecillas, and Josep Bassaganya-Riera.

1.1 Summary

The mucosal immune system of the gastrointestinal tract is a highly specialized and regulated network of immune components responsible for the immune protection against external threats while maintaining proper gut homeostasis. The regulatory component is a key player of the mucosal immunity. Disruption or failure during the induction of regulatory mechanisms results in severe tissue destruction, leading to important pathological conditions, such us unresolved infections, chronic and autoimmune diseases. Currently, the primary treatment for infectious diseases is antibiotic administration, however, the significant emergence of resistant strains, the collateral disruption of commensal bacteria, as well as the correlation between antibiotic administration and development of specific infections, i.e. *Clostridium difficile*, point out the unmet clinical need of new therapeutics. Development of therapeutic approaches that target the regulatory component of the immune response, is a novel promising path for the treatment of inflammatory and infectious disease. In this study, we aim to deeper characterize host-pathogen interaction to identify novel immunoregulatory mechanisms and markers of the gastrointestinal immunity during *Helicobacter pylori* and *Clostridium difficile* infection that give new insights in the development of new host-centered therapeutics.

1.2 Mucosal immune system of the gastrointestinal tract and enteric pathogens

The mucosal immunity of the gastrointestinal (GI) tract consist of a complex, dynamic, and deeply regulated system constantly maintained in a fine balance between initiation of inflammatory responses and induction of intestinal immune tolerance. The GI mucosa constitutes of an extended surface of approximately 32 to 400 square meters, depending on the counting method, in continuous contact with an enormous number of foreign antigens [1-3]. The main challenge of this highly specialized immune system is the distinction between commensal bacteria and innocuous antigens, versus pathogenic microbes and harmful threats. Indeed, the disruption of this equilibrium, due to initiation or maintenance of uncontrolled inflammatory processes, can result in the development of severe infectious, chronic, and autoimmune diseases, as well as hypersensitive reactions to harmless antigens [2]. Therefore, the presence of a highly regulatory component is critical to maintain gastrointestinal homeostasis and prevent the development of pathogenic conditions.

The first line of defense in the GI tract is the epithelial barrier, a monolayer of epithelial cells that covers the entire GI tract, preventing the translocation of commensal bacteria

and foreign threats. The gastrointestinal epithelium is constituted by a variety of specialized cells. Indeed, the monolayer includes M and goblet cells, that are continuously sampling the lumen and uptaking antigens to dendritic cells and lymphocytes, being a critical component for the generation of intestinal immune tolerance. In addition, there is also the presence of secretory cells, including Paneth cells, that produce antimicrobial peptides (AMP), and mucin-producer cells, such as goblet cells. Together, these secreted molecules constitute the mucus layer, a physical barrier that separates the intestinal bacterial species from the epithelium [4, 5]. In addition to the physical barrier and the lumen sampling functions, the intestinal epithelium is actively involved in the activation of the immune response through production of chemokines and cytokines responsible for the initiation of the immune signaling [5]. The mucosal immune system is mainly located in the gut lamina propria (LP), a layer adjacent to the epithelium, and the organized secondary lymphoid tissues, including the mesenteric or gastric lymph nodes, Peyer patches, etc. Translocation of microbes into lamina propria through disruption of the epithelial barrier, induces activation of macrophages and DCs. Upon recognition of foreign antigens, antigen presenting cells (APC) migrate to the lymph nodes and present the antigens to naïve T cells. Naïve T cells will differentiate into effector cells (Th1, Th17, etc.) and regulatory (Treg) cells, depending on the cytokine context. Activated lymphocytes will then initiate the adaptive immune responses. Upon clearance of the external threat, the resolution of the inflammatory process is initiated through induction of regulatory responses and tissue healing [6]. Failure of the regulatory component leads to uncontrolled inflammation, resulting in extreme damage of the gastrointestinal tissue, disrupting the epithelial barrier and preventing the resolution of the infection.

Infectious diseases are a current major health concern worldwide. According to the Centers for Disease Control and Prevention (CDC), 15.5 million visits to physician office in the US during 2016 concluded with a primary diagnosis of infectious and parasitic diseases. Acute diarrhea illnesses, frequently caused by enteric pathogenic infections, are a main cause of morbidity and mortality worldwide. In 2015, there was an estimate of 1.3 million deaths associated to diarrhea [7, 8]. Historically, treatment with antibiotic regimens to eliminate the pathogen has been the primary therapeutic approach to resolve infections. However, the emergence of hyper-virulent multi-resistant strains together with the increased awareness of commensal bacteria's role in host homeostasis, support the unmet clinical need to develop novel therapeutic approaches as an alternative to antibiotic administration. Modulation of the immune response, through activation of regulatory mechanisms, is a novel promising pathway to develop new therapeutics for infectious diseases. With this novel approach, the collateral tissue damage is reduced without compromising the ability of the immune system to fight other potential external threats.

1.3 *Helicobacter pylori* infection

Helicobacter pylori is a gram-negative, microaerophilic, unipolar, flagellated bacterium identified by Warren and Marshall in 1983 [9-12]. *H. pylori* colonizes the gastric tissue of over half of the population worldwide and has co-evolved with human beings since humans expanded out of Africa more than 50,000 years ago [13]. *H. pylori* constitutes the

predominant member of the gastric microbiome in infected individuals and selectively establishes a chronic, lifelong colonization that courses asymptomatically in the majority of carriers [14]. Several epidemiology studies have reported a beneficial component to *H. pylori* infection, observing negative correlations with several inflammatory and autoimmune conditions, including asthma, type-2 diabetes, and esophageal adenocarcinoma [15-19]. Controversially, *H. pylori* has been classified as a class I carcinogen by the International Agency for Research on Cancer and is considered the leading cause for the development of gastro-duodenal ulcers and gastric cancer [20, 21]. Indeed, in approximately 10% of infected individuals *H. pylori*-associated gastritis will eventually develop into peptic ulcers, and in 1-3% of cases, into gastric cancer [22].

The unique dual role of *H. pylori* as a beneficial bacterium and a pathogenic agent can be attributed to the induction of antagonistic immune responses that encompass both effector and regulatory components. Effector mechanisms are characterized by a dominant Th1 [23, 24], as well as Th17 [25-28] cellular immune responses, the main cause of the *H. pylori*-associated gastritis. In contrast, the regulatory mechanisms induced during the infection suppress the inflammation and prevent bacterial clearance [29]. Particularly, *H. pylori* prevents dendritic cells maturation and promotes the generation of tolerogenic dendritic cells, that together suppress the activation of effector T cells and promote the generation of regulatory T cells [30-32]. The accumulation of regulatory T cells in gastric mucosa will maintain tissue integrity and impede bacterial eradication, leading to a long-term colonization [29, 33, 34]. Recently, regulatory macrophages have also been described as relevant immune cells in *H. pylori*-induced regulatory mechanisms [35]. Despite the established role of certain subsets of immune cells, the extension of the regulatory component present during *H. pylori* colonization still remains unclear.

The current treatment regimen upon detection of *H. pylori* in humans is the eradication through antibiotics administration [36]. However, the chronic, asymptomatic colonization observed in most *H. pylori* carriers, together with the emerging epidemiologic studies that attribute protector roles to this bacterium, and the increased prevalence of bacterial multi-resistant strains, suggest the need to identify novel biomarkers to better stratify *H. pylori* carriers as well as to apply a novel personalized treatment approach. Additionally, the significant impact of the *H. pylori*-induced regulatory mechanisms suppressing inflammation, infers their critical ability to shape the immune response. Thus, it gives new insights to the potential of these novel immunoregulatory mechanisms to advance in the development of new therapeutic strategies, not only for *H. pylori* infection, instead, with the potential to be benefit for a wide spectrum of diseases through modulation of the immune response.

1.4 *Clostridium difficile* infection

Clostridium difficile is an obligate anaerobic, gram-positive, spore-forming bacterium that opportunistically infects the human gastrointestinal tract after gut microbiome disruption, commonly associated to antibiotic treatment [37]. *C. difficile* is the leading cause of nosocomial diarrhea in developed countries [38]. *C. difficile*-associated disease (CDAD) includes a range of conditions from asymptomatic colonization and mild

diarrhea, to pseudomembranous colitis, toxic megacolon, or even death [39]. CDAD severity is dependent on both the pathogen characteristics and the interaction with the host. For instance, infection with non-toxicogenic bacteria or generation of humoral immune responses against *C. difficile* toxins results in asymptomatic colonization. However, infection of toxicogenic strains together with microbiome disruption and lack of anti-toxin antibodies lead to clinical symptomatology [39]. *C. difficile* infection causes an estimate of almost half a million cases, and 29,000 deaths annually only in the United States [40]. The leading risk factor in *C. difficile* infection is antibiotic administration, resulting in a disruption of the normal microbiome that allow endospore proliferation and consequent *C. difficile* infection (CDI) [39]. Indeed, almost two thirds of the new diagnostic cases are associated to healthcare [40].

Over the last years, an alarming increased incidence and severity, including case-fatality, mortality and morbidity rates, of CDAD have been reported [41-43]. These reported CDAD outbreaks seem to be associated to the emergence of new hyper-virulent strains, i.e. BI/NAPI/027, resistant to fluoroquinolone and characterized by higher production of *C. difficile* toxin A (TcdA) and B (TcdB), together with the secretion of a third toxin, the binary toxin [43-45]. In the United states, the annual *C. difficile* infection-associated healthcare cost surpass $1.1 billion [46].

Currently, the standard treatment for *C. difficile* infection (CDI) is further antibiotic administration to eliminate the pathogen [47]. However, the continuous blockage of commensal bacteria regrowth due to the antibiotic regimen, together with the host-secreted antimicrobial peptides, results in infection relapse in 20-25% cases [48, 49]. The relapse episode frequently occurs in multiple occasions, and normally appears in a 3-week period post initial antibiotic administration [50]. Additionally, incidence of CDI recurrence in infected individuals has significantly increased in the last years [51, 52]. Several factors have been associated to increased risk of CDI recurrence, including advanced age, number of previous CDI, long-term hospitalizations, prior colectomy, disruption of gut microbiome, association to antibiotic exposure but also, to the host inflammatory immune response, and the lack of a humoral adaptive response against TcdA and TcdB [50, 52-55].

Fecal microbiota transplantation (FMT) from a healthy donor is an alternative therapeutic strategy currently utilized in CDI relapses that report greater efficacy than the standard treatment [56, 57]. However, the potential introduction of pathogenic microbes, the limited information regarding adverse effects, and the unknown impact in other host systems [58-61] raises concerns regarding the safety of this approach. A safer and promising alternative to FMT for CDI treatment is the development of novel host-targeted strategies to regulate the effector mechanisms through immunomodulatory approaches. Induction of a regulatory shift of the immune response would prevent the disruption of the gut microbiome observed during CDI, as well as the destruction of self-structures, while the immune system's functions would remain intact.

1.5 Conclusions

The characterization and study of the mucosal immune responses against *H. pylori* and *C. difficile* infection will bring new insights regarding the complex network of molecular mechanisms triggered during enteric infections. An in-depth dissection of pathogen-host interactions, will enable the discovery of novel regulatory mechanisms and molecular targets that will not only be beneficial for the investigated pathogen, instead, through their ability to shape the immune response, can contribute to the development of novel host-centered therapeutic approaches for the treatment of a wide-range of infectious and chronic diseases.

Chapter 2

Gastric Mononuclear Phagocytes Cooperate with *Helicobacter pylori* and Induce Regulatory Mechanisms During Colonization

Nuria Tubau Juni, Josep Bassaganya-Riera, Andrew Leber, Victoria Zoccoli-Rodriguez, Monica Viladomiu, Barbara Kronsteiner, Casandra W. Philipson, and Raquel Hontecillas.

Sections of this chapter where originally published in *The Journal of Immunology*. Viladomiu M, Bassaganya-Riera J, Tubau-Juni N, Kronsteiner B, Leber A, Philipson CW, Zoccoli-Rodriguez V, and Hontecillas R. 2017. Cooperation of Gastric Mononuclear Phagocytes with *Helicobacter pylori* during Colonization. *J Immunol*. 198(8):3195-3204. Copyright © 2017 by The American Association of Immunologists, Inc. (https://www.jimmunol.org/content/198/8/3195.long)

2.1 Summary

Helicobacter pylori, the dominant member of the human gastric microbiota, elicits immunoregulatory responses implicated in protective versus pathological outcomes. To evaluate the role of macrophages during infection, we employed a system with a shifted pro-inflammatory macrophage phenotype by deleting PPARγ in myeloid cells and found a 5- to 10-fold decrease in gastric bacterial loads. Higher levels of colonization in wild-type mice were associated with increased presence of mononuclear phagocytes and in particular with the accumulation of $CD11b^{+}F4/80^{hi}CD64^{+}CX_3CR1^{+}$ macrophages in the gastric lamina propria. PPARγ-deficient mice presented decreased IL-10–mediated T cell responses while presenting increased secretion of pro-inflammatory cytokines. IL-10 neutralization during *H. pylori* infection led to increased IL-17-mediated responses and increased neutrophil accumulation at the gastric mucosa. Depletion of phagocytic cells resulted in a reduction of gastric *H. pylori* colonization and increased neutrophil infiltration. Additionally, $CD11b^{+}F4/80^{hi}CD64^{+}CX_3CR1^{+}$ macrophages presented *in situ* proliferative capacity and their accumulation was independent of CCR2 expression. In conclusion, we report the induction of IL-10–driven regulatory responses mediated by $CD11b^{+}F4/80^{hi}CD64^{+}CX_3CR1^{+}$ mononuclear phagocytes that contribute to maintaining high levels of H. pylori loads in the stomach by modulating effector T cell responses at the gastric mucosa.

2.2 Introduction

Helicobacter pylori is a microaerophilic, gram-negative, spiral-shaped bacterium that selectively establishes lifelong colonization of the gastric mucosa in more than 50% of the human population [62, 63]. Approximately 10–15% of *H. pylori*–infected individuals will eventually develop gastroduodenal ulcers, and *H. pylori* carriers have a >2-fold greater risk of developing gastric cancer in the form of B cell lymphoma of MALT lymphoma or adenocarcinoma [64, 65]. Despite the reported links between gut

pathologies and *H. pylori*, its role as a beneficial and dominant member of the human gastric microbiota is emerging through epidemiological, clinical, and experimental data illustrating that it might actually protect from esophageal cancer, asthma, obesity-induced insulin resistance, and inflammatory bowel disease (IBD) [19, 66-70]. This dual role of *H. pylori* as a commensal and pathogenic organism denotes a complex, context dependent interaction with its host and provides a means of tracking the induction of mucosal effector or regulatory responses to a single organism.

H. pylori is mainly found free-floating on the thick mucus layer of the stomach or on the apical side of epithelial cells. However, a small fraction of the *H. pylori* population can invade the lamina propria (LP) following disruption of tight junctions. Although effector immune mechanisms of elimination have not been dissected in depth, the type of immune response elicited may depend on the location and kind of cell that first comes in contact with H. pylori. Colonization of the gastric mucosa by H. pylori induces mixed effector and regulatory immune responses [71]. However, its chronic persistence in the host suggests that the regulatory immune responses might predominate over effector mechanisms [33, 72-79]. Computational modeling of immune responses to *H. pylori* predicted that macrophages are central regulators of the mucosal immune response [28, 80, 81]. Interestingly, in line with our computational prediction, the loss of protein-activated receptor 1, matrix metalloproteinase (MMP)7, or heme oxygenase (HO) results in lower rates of colonization, more severe pathology, and changes in macrophages toward a pro-inflammatory or classically activated state [82-84]. Thus, macrophages could be critical in tipping the balance between pro-inflammatory/effector and regulatory responses and significantly affect the outcome of this bacteria–host interaction. Macrophages and dendritic cells (DCs) belong to the mononuclear phagocytic compartment, which comprises a heterogeneous class of cells that perform functions ranging from tissue development, remodeling and repair, to pathogen recognition and initiation of inflammation and antigen specific immune responses [85, 86]. Functional characterization based on phenotypic traits and the establishment of a clear division of labor among mononuclear phagocytes (MNPs) has been challenging because these cells arise from common progenitors and undergo radical reprogramming in the presence of danger signals [87-89].

Macrophages are highly specialized tissue-resident immune cells with extreme heterogeneous function, morphology and origin. Tissue resident macrophages are long-lived cells originally from the embryogenic yolk sac and fetal liver that are distributed to the tissues. During adulthood, the macrophage pool is supplemented by bone-marrow derived monocytes [90, 91]. In several tissues, including the brain, liver, lungs, spleen and adipocyte tissue, resident macrophages have the ability to proliferate *in situ*, presenting local self-renewal not dependent to bone-marrow monocytes [86, 92-94]. The gastrointestinal tract contains the largest pool of macrophages in the body in steady-state [95, 96]. The current paradigm states that, in contrast to many other tissues, gastrointestinal macrophages require a constant replenishment from $Ly6C^{hi}$ blood monocytes from bone marrow during the adulthood [97]. Moreover, this monocyte recruitment is dependent on CCR2 axis [98]. However, different populations of self-maintained macrophages with unique transcriptomic profile have been identified in the

gut [99, 100]. Thus, this suggests that the pool of tissue resident macrophages in the gastrointestinal tract is constituted by both self-renewal primitive macrophages and blood monocytes-derived macrophages, with heterogeneous functions.

In the present study, we show that during *H. pylori* infection phagocytic cells promote high *H. pylori* loads rather than contributing to bacterial clearance. However, disruption of the phenotype of MNPs through either genetic ablation of PPARγ or phagocytic cell depletion results in more efficient bacterial elimination although not complete clearance. By performing a detailed immunological profiling of MNPs in the stomach of *H. pylori*–infected mice, we have identified and traced a subset of $CD11b^{+}F4/80^{hi}CD64^{+}CX3CR1^{+}$ macrophages that begin to accumulate in the gastric LP between days 21 and 24 post-infection in wild-type (WT) mice but not in mice lacking PPARγ in myeloid cells. These cells produce IL-10 and thus could be responsible for establishing a microenvironment that facilitates *H. pylori* colonization of the stomach. We also show that IL-10 deficiency leads to low colonization and significant infiltration by neutrophils. Additionally, $CD11b^{+}F4/80^{hi}CD64^{+}CX3CR1^{+}$ macrophage accumulation in gastric tissue is independent of CCR2 expression and this population of macrophages is able to proliferate *in situ*. Our studies demonstrate the presence of a very complex system of MNPs associated with the gastric mucosa that is predominantly regulatory and highly susceptible to modulation by environmental changes. Furthermore, the state of the gastric MNP system can also impact the microbial composition by facilitating colonization by certain bacterial species, such as *H. pylori*. Moreover, we have identified a novel MNP subset that could provide new insights into the mechanisms of mucosal immunoregulation underlying the protective versus pathogenic behavior of gastrointestinal bacteria.

2.3 The complex system of myeloid cells identified in gastric tissue is significantly subjected to the loss of PPARγ and these alterations are associated to a decrease of bacterial colonization.

To determine the impact of macrophages and mononuclear phagocytes during *H. pylori* infection. The NIMML team previously performed a 6-month *H. pylori* infection *in vivo* employing wild-Type (WT), PPARγ fl/fl;$LysCre^{+}$ (LysMCre, cell-specific PPARγ deficiency in myeloid cells), and PPARγ fl/fl;$CD4Cre^{+}$ (CD4Cre, cell specific PPARγ deficiency in $CD4^{+}$ T cells) mice. Loss of PPARγ in myeloid cells induces upregulation of pro-inflammatory cytokine expression [101-103], inducing a phenotyping switch towards a pro-inflammatory state. LysMCre mice were chosen in this study for the stated phenotypic switch in myeloid cells associated to the loss of PPARγ, and not to investigate the PPARγ role in *H. pylori* infection. The performed 6-month infection reported a significant drop in bacterial burden between 2 and 3 weeks post-infection in LysMCre mice not observed in the WT and the CD4Cre groups (Figure 2.1A). Interestingly, this decrease in colonization levels in LysMCre mice was maintained throughout the entire infection.

The reported differences in LysMCre mice not observed in CD4Cre, lead to an in-depth analysis of the myeloid compartment in gastric tissue using a wide-range of MNPs

markers, including CD11b, CD11c, MHC-II, CX_3CR1, F4/80, CD103, CD64 and Gr1, which revealed substantial alterations in the myeloid compartment due to the loss of PPARγ. The stomach mucosa of WT mice was enriched in a population of $F4/80^+CD11b^+$ cells, as opposed to LysMCre mice (Figure 2.1C). Within these $F4/80^+CD11b^+$ cells, we characterized two gastric mucosal subsets based on the level of expression of F4/80: an F4/80hi subset corresponding to macrophages based on the expression of CD64, and an F4/80lo subset. The percentage of $F4/80^{hi}$, corresponding to macrophages, was suppressed in mice lacking PPARγ in myeloid cells (Figure 2.1B). Additionally, within the $CD64^-MHC\text{-}II^+$ fraction, we characterize two major DC subsets based on CD11c and CD103 expression: $CD11c^+CD103^+$, and $CD11c^+CD103^-$, the latter of which constituted most DC. Of note, whereas the $CD11c^+CD103^+$ cells were negative in CD11b and F4/80, the $CD11c^+CD103^-$ cells had heterogeneous expression of F4/80 and CD11b, although F4/80 was always expressed in low levels (Figure 2.2), in contrast to the CD64+ macrophages, which expressed high levels of F4/80. Alternatively, neutrophils could be easily identified as $CD11b^{hi}$ cells that expressed also high levels of GR1. This phenotypic analysis showed significant differences between WT and LysMCre mice with regard to the percentage of $F4/80^+CD11b^+$ cells, which were significantly higher in WT mice. In particular, PPARγ deletion affected the proportion of macrophages in the gastric mucosa (Figure 2.1B). We further characterized the myeloid compartment in the stomach mucosa of naïve mice using $CX_3CR1\text{-}GFP^{+/+}$ reporter mice (Figure 2.1D). We show that the $F4/80^{hi}CD11b^+CD64^+$ cells were all in the CX_3CR1^+ fraction, whereas the $CD11b^+F4/80l^o$ cells, including $CD11c^+MHC\text{-}II^+CD64^-$ DC could be either CX_3CR1^+ or CX_3CR1^-. These analyses demonstrate the presence of a complex system of myeloid cells in the stomach mucosa that has not been previously described, and its composition is significantly altered due to the loss of PPARγ in LysMcre mice.

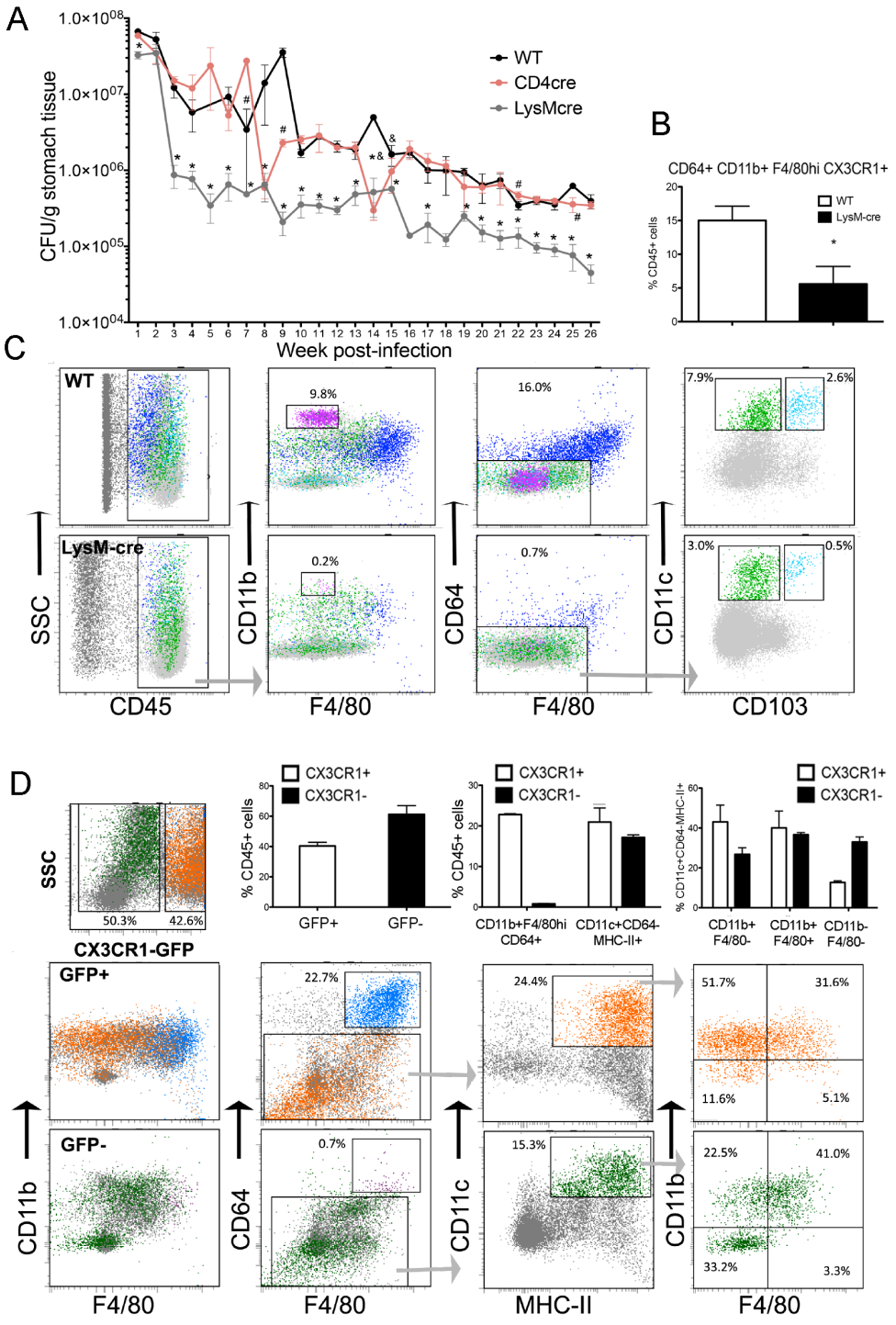

Figure 2.1. Loss of PPARγ in myeloid cells results in lower colonization with *Helicobacter pylori* and altered myeloid compartment. (A) WT, PPARγ myeloid cell-deficient (LysMcre) or PPARγ T cell-deficient (CD4cre) mice were infected with *H. pylori* SS1. Bacterial burden measured weekly up to 6 mo postinfection show a significant reduction in colonization due to the loss of PPARγ in myeloid cells. Data

represents mean ± SEM (n=10). (B) Loss of PPARγ in myeloid cells results in significantly lower percentage of $CD64^{+}CD11b^{+}F4/80^{hi}CX3CR1^{+}$ macrophages. Data represent means ± SEM (n = 5). (C) Phenotypic analysis of gastric myeloid cells in WT and LysMcre mice show a significant depletion in myeloid cells in LysMcre mice including $CD11b^{+}F4/80^{hi}CD64^{+}$, neutrophils ($CD11b^{hi}$) and DCs. (D) Phenotypic analysis of myeloid cells in naïve $CX_3CR1\text{-}GFP^{+/+}$ reporter mice. Macrophages, defined by CD64 expression, were found to be $CX_3CR1\text{-}GFP^{+}$and DCs were analyzed in the $CD64^{-}$ fraction, after negative gating of CD3 and CD19 expression, and defined based on MHC-II, CD11c, and CD103 expression. Top panel represents CX_3CR1^{+} cells, and bottom panel represents CX_3CR1^{-} cells. Results from (B)-(D) are representative of three independent replicate experiments with the same results. *$p < 0.05$ when compared with the control (WT) group.

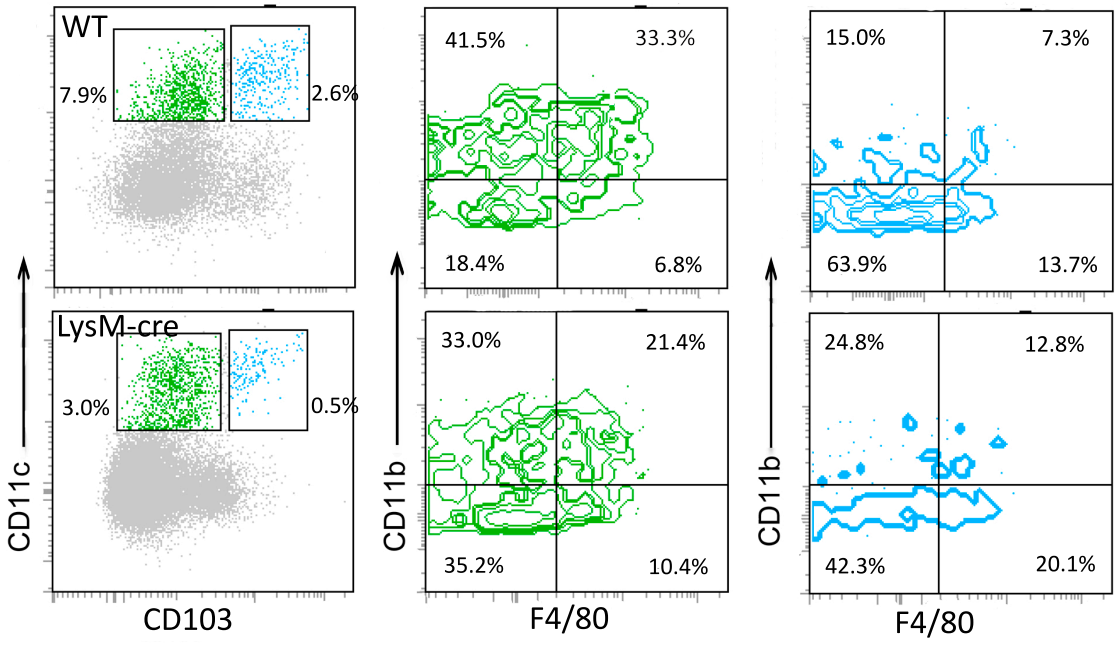

Figure 2.2. F4/80 and CD11b expression by gastric DC. We identified two main subsets of DC present in the stomach of both WT and LysMCre as $CD64^{-}MHC\text{-}II^{+}CD11c^{+}$ which were either $CD103^{-}$ (green) or $CD103^{+}$ (blue). The $CD103^{-}$ subset has heterogeneous expression of CD11b and F4/80, whereas the $CD103^{-}$ were mostly $CD11b^{-}$ and $F4/80^{-}$.

2.4 Macrophages accumulate in the gastric mucosa of *H. pylori*-infected mice

We performed a time-course study spanning the first 7 wk post-infection because the drop in *H. pylori* loads in LysMcre mice consistently occurs between weeks 2 and 3 post-infection. The results show a significant increase in numbers of $F4/80^{hi}CD11b^{+}CD64^{+}CX_3CR1^{+}$ cells in WT mice in comparison with LysMcre mice (Figure 2.3A, E). These cells accumulated in the stomach mucosa starting on day 14 post-infection in the WT but not in the LysMcre mice. We also found increased

percentages of neutrophils on days 14 and 28 and total numbers on day 28 post-infection in WT mice (Figure 2.3B, F), as well as in the percentages of $CD11c^{+}CD103^{+}$ and $CD11c^{+}CD103^{-}$ DCs (gated within $CD64^{-}MHC\text{-}II^{+}$), which were increased in WT mice when compared with LysMcre mice (Figure 2.3C, D, G, H), although no differences were found in absolute numbers. Overall, our data indicate that the major sustained difference between strains was in the accumulation of $F4/80^{hi}CD11b^{+}CD64^{+}CX_3CR1^{+}$ in the stomach of WT mice following infection. We then determined whether macrophages proliferate *in situ* in the gastric mucosa via Bromodeoxyuridine (BrdU) staining. WT and LysMcre mice infected with *H. pylori* SS1 received 1mg of BrdU i. p. followed by 0.8mg/mL in drinking water for 3 d. BrdU was withdrawn and incorporation was measured the same day, corresponding to day 15 post-infection, and on days 18 and 21 in cells isolated from the stomach. The results show that $F4/80^{hi}CD64^{+}$ cells, which correspond to $F4/80^{hi}CD11b^{+}CD64^{+}CX_3CR1^{+}$, incorporated BrdU with a slightly higher increase in WT compared with LysMcre mice on day 18 (Figure 2.3I). We also detected positive BrdU staining in $F4/80^{lo}$ $CD64^{-}$ cells, although only an average of 15% were positive by day 21 (Figure 2.3J**),** whereas the percentages of $F4/80^{hi}CD64^{+}$ stained with BrdU remained higher in both WT and LysMcre mice. These results indicate that $F4/80^{hi}CD11b^{+}CD64^{+}CX_3CR1^{+}$ cells can proliferate *in situ* in the gastric mucosa during *H. pylori* infection.

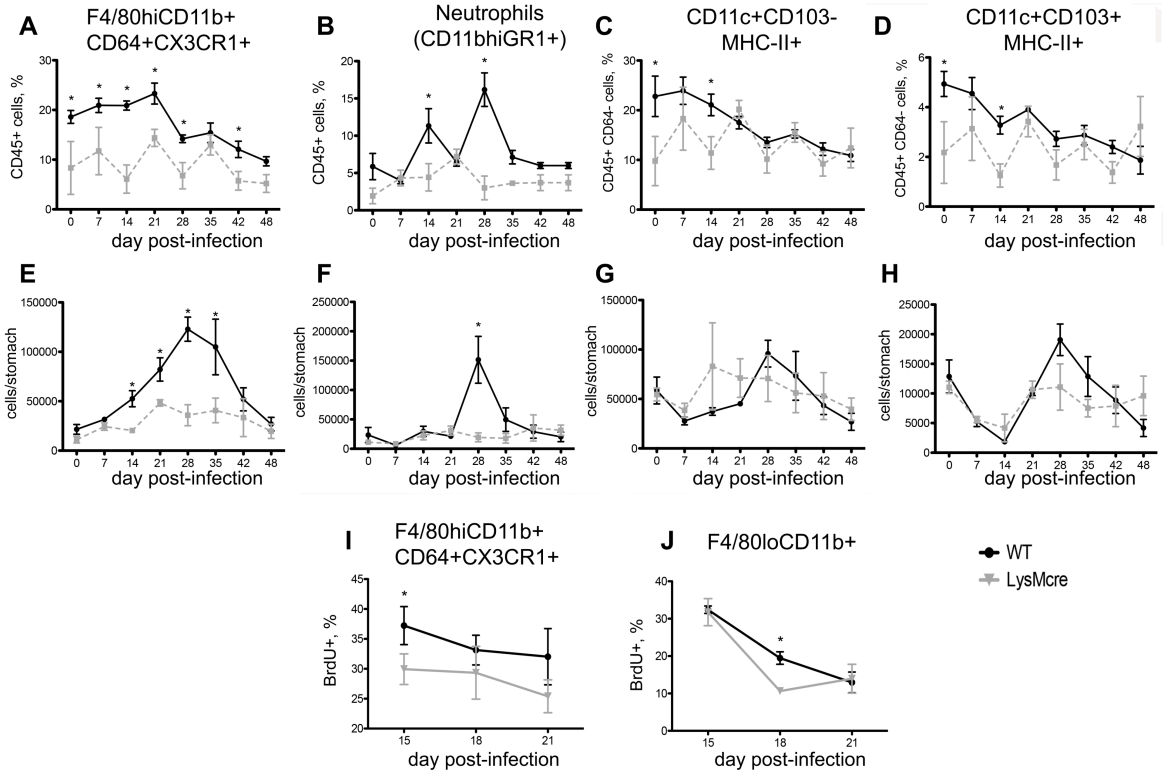

Figure 2.3. *H. pylori* infection causes accumulation of $CD11b^{+}F4/80^{hi}CD64^{+}CX3CR1^{+}$ macrophages in gastric mucosa. Time-course FACS analysis of gastric myeloid cells after *H. pylori* infection of WT and LysMcre mice is

shown. The analysis was performed at the indicated times in cells isolates from mouse stomachs. Plots represent percentages (top row) and absolute number (middle row) of $CD11b^{+}F4/80^{hi}CD64^{+}CX_3CR1^{+}$ macrophages (A and E), neutrophils (B and F), and $CD11c^{+}CD103^{-}$ (C and G) and $CD11c^{+}CD103^{+}$ DC (D and H) subsets. DC gating was done on $MHC\text{-}II^{+}CD64^{-}$ cells. Results are averages of five mice per time point and are presented as means ± SEM (n = 5 per time point). (I and J) BrdU incorporation was measured by flow cytometry in $CD11b^{+}F4/80^{+}CX_3CR1^{+}$ and $F4/80^{lo}CD11b^{+}$ cells isolated from the stomach of *H. pylori*-infected mice on days 15, 18 and 21 post-infection. Results are representative of five independent replicate experiments with the same results. *$p<0.05$ when compared with the control (WT) group.

We also analyzed changes in the lymphocyte compartment due to infection in both WT and LysMcre genotypes. The results show higher percentages and numbers of $CD4^{+}$ T cells (Figure 2.4A, B), $CD8^{+}$ T cells (Figure 2.4C, D) and B cells in PPARγ mice (Figure 2.4E, F), suggesting that defects derived from the loss of PPARγ in myeloid cells of the stomach lead to suppressed numbers of $F4/80^{hi}CD11b^{+}CD64^{+}CX_3CR1^{+}$ and secondary increase of lymphocytes in the gastric mucosa. Interestingly, the elevated numbers of $F4/80^{hi}CD11b^{+}CD64^{+}CX_3CR1^{+}$ detected in WT mice was specific to the stomach, at least in naïve mice, since WT and LysMcre naïve mice had similar percentages of $F4/80^{hi}CD11b^{+}CD64^{+}CX_3CR1^{+}$ in the duodenal and colonic mucosa (Figure 2.5).

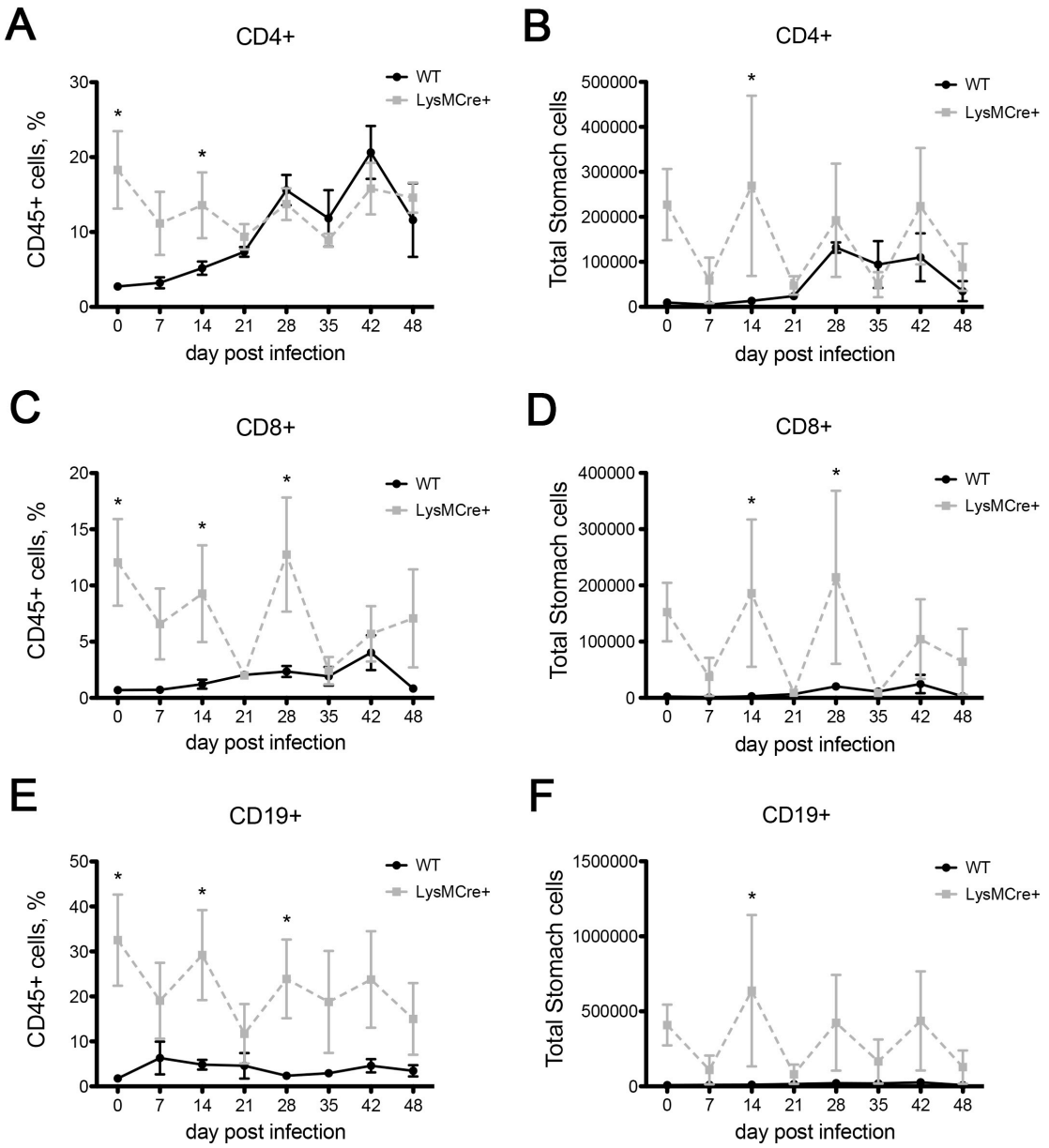

Figure 2.4. PPARγ deficiency in myeloid cells leads to increased numbers of lymphocytes in the gastric mucosa. Time-course FACS analysis of gastric lymphocytes after *H. pylori* infection of WT and LysMcre mice with strain SS1. Mice were infected during indicated times and analysis was performed on cells isolated from whole stomach. Percentages and absolute numbers of $CD4^+$ T cells, $CD8^+$ T cells and $CD19^+$ B cells were increased in LysMcre mice at the time points indicated with asterisks. $CD4^+$ T cells of WT mice increased with respect to day 0 of experiment between days 21 and 28, suggesting the initiation of T cell responses to the infection. Data represents mean ± SEM of 4-5 mice per group. Points with different superscripts are significantly different when compared to the control group ($P<0.05$).

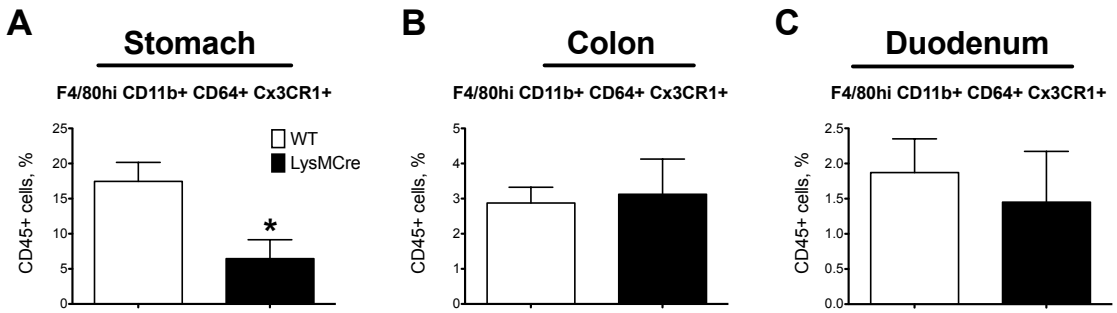

Figure 2.5. The reduced percentage of $CD64^{+}CD11b^{+}F4/80^{hi}CX_3CR1^{+}$ macrophages in gastric tissue of LysMCre mice is not reported in colonic tissue and duodenum. FACS analysis of $CD64^{+}CD11b^{+}F4/80^{hi}CX3CR1^{+}$ macrophages in stomach (A), Colon (B) and Duodenum (C) of WT and LysMCre non-infected mice. Data represent means ± SEM of 4-6 mice per group. *$p<0.05$ when compared with the control (WT) group.

2.5 Loss of Pparγ in myeloid cells alters *H. pylori*-antigen specific immune response in gastric lymph nodes

While gastric $CD64^{+}CD11b^{+}F4/80^{hi}CX_3CR1^{+}$ macrophages constitutively express IL-10, *H. pylori* infection induces CD4+ T and B cell production of IL-10 in WT mice. Moreover, Pparγ deficiency in myeloid cells suppresses both macrophage constitute IL-10 expression as well as the *H. pylori*-associated IL-10 upregulation from the gastric lymphocytic compartment, suggesting that the accumulation of gastric macrophages upon infection facilitates the generation of a regulatory environment in lymphocytes [104].

In order to further dissect the impact of IL-10 producing gastric $CD64^{+}CD11b^{+}F4/80^{hi}CX_3CR1^{+}$macrophage accumulation into downstream immune responses against *H. pylori,* WT and LysMcre mice were infected with *H. pylori* SS1 and euthanized at day post-infection 24. Cells from gastric lymph nodes (GLN) were isolated and cultured for 72h with formalin-inactivated *H. pylori* SS1 antigen. Cytokine profile was assessed through cytokine quantification of the collected supernatants with the cytometric bead array. *H. pylori* challenge induces a significant upregulation of IL-10 secretion in WT GLN-isolated cells that is prevented in the LysMcre group (Figure 2.6A). Additionally, upon *H. pylori* recognition, LysMcre cells report an increased production of pro-inflammatory cytokines, including IL-17 (Figure 2.6B), IFNγ (Figure 2.6C) and TNFα (figure 2.6D) not observed or very limited in the WT group. Therefore, these results support that accumulation of $CD64^{+}CD11b^{+}F4/80^{hi}$CX3CR1+ upon *H. pylori* infection favors the generation of an IL-10-driven regulatory environment in both gastric mucosa and gastric lymph nodes potentially associated to increased bacterial colonization in WT mice.

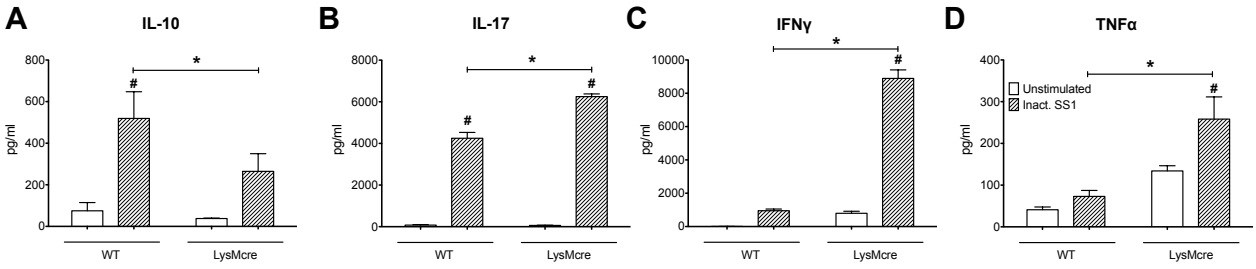

Figure 2.6. Loss of PPARγ in myeloid cells alters subsequent effector responses in gastric lymph nodes. Isolated cells from gastric lymph nodes of WT and LysMcre mice were cultured *ex vivo* and stimulated with 5 µg/ml formalin-inactivate *H. pylori* SS1. Cytokine profile was measured 72-h post incubation in cell culture supernatant using a cytometric bead array. Production of (A) IL-10, (B) IL-17, (C) IFNγ, and (D) TNFα was assessed. Data represent mean ± SEM of three to five samples of pooled cells from mice of same sex and genotype. * $P < 0.05$ when compared with the WT group. # $P < 0.05$ when compared with the unstimulated group.

2.6 IL-10 is required for high levels of *H. pylori* colonization

To further evaluate the role of IL-10 during the initial phases of colonization, we performed IL-10 neutralization studies in mice infected with *H. pylori* and compared their response to control mice that received an isotype Ab. Mice received three doses of either control or neutralizing Ab (100 µg per mouse) on days 17, 19 and 21. Measurement of bacterial loads on day 22 post-infection showed that indeed IL-10 is required for optimal gastric colonization, because gastric *H. pylori* burden was significantly lower in the group of mice in which IL-10 was neutralized (Figure 2.7A). IL-10 blockade also significantly increased neutrophils (Figure 2.7C) in the gastric mucosa but did not affect the levels of F4/80hiCD11b+CD64+CX_3CR1+ macrophages (Figure 2.7B), which indicates that IL-10 is dispensable for the accumulation of these cell type in the stomach. In contrast, MHC-II+CD11c+CD64- DCs were slightly but significantly suppressed by IL-10 depletion (Figure 2.7D). In addition to IL-10 neutralization, we infected IL-$10^{-/-}$ mice and obtained the same results, that is, *H. pylori* loads were suppressed and neutrophil influx increased (Figure 2.8).

IL-10-producing MNP accumulate in the stomach of *H. pylori*-infected mice, and this initial response influences CD4+ T cell and B cell compartments. To assess how the absence of IL-10 could affect downstream effector responses, we cultured cells obtained from gastric lymph nodes of *H. pylori*-infected mice that were either treated with IL-10 neutralizing or control Abs, and stimulated them *ex vivo* with inactivated whole *H. pylori* SS1. Supernatants were collected 72 h after stimulation and cytokine levels measured using a cytometric bead array. As observed in the study above, the results (Figure 2.7 E-H) show that *ex vivo* stimulation with inactivated *H. pylori* induces significant production of IFNγ, IL-10 and IL-17 as well as IL-6 in gastric lymph nodes from infected mice. However, IL-10 neutralization was associated with a suppression of IFNγ and IL-10 (Figure 2.7E, F) and increased production of IL-17 (Figure 2.7G).

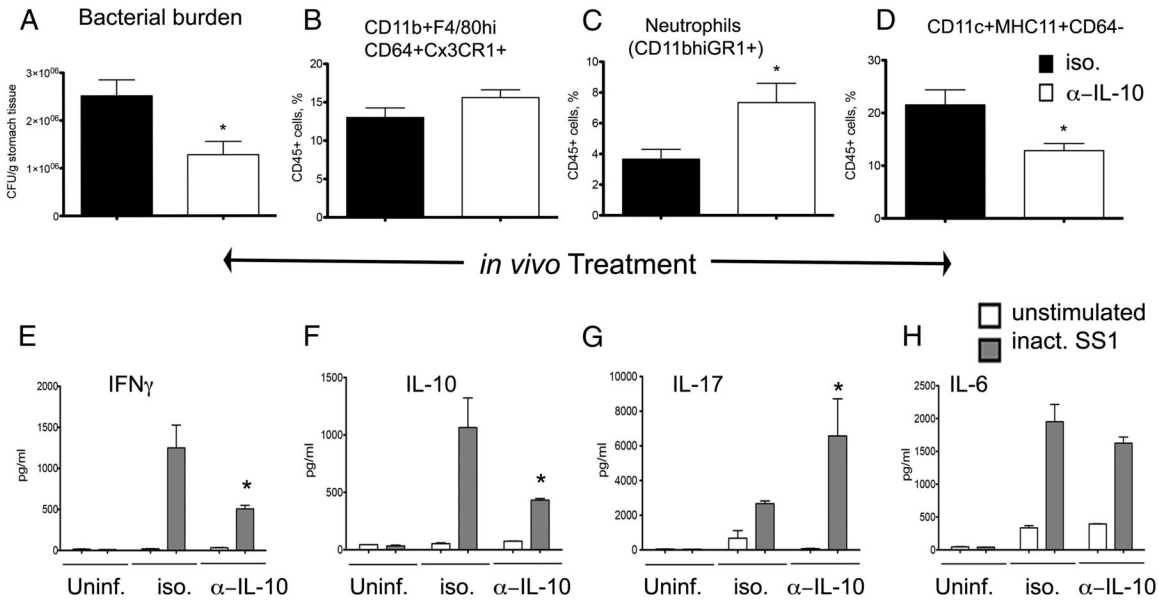

Figure 2.7. IL-10 neutralization during *H. pylori* infection. WT mice were infected with *H. pylori* and on days 17, 19, and 21 post-infection they were treated with 100 µg of either neutralizing anti-mouse IL-10 or rat IgG1 isotype control Abs. Mice (n = 6) were euthanized on day 22 post-infection to measure (A) bacterial burden in the stomach and percentages of (B) $CD11b^{+}F4/80^{hi}CD64^{+}CX_3CR1^{+}$ cells, (C) neutrophils, and (D) DCs. Cells from the gastric lymph nodes of three to four mice of the same sex and treatment were stimulated *ex vivo* with RPMI 1640 (unstimulated) or 5 µg/ml formalin-inactivate *H. pylori* SS1. Production of (E) IFNγ, (F) IL-10, (G) IL-17, and (H) IL-6 were measured in 72-h cell culture supernatant using a cytometric bead array. Results are expressed as the average of three to five samples of pooled cells, and data represent mean ± SEM. Results are representative of two independent replicate experiments with same results. * $P < 0.05$ when compared with the control (WT) group.

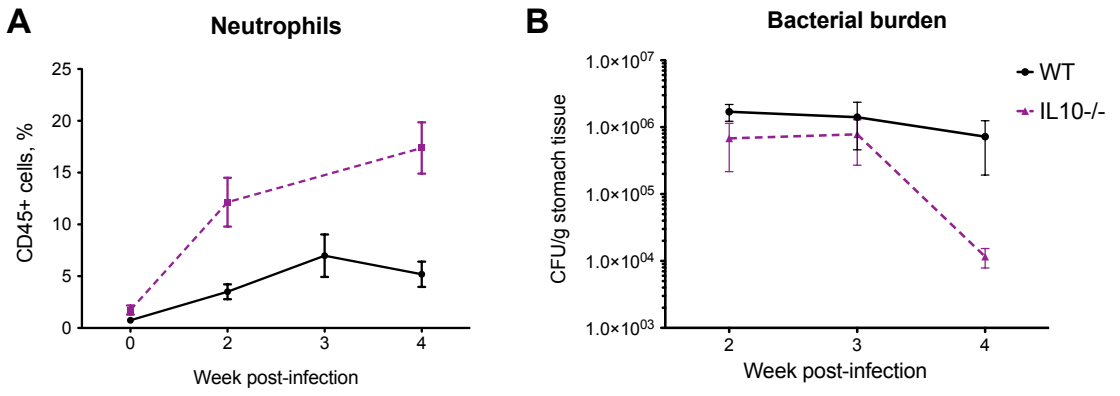

Figure 2.8. Infection of IL-10 deficient mice. WT and IL-10 deficient mice were infected with *H. pylori* SS1 and at the indicated times, bacterial reisolation from stomach was performed to measure bacterial burden. (A) Percentages of neutrophils ($CD11b^{hi}$

GR1$^+$) were determined by flow cytometry. The results show that lack of IL-10 induces significant accumulation of neutrophils, induced by *H. pylori* infection, since no differences were found between strains prior to challenge. (B) Bacterial loads were significantly lower at week 4 post-infection. Data represent mean ± SEM of 8 mice per group. Points with different superscripts are significantly different when compared to the control group ($P < 0.05$).

2.7 Depletion of phagocytic cells suppresses high levels of *H. pylori* colonization

Phagocytic depletion employing a chemical method through administration of clodronate liposomes results in decreased bacterial burden in WT mice, mimicking colonization levels observed in LysMcre mice [104]. To further confirm the significance of gastric phagocytes, and specifically CD11b$^+$F4/80^{hi}CD64$^+$CX$_3$CR1$^+$ cells, in allowing high levels of *H. pylori* colonization in gastric tissue, we employed a mouse model, CD11c-DTR mice, to deplete phagocytic cells as an alternative method. Due to the expression of the diphtheria toxin receptor in CD11c$^+$ cells in CD11c-DTR mice, upon administration of diphtheria toxin, depletion of CD11c$^+$ is achieved. Of note, even that CD11c-DTR mice have been extensively employed to specifically deplete DCs [105-108], CD11b$^+$F4/80^{hi}CD64$^+$CX$_3$CR1$^+$ cells also express the CD11c molecule and can be depleted using this method. WT and CD11c-DTR mice were infected with *H. pylori* SS1. At day post-infection 17 and 20, diphtheria toxin was administered to prevent the CD11b$^+$F4/80^{hi}CD64$^+$CX$_3$CR1$^+$ accumulation in gastric mucosa. Results report a decrease in bacterial colonization starting at day post-infection 21 and achieving a significant drop at day post-infection 23 in the CD11c-DTR diphtheria toxin-administered group (Figure 2.9A). The bacterial burden drop observed at day post-infection 23 correlated with a significant depletion of CD11b$^+$F4/80^{hi}CD64$^+$CX$_3$CR1$^+$ cells in gastric tissue (Figure 2.9B). Interestingly, as observed during IL-10 neutralization, the phagocytic depletion is associated to higher infiltration of neutrophils in gastric tissue (Figure 2.9C).

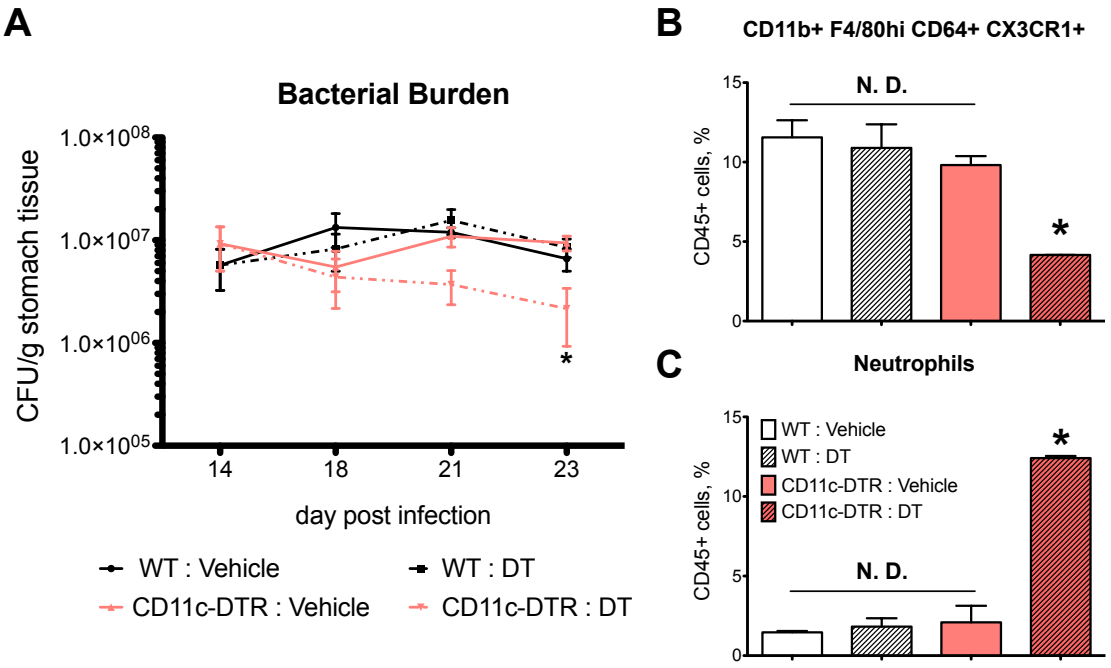

Figure 2.9. Phagocytic depletion through the employment of a mouse model of CD11c^{+} cell depletion results in lower *H. pylori* colonization in gastric tissue. WT and CD11c-DTR mice were infected with *H. pylori* SS1. 25ng/g of diphtheria toxin were injected through i. p. at day post-infection 17 and 20. (A) At day post-infection 14, 18, 21 and 23 mice were euthanized and bacterial colonization assessed through quantification of gastric bacterial burden. Flow cytometry analysis of (B) CD11b^{+}F4/80^{hi}CD64^{+}CX$_3$CR1^{+} and (C) neutrophils in gastric tissue was performed at day post-infection 23. Data represents mean ± SEM of 4-5 mice per group. Points with different superscripts are significantly different when compared to the control group (P<0.05).

2.8 Expression of the CCR2 receptor is not required for macrophage accumulation in gastric tissue upon *H. pylori* infection

To determine the origin of CD11b^{+}F4/80^{hi}CD64^{+}CX$_3$CR1^{+} macrophages, with proliferative capacity, that accumulate in gastric tissue upon *H. pylori* infection, WT, LysMcre and CCR2$^{-/-}$ mice were infected with *H. pylori* SS1. Flow cytometry analysis of myeloid and lymphocyte populations in gastric tissue at day post-infection 24 revealed no differences in CD11b^{+}F4/80^{hi}CD64^{+}CX$_3$CR1^{+} macrophages (Figure 2.10A) in the absence of CCR2. In contrast, CCR2 deficiency resulted in a significant decrease of infiltrated neutrophils (Figure 2.10D), as reported in the LysMCre group, as well as a heterogeneous response in DCs (Figure 2.10B, C). Additionally, no differences were observed in CD4^{+} T cells (Figure 2.10E) and B cells (Figure 2.10F).

H. pylori colonization at day post-infection 24 was also quantified in WT and CCR2$^{-/-}$ mice. In correlation with the results obtained in the immune cell analysis, no differences were reported in bacterial burden due to the loss of CCR2 (Figure 2.11). These results

demonstrate that the accumulation $CD11b^{+}F4/80^{hi}CD64^{+}CX_3CR1^{+}$ macrophages is not dependent of monocyte recruitment in gastric tissue, suggesting that this population of gastric phagocytic cells have a tissue resident origin.

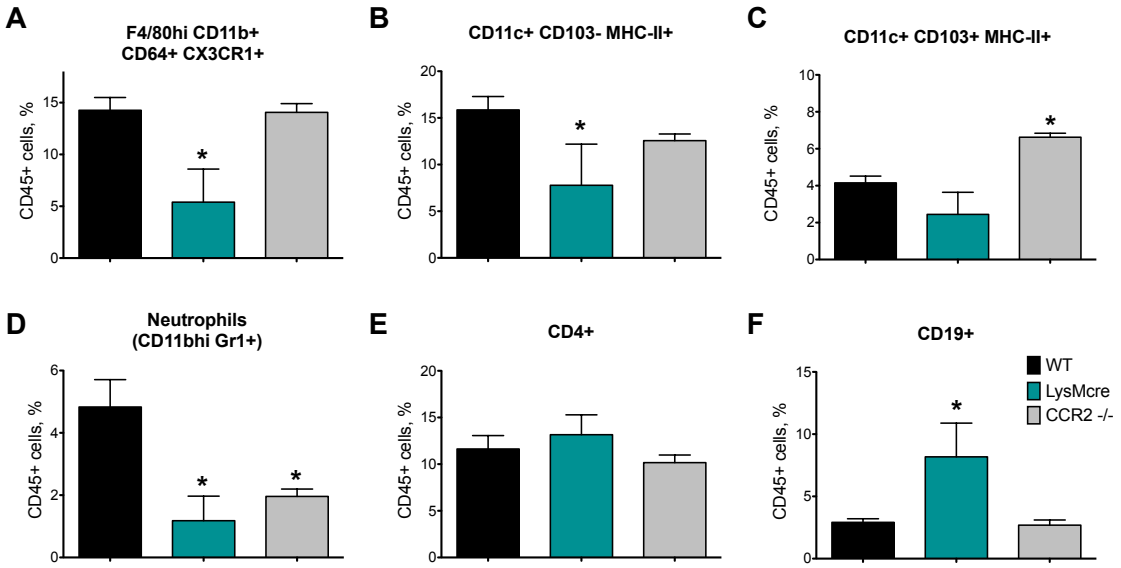

Figure 2.10. *H. pylori*-induced accumulation of gastric $CD11b^{+}F4/80^{hi}CD64^{+}CX_3CR1^{+}$ macrophages is independent of CCR2 expression. Flow cytometry analysis of myeloid cells and lymphocytes in gastric tissue. WT, LysMcre and CCR2-/- mice were infected with *H. pylori* SS1 and stomachs collected at day post-infection 24. (A) $CD11b^{+}F4/80^{hi}CD64^{+}CX_3CR1^{+}$ macrophages, (B) CD11c+CD103-MHC-II+, (C) CD11c+CD103+MHC-II+, (D) Neutrophils, (E) CD4+ T cells and (F) B cells were analyzed. Data represents mean ± SEM of 5 mice per group. Results are representative of two independent replicate experiments with same results. Points with different superscripts are significantly different when compared to the control group (P<0.05).

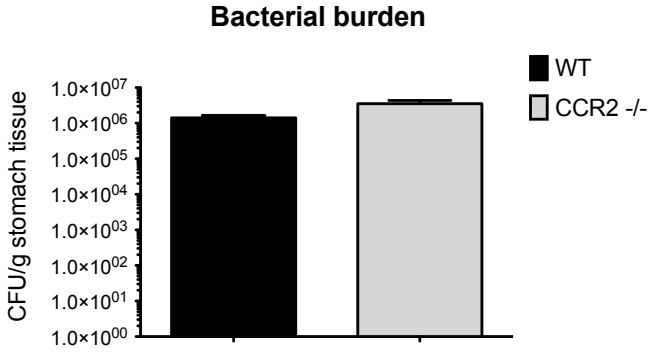

Figure 2.11. CCR2 deficiency does not prevent high colonization of *H. pylori* in gastric tissue. Bacterial burden at day post-infection 24 was quantified in WT and

$CCR2^{-/-}$ mice. Data represents mean ± SEM of 10 mice per group. Results are representative of two independent replicate experiments with same results. Points with different superscripts are significantly different when compared to the control group ($P<0.05$).

2.9 Discussion and conclusions

H. pylori has colonized the human stomach since early evolution, diverged with prehistoric human migrations [13, 109-111], and coevolved with its human host for over 60,000 years [62, 63]. However, its identification as the main etiologic agent of gastro-duodenal ulcers, and gastric cancer [21] set the stage for the pre-conceived notion of *H. pylori* as pathogen. Thirty years after this discovery, it is broadly accepted that *H. pylori* can predispose carriers to develop serious gastric pathologies [112, 113]. However, emerging clinical and epidemiological data support the theory that *H. pylori* might also be a beneficial commensal organism and its disappearance has been linked to increased incidence of diseases like asthma or IBD [114, 115]. Indeed *H. pylori'*s ability to establish life-long chronic colonization of the gastric mucosal niche has been linked to the induction of potent regulatory responses that dampen effector mechanisms of bacterial eradication, although the induction of these responses has been attributed mainly to the modulation of DC*,* as opposed to macrophages [116-118]. In any case, the mechanisms underlying the induction of these protective responses are not fully understood. This study reports a complex network of MNPs, which include DCs and a subset of $CD11b^{+}F4/80^{hi}CD64^{+}CX_3CR1^{+}$ macrophages not previously described in the stomach. We provide evidence that MNPs can facilitate *H. pylori* colonization by promoting IL-10 responses.

The prevailing theory is that the regulatory/suppressor responses associated with of *H. pylori* gastric infection are induced by DCs [77, 78, 116, 119] and not by macrophages. Moreover, it has been suggested that macrophages contribute to the initiation of gastritis. For instance, Shumacher and colleagues identified a subset of $CD11b^{+}F4/80^{+}Ly6C^{hi}$ cells that is recruited to the stomach of mice as early as 2 days post-infection, and the loss of this subset was associated with reduced gastritis [120]. Others have shown that the expression of matrix metalloproteinase 7, heme oxygenase and protease-activated receptor 1 ameliorates *H. pylori*-induced gastritis through the regulation of pro-inflammatory gene expression in macrophages [121-123]. To investigate how macrophage phenotype influences the outcome of infection we used myeloid-specific PPARγ deficient mice with inflammatory-prone macrophages driven by the deletion of PPARγ, an important regulatory transcription factor. Interestingly, our data shows that loss of PPARγ results in a significant drop in bacterial loads, which consistently occurs between weeks 2 and 3 post-infection, and is paralleled mainly by impaired accumulation of $CD11b^{+}F4/80^{hi}CD64^{+}CX_3CR1^{+}$ macrophages at the gastric mucosa when compared to WT mice. Our finding that mice with a targeted deletion of PPARγ in myeloid cells failed to expand and maintain this population was unexpected, since loss of PPARγ in myeloid cells does not affect their differentiation or survival [103, 124]. Of note, inducible NO synthase levels are higher in *H. pylori*-associated atrophic gastritis compared to uncomplicated gastritis, indicating the potential contribution of M1-like

macrophages to lesion development [125]. Furthermore, PPARγ polymorphisms in humans are associated with an increased risk of developing *H. pylori*-related gastric cancer [126]. Although the importance of PPARγ in the host response to *H. pylori* has been established in previous studies, the mechanisms underlying the protective actions of gastric *H. pylori* colonization remain incompletely understood. Here we provide novel evidence that PPARγ is essential for mounting a regulatory immune response to *H. pylori* via accumulation of $CD11b^{+}F4/80^{hi}CD64^{+}CX_3CR1^{+}$ macrophages and IL-10 production. A possible mechanism is that *H. pylori* infection favors endogenous PPARγ agonist production locally. Interestingly, differentiation of monocytes into macrophages in the presence of endogenous PPARγ agonists 9-HODE and 13-HODE, two major oxidized linoleic acid metabolite components of oxLDL, induced a shift from CCR2 to CX_3CR1 surface expression and upregulation of CD36. This phenotypic switch occurred in the presence of lipid-induced TNFα, IFNγ and IL-1β, and it was inhibited by RNAi-mediated knockdown of PPARγ and treatment with its antagonist GW9662. Although CX_3CR1 was constitutively expressed in monocytes, only PPARγ activation upregulated CX_3CR1 expression by directly binding to PPARγ response element (PPRE) consensus sites on the CX_3CR1 promoter [127]. Indeed, infection with *H. pylori* CagA+ strains has been associated with increased levels of oxidized low-density lipoprotein (oxLDL) in the plasma of human subjects with more severe coronary atherosclerosis [128]. In line with this, our unpublished observations demonstrate that co-culture of H. *pylori* with BMDM upregulates CX_3CR1 although mRNA expression is suppressed in PPARγ-deficient BMDM.

Clodronate-induced depletion of phagocytic cells resulted in lower *H. pylori* colonization in gastric tissue correlated with a decreased production of IL-10 by $CD3^{+}CD4^{+}$ T cells and $CD11b^{+}$ cells, while neutrophils infiltration significantly increased [104]. To further validate that the temporary loss of phagocytic cells leads to decreased bacterial colonization, we employed a mouse model of depletion of $CD11c^{+}$ cells using CD11c-DTR mice. Oertli el al., previously employed this model to investigate the implication of DCs in *H. pylori*-induced tolerance, observing a significant reduction of *H. pylori* burden in the stomach due to enhanced IFNγ responses. Our phenotypic analysis shows that in addition to DC ($MHC\text{-}II^{+}CD11c^{+}CD103^{+}$ and $MHC\text{-}II^{+}CD11c^{+}CD103^{-}$), $CD11b^{+}F4/80^{hi}CD64^{+}CX_3CR1^{+}$ macrophages also express CD11c (not shown). The results obtained from the $CD11c^{+}$ cells depletion consistently demonstrated a decrease of gastric *H. pylori* colonization upon depletion of phagocytic cells. As hypothesized, the phagocytic depletion significantly affected $CD11b^{+}F4/80^{hi}CD64^{+}CX_3CR1^{+}$ population in gastric tissue, supporting the role of this population in facilitating bacterial colonization. As observed in the clodronate-induced depletion, a significant influx of neutrophils was also observed. Taken together, these data indicate that MNPs contribute to high levels of bacterial colonization in the gastrointestinal tract by inducing IL-10-mediated regulatory responses at the mucosa and creating a host tolerant environment that favors colonization. Follow-up challenge studies in mice revealed that $F4/80^{lo}CD11b^{+}$, and $F4/80h^{i}CD11b^{+}CD64^{+}CX_3CR1^{+}$ cells from WT mice produce significant amounts of IL-10 [104]. Notably, IL-10 levels on a per cell basis were not augmented in WT mice following infection with *H. pylori*, which suggests that these cells have innate regulatory function and produce IL-10 in the steady state to maintain mucosal homeostasis. As

opposed to MNPs, *H. pylori* infection induced IL-10 production by gastric $CD19^+$ B cells and $CD4^+$ T cells on day 24 post-infection [104]. Additionally, *ex vivo* culture with isolated cells from GLN, reported an antigen-specific response characterized by production of IL-10 and IL-17. Interestingly, loss of PPARγ in myeloid cells upregulated IL-17 expression together with other pro-inflammatory cytokines, including IFNγ and TNFα, while IL-10 expression was suppressed. This increase in IL-10 production by lymphocytes in response to *H. pylori* in both gastric tissue and gastric lymph nodes suggests that IL-10-producing MNPs are the main source and promoters of IL-10-mediated responses at the gastric mucosa. Interestingly, in an attempt to characterize resident MNPs in the kidneys, Duffield and colleagues have identified a $CD11b^{int}$ $CD11c^{int}$ $F4/80^{hi}$ subpopulation that expresses high levels of CX_3CR1 and IL-10 [129]. Also, depletion of CX_3CR1^+ MNPs results in more severe colitis in the *Citrobacter rodentium* infection colitis model. The mechanism is mediated by CX_3CR1^+ MNP's ability to promote IL-22 secretion from ILC3. An equivalent CX_3CR1^+ cell subset was identified in the human intestine, which additionally expressed CD64 and CD68 [130].

To evaluate the potential mechanism by which IL-10-producing MNPs could modulate the gastric environment early post-infection, we neutralized IL-10 in WT mice infected with *H. pylori*. As expected, IL-10 ablation lead to suppressed colonization and, similarly to our results during MNPs depletion, to a significant influx of neutrophils. Surprisingly, IL-10 neutralization did not affect numbers of $F4/80^{hi}CD11b^+CD64^+CX_3CR1^+$ cells, which suggest that IL-10 is dispensable for their accumulation in the stomach. We also report that *H. pylori* infection induced IFNγ, IL-10, IL-6 and IL-17 responses in gastric lymph nodes, which is in line with the mixed response to infection that has been reported previously. However, IL-10 blockade led to increased IL-17 and diminished IFNγ and IL-10 production. This response fits well with the enhancement of a TH17 responses and can explain the effect of neutrophil accumulation after neutralization of IL-10 or depletion of IL-10-producing MNPs.

Recent studies suggest that the pool of tissue-resident macrophages in the gastrointestinal tract is comprised by self-renewal macrophages with embryogenic origin supplemented by blood monocyte-derived macrophages originated from the bone marrow [97, 99, 100]. BrdU data indicate that $CD11b^+F4/80^{hi}CD64^+CX_3CR1^+$ macrophages have the ability to proliferate in gastric tissue. Additionally, $CD11b^+F4/80^{hi}CD64^+CX_3CR1^+$ accumulation is independent of expression of CCR2, a key receptor for the recruitment of bone marrow monocytes into to the inflammatory tissues [131, 132]. Indeed, the alteration in the myeloid compartment reported in $CCR2^{-/-}$ does not affect CD11b+F4/80hiCD64+CX_3CR1+ macrophages, that presented a similar behavior to the WT group. These results suggest that $CD11b^+F4/80^{hi}CD64^+CX_3CR1^+$ are tissue resident macrophages that accumulate during *H. pylori* infection through self-renewal expansion.

In summary, we provide data showing that MNPs facilitate *H. pylori* colonization early post-infection. We show that the gastric mucosa hosts a large and heterogeneous population of myeloid cells, including DC and a newly identified $CD11b^+F4/80^{hi}CD64^+CX_3CR1^+$ macrophage subset. Although our profiling data does not provide definitive evidence of this subset being responsible for the induction of the

regulatory responses that facilitate optimal colonization, the fact that they: 1) accumulate in the stomach following *H. pylori* infection, 2) are the subset most affected cell by clodronate treatment and are significantly affected by $CD11c^+$ depletion, and 3) produce IL-10 constitutively, makes them the cell type most likely responsible for inducing a regulatory microenvironment in the gastric mucosa during *H. pylori* infection. Our results also suggest that $CD11b^+F4/80^{hi}CD64^+CX_3CR1^+$ MNPs are resident cells of the gastric immune system that promote tolerogenic responses. Moreover, this population impose an IL-10-dominated tissue microenvironment that dampens effector responses, particularly TH17, against *H. pylori* and thereby facilitate a more effective colonization. An interesting finding of this study is the very critical role of PPARγ in macrophages for the maintenance of regulatory homeostasis in the stomach. The mechanism by which the loss of PPARγ results in more efficient *H. pylori* elimination does not seem to be related to increased neutrophil influx, although it was associated with lower production of IL-10. While neutralization of IL-10 did not affect accumulation of CD11b+F4/80hiCD64+CX_3CR1+ MNPs in the stomach, the myeloid compartment was severely affected by genetic ablation of PPARγ. Three immediate implications derived from this work that deserve further investigation. First, to what extent do these host tolerance mechanisms contribute to the role of *H. pylori* as a beneficial commensal that protects from immune-mediated diseases? Second, do CD11b+F4/80hiCD64+CX_3CR1+ MNPs facilitate colonization by other members of the gastrointestinal microbiota? Finally, are there other master regulators of homeostasis in the GI mucosa that target this cell type and can the used for therapeutic development?

2.10 Materials and Methods

Animal housing and ethic statement

6 to 10 week old C57Bl/6J wild-type (WT), PPARγ fl/fl;LysCre+ (LysMCre), CD11c-DTR, IL10 whole body knock-out (IL10-/-) and CCR2 whole body knock-out (CCR2-/-) mice were utilized for these study. LysMCre mice, tissue specific knock out mice PPARγ-deficient in myeloid cells, were originally generated through breeding of PPARγ fl/fl into Lys-Cre mice. WT and LysMCre mice have been bred in a Virginia Tech's animal facilities for 10 years. CD11c-DTR, IL10-/- and CCR2-/- mice were purchased form Jackson Laboratories and bred and maintained in the same animal facilities. Mice were kept in ventilated racks and under a 12:12h light-dark cycle. All experimental procedures performed were approved by the Institutional Animal Care and Use Committee (IACUC) and met or exceeded requirements of the Public Health Service/National Institutes of Health and Animal Welfare Act.

Preparation of the inoculum and in vivo H. pylori infection

H. pylori SS1 was grown in Difco Columbia blood agar plates (BD Biosciences, San Jose, CA) supplemented with 7% of Horse Laked blood (Lampire Biological Laboratories, Pipersville, PA) and the *H. pylori* selective supplement (Dent, Oxoid, Altrincham, England) containing 5mg of Vancomycin, 2.5mg of Trimethoprim, 2.5mg of Cefsulodin and 2.5mg of Amphotericin B, at 37ºC and under microaerophilic conditions. Colonies were harvested and adjusted in 1X sterile Phosphate-Buffered Saline (PBS) to an optimal density (OD) of 1.2 at a 600-nm wavelength that corresponds to $2.5x10^8$

colony forming units (cfu) per mL. For *in vivo* infection, mice were challenged with 2 doses of $5x10^7$ cfu of *H. pylori* SS1 in 200µL of fresh inoculum through intragastric at day 0 and day 2. Non-infected control mice received 200µL of sterile 1X PBS. Mice were euthanized through CO_2 narcosis followed by cervical dislocation as secondary method of euthanasia.

Cell isolation from gastric lamina propria

Collected stomachs where opened through the large curvature and rinsed twice with 1X PBS. Tissues were digested at 37ºC in RPMI media containing RPMI 1640 (Corning Incorporated, Corning, NY), 10% Fetal Bovine Serum (Corning Incorporated, Corning, NY), 2.5% Hepes (Corning Incorporated, Corning, NY) and 1% Sodium pyruvate (Corning Incorporated, Corning, NY), supplemented with 300U/mL of collagenase (Sigma Aldrich, St. Louis, MO) and 50U/mL of DNase I (Sigma Aldrich, St. Louis, MO) stirring. Samples were filtered through 100µM cell strainers and washed. Immune cell population was enriched using a Percoll gradient of density (44/67%). The interphase containing the enriched immune cell fraction was collected, washed and counted.

Flow cytometry

Between $3x10^5$ and $5x10^5$ cells were seeded in 96-well plates and incubated with Fc block for 10 minutes. Samples were then incubated with a mix of fluorochrome-conjugated antibodies against extracellular markers, including anti-CD45 APC-cy7, anti-CD64 PE, anti-Cd11b AF700, anti-CD4 BV605, anti-CD3 BV421, anti-CD11c PeCy7, anti-CD19 APC (BD Biosciences, San Jose, CA), anti-F4/80 PeCy5, anti-MHC II Biotin, anti-Gr1 PeCy7, anti-CD103 FITC, Anti-CD4 AF700, anti-CD8 PerCPCy5.5 (ThermoFisher Scientific, Waltham, MA), and anti-CX3CR1 unconjugated (Bio-Rad, Hercules, CA) for 20 minutes at 4ºC in the dark. Samples requiring a secondary staining were then incubated with Streptavidin-Texas Red (BD Biosciences, San Jose, CA) and anti-rabbit IgG (H+L) FITC (southern Biotech, Birmingham, AL). For intracellular staining, samples were initially fixed and permeabilized using the eBiosciences reagent kit and then incubated with anti-IL10 APC (BD Biosciences, San Jose, CA) for 20 minutes at 4ºC in the dark. Data was acquired with a BD LSRII flow cytometer and analyzed with the FACSDiva software (BD Biosciences, San Jose, CA).

In vivo BrdU challenge

WT mice were intraperitoneally injected with one dose of 1mg of BrdU (BD Biosciences, San Jose, CA) followed by 3 days of 0.8mg/mL BrdU (Sigma Aldrich, St. Louis, MO) administration in drinking water 12 days after the first *H. pylori* infection. Mice were euthanized at days 0, 3 and 6 post BrdU challenge, corresponding to days 15, 18 and 21 post infection. A control group of non-infected mice were also included in each timepoint. Following stomach collection and isolation of gastric lamina propia leukocytes, the BD BrdU Flow kit (BD Biosciences, San Jose, CA) was used to assess BrdU incorporation in immune populations.

Ex vivo culture

Following euthanasia, gastric lymph nodes (GLN) were collected, washed in sterile 1XPBS and digested for 60 minutes at 37ºC in RPMI 1640 media containing 10% FBS,

2.5% Hepes, and 1% Sodium pyruvate with collagenase (Sigma Aldrich, St. Louis, MO) at 300U/mL and DNase I (Sigma Aldrich, St. Louis, MO) at 50U/ml under stirring. After filtration, samples were washed and adjusted to $1x10^6$cells/mL with cRPMI containing RPMI 1640, 10% FBS, 2.5% Hepes, 1% Sodium pyruvate, 2% Essential Amino Acids (ThermoFisher Scientific, Waltham, MA), 1% Non-essential Amino acids (ThermoFisher Scientific, Waltham, MA), 1% L-glutamine (Corning Incorporated, Corning, NY), 1% Penicilin/Streptamicin (Corning Incorporated, Corning, NY) and 50uM β-mercaptoethanol (Sigma Aldrich, St. Louis, MO). $2x10^5$ cells were seeded in a 96-well plate. Samples were stimulated with 5ug/mL of *H. pylori* SS1 antigen and cultured at 37ºC, 95% humidity and 5% CO_2. After 72 hours of culture, supernatants were collected for assessment of cytokine profile.

Cytokine bead array

The mouse Th1, Th2 and Th17 Cytokine kit (BD Biosciences, San Jose, CA) was utilized to assess the secreted cytokine profile form the *ex vivo* cultures. Following manufacturer's instructions, collected supernatants and diluted standards were incubated with the mouse capture bead mix and the PE detection reagent for 2 hours. Samples were washed, centrifuged at 200 x g for 5 min and re-suspended with wash buffer. Data was acquired with a BD LSRII flow cytometer and analyzed with the FACSDiva software. Cytokines assessed included IL-10, IFNγ, TNFα, IL-6 and IL-17.

IL-10 neutralization

To neutralize IL-10, WT mice were injected with a rat anti-mouse IL-10 antibody (R&D systems, Minneapolis, MN) at days 17, 19 and 21 post *H. Pylori* infection. Each dose consisted of 100µg of IL-10 antibody in 100µL of sterile 1X PBS administered via intraperitoneal injection. A group of control mice receiving 100µg of Rat IgG1 isotopye control (R&D systems, Minneapolis, MN) in 100µL of sterile 1X PBS was also included. Mice were euthanized at days 22 post infection.

Bacterial reisolation from gastric tissue

Opened and cleaned stomachs were weighed and collected in 200 µL of sterile bacterial broth. Tissues were homogenized using a grinder. Homogenates were employed to perform serial dilutions (10^{-1}, 10^{-2}, 10^{-3}). Homogenates and diluted samples were plated in Difco Columbia blood agar plates for *H. pylori* culture prepared as described above. Plates were cultured at 37ºC under microaerophilic conditions for 4 days. Number of colonies were counted and normalized to initial stomach weight.

Mononuclear phagocyte depletion

The tissue engineered CD11c-DTR mice characterized by the expression of the diphtheria toxin receptor in CD11c-positive cells were employed. WT and CD11c-DTR mice were intraperitoneally injected with 2 doses of 25ng/g of diphtheria toxin (Sigma Aldrich, St. Louis, MO) in 100µL of sterile 1X PBS at day post infection 17 and 20. Two control groups of WT and CD11c-DTR mice receiving 100µL of 1X PBS without toxin were also included. Mice were euthanized at day post infection 14, 18, 21 and/or 23.

Statistics

Data are expressed as means ± standard error of the mean represented in error bars. Statistical analysis to determine significance was performed through Analysis of variance (ANOVA) using the general linear model procedure in SAS (SAS Institute). We employed a 2 X 2 factorial arrangement in order to compare genotype and infection. Significance was considered at $p \leq 0.05$ and significant differences were identified with an asterisk.

Chapter 3

Identification of Regulatory Genes through Global Gene Expression Analysis of a *Helicobacter pylori* Co-culture System

Nuria Tubau Juni, Josep Bassaganya-Riera, Andrew Leber, Victoria Zoccoli-Rodriguez, Barbara Kronsteiner, Monica Viladomiu, Vida Abedi, and Raquel Hontecillas.

Tubau-Juni N, Bassaganya-Riera J, Leber A, Zoccoli-Rodriguez V, Kronsteiner B, Viladomiu M, Abedi V, and Hontecillas R. 2019. Identification of regulatory genes through global gene expression analysis of a *Helicobacter pylori* co-culture system. bioRxiv. 2019:523274

3.1 Summary

Helicobacter pylori is a gram-negative bacterium that establishes life-long infections by inducing immunoregulatory responses. We have developed a novel *ex vivo H. pylori* co-culture system to identify new regulatory genes based on expression kinetics overlapping with that of genes with known regulatory functions. Using this novel experimental platform, in combination with global transcriptomic analysis, we have identified 5 lead candidates, validated them using mouse models of *H. pylori* infection and *in vitro* co-cultures under pro-inflammatory conditions. Plexin domain containing 2 (*Plxdc2*) was selected as the top lead immunoregulatory target. Gene silencing and ligand-induced activation studies confirmed its predicted regulatory function. Our integrated bioinformatics analyses and experimental validation platform has enabled the discovery of new immunoregulatory genes. This pipeline can be used for the identification of genes with therapeutic applications for treating infectious, inflammatory, and autoimmune diseases.

3.2 Introduction

Chronic bacterial infections trigger complex and dynamic host-bacterial interactions that modulate immunometabolic host responses. The phenotypic manifestation of these dynamic interactions results from the coordinated expression of blocks of genes with overlapping functions that cooperate in modulating host responses. In addition to pathogen associated molecular patterns (PAMPs) that signal infection and are associated with induction of innate anti-bacterial and inflammatory responses, other lesser known bacterial components elicit compensatory immunoregulatory responses that when exploited by pathogens, promote bacterial persistence. For instance, *Mycobacterium tuberculosis* induces IL-10-driven regulatory responses that suppress the activated immune mechanisms and contribute to long-term infection [133-136]. Therefore, the activation of host immunoregulatory mechanisms by certain bacterial organisms inhibit the effector immune response and prevent bacterial clearance.

Helicobacter pylori is a gram-negative, microaerophilic, spiral-shaped bacterium with unipolar, sheathed flagella [12, 137], that constitutes the primary member of the gastric

mucosa in infected individuals [138, 139]. *H. pylori* is highly specialized to colonize the human gastric niche. The infection is chronic and affects more than 50% of the world's population [140]. *H. pylori* infection is mostly asymptomatic; however, approximately 10% of carriers will develop peptic ulcers [22, 141], and 1-3% gastric cancer [22]. Interestingly, *H. pylori* infection may be an important driver of systemic tolerance in asymptomatic individuals with an inverse correlation between the presence of this bacterium and the development of autoimmune diseases, asthma, esophageal adenocarcinoma and type-2-diabetes [15-19]. These conflicting implications may stem from the relative predominance of antagonistic immune responses that encompass both effector and regulatory components elicited by *H. pylori [23, 25, 29, 30]*. However, long-term colonization by the bacterium, due to failure of the immune system to clear the infection, suggests that the strong *H. pylori*-induced regulatory responses can shift inflammatory/effector responses leading to chronicity of infection.

Macrophages have been described as key immune cells in *H. pylori*-induced regulatory mechanisms [35]. Particularly, *H. pylori* interacts with a specific subset of mononuclear phagocytes that generate IL-10-driven regulatory responses facilitating optimal colonization of the gastric mucosa [104]. We demonstrated that macrophage peroxisome proliferator-activated receptor gamma (PPARγ), an anti-inflammatory transcription factor, was needed for the induction of the full spectrum regulatory response [104]. Additional macrophage-expressed genes (*Par1*, *HO-1*) have been shown to play a similar role to PPARγ and contribute to keeping high levels of colonization while reducing pathology and disease [121, 142].

Early after the initiation of the immune response, both macrophages and dendritic cells (DC) endure strong metabolic and transcriptional changes. To increase the speed of energy production and facilitate the execution of effector responses, activated macrophages are subjected to a metabolic switch, in which glycolysis and lactate production predominate, while Krebs cycle and oxidative phosphorylation are reduced into secondary roles [143, 144]. This substantial change implies that the metabolic shift towards higher glucose consumption and glycolysis rate is key to enable the required spectrum of host responses in inflammatory macrophages. In contrast, alternatively-activated macrophages present a metabolic component in which oxidative phosphorylation is dominant and fatty acid consumption is increased [144-146]. Moreover, IL-10 was found to suppress glycolysis while stimulating oxidative metabolism [147], suggesting that some metabolic changes are essential for the induction of regulatory responses in macrophages. Interestingly, PPARγ-driven regulatory responses encompass a profound metabolic component, since PPARγ is required for glucose and fatty acid uptake, achieve greater fatty acid β-oxidation in macrophages, and maintain mitochondrial biogenesis, both dominant processes in alternatively activated macrophages [148]. These metabolic changes are tightly coupled to the suppression of proinflammatory gene expression [146, 149].

Transcriptional changes play crucial roles in modulating immunomodulatory and metabolic responses to infection. Gene expression is highly coordinated in time, with sets of genes with overlapping roles sharing the same expression pattern by being upregulated

and downregulated simultaneously. The loss of a single gene can affect the equilibrium of the whole system and have a significant impact in the outcome of the response. Indeed, suppression or inactivation of a single regulatory protein, for instance PPARγ, results in stronger inflammation, while activation or enhanced expression leads to a balanced response, maintained by induction of immunoregulation [104, 148, 150, 151].

In this study, we used an *ex vivo H. pylori* co-culture system to identify genes with putative regulatory function based on the kinetic pattern of expression of known genes using WT and PPARγ-deficient bone marrow-derived macrophages (BMDM). Using a global transcriptomic assay together with a bioinformatics pipeline based on expression pattern-analysis approaches, we have identified 5 potential new regulatory genes. Extensive *in vitro* and *in vivo* validation studies, in both pro-inflammatory as well as regulatory-induced conditions, support the regulatory functions of the selected group of candidate genes. In particular, the plexin domain containing 2 (Plxdc2) gene was selected as the lead immunoregulatory target, based on its characteristics and expression pattern, for further validation of its regulatory behavior. In conclusion, this manuscript establishes a novel integrated platform for the identification of genes such as *Plxdc2* with promising regulatory and immunometabolic functions that could become new molecular targets to treat inflammatory and autoimmune diseases.

3.3 *H. pylori* induces expression of regulatory genes in WT but not in PPARγ-deficient macrophages

The *in vivo* interplay between *H. pylori* and the myeloid cell compartment revealed that macrophages are highly responsive to *H. pylori*-induced regulatory responses [104]. Here, we sought to explore *H. pylori* interactions with macrophages employing a synchronized gentamycin protection co-culture system comparing cells obtained from WT and PPARγ fl/fl;LysCre+ (LysCre+) mice. Gentamycin was applied to the culture system 15 min after cells were exposed to live *H. pylori* to avoid constant extracellular stimulation and synchronize the cellular response. Of note, *H. pylori* can be internalized and replicate in the intracellular compartment [152-155]. Here, we used intracellular replication post-gentamycin treatment as a marker of the effect and status of the anti-bacterial response. LysCre+ mice lack PPARγ transcription factor in myeloid cells, which results in defective expression of genes with regulatory function and overexpression of pro-inflammatory and anti-bacterial response genes [101-103]. Cells were harvested at several time-points from 0 to 12 hours post-gentamycin exposure to assess bacterial burden and changes in gene expression in response to *H. pylori*. The same pattern of bacterial replication was observed for both genotypes. Initial replication was first detected 30 min post-gentamycin treatment and the peak occurred at 120 min (Figure 3.1A). However, bacterial counts in co-cultures of LysCre+ macrophages were significantly reduced throughout the time course, starting at 60 min post-challenge and up to 240 min post-challenge. This phenotype was compatible with an inflammatory shift in LysCre+ BMDM due to the loss of PPARγ resulting from altered activation of certain regulatory *H. pylori*-induced mechanisms and consequently a more efficient anti-bacterial response. To validate this assessment, WT and LysCre+ macrophages were classically activated through LPS/IFNγ stimulation 24 hours prior the infection. Generation of pro-

inflammatory WT macrophages resulted in a drastic suppression of *H. pylori* loads at the 120 min time point, compared to the WT control (Figure 3.1B). Moreover, the bacterial burden peak was entirely abrogated in LPS/IFNγ-treated LysCre+ cells. Regarding the *H. pylori*-induced gene expression profile, IFNγ expression following *H. pylori* challenge was remarkably increased in LysCre+ cells compared to WT. The WT group showed minimal increase at all timepoints relative to time 0 (Figure 3.1F). In contrast, WT macrophages displayed a dramatic increase of the anti-inflammatory cytokine IL-10 at 60 min post-*H. pylori* co-culture, that was significantly diminished in LysCre+ BMDM (Figure 3.1E). Therefore, *H. pylori* promotes the activation of cytokine-driven regulatory mechanisms in WT macrophages, that modulate the immune response and generate a regulatory microenvironment that facilitates bacterial proliferation reaching the greatest peak at 2 hours post gentamycin treatment.

To elucidate the underlying regulatory molecular mechanisms activated upon *H. pylori* co-culture in WT macrophages, we performed a global transcriptomic analysis on a gentamycin protection assay time course (0, 60, 120, 240, 360 and 720 min). RNAseq analysis demonstrated important differences in the gene expression profile within both genotype (Figure 3.1C) and treatment (Figure 3.1D). Almost 50% of genes exhibited a significant differential expression based on the treatment, with a substantial upregulation after *H. pylori* challenge. Thus, *H. pylori* strongly influences the macrophage transcription profile, resulting in drastic modifications in macrophage function that favor the generation of a regulatory phenotype. Therefore, we sought to utilize the new co-culture system to explore novel regulatory pathways activated upon *H. pylori* infection to discover new host regulatory genes that modulate the immune response, with potential to become molecular targets for the development of therapeutics for infectious, inflammatory and autoimmune diseases.

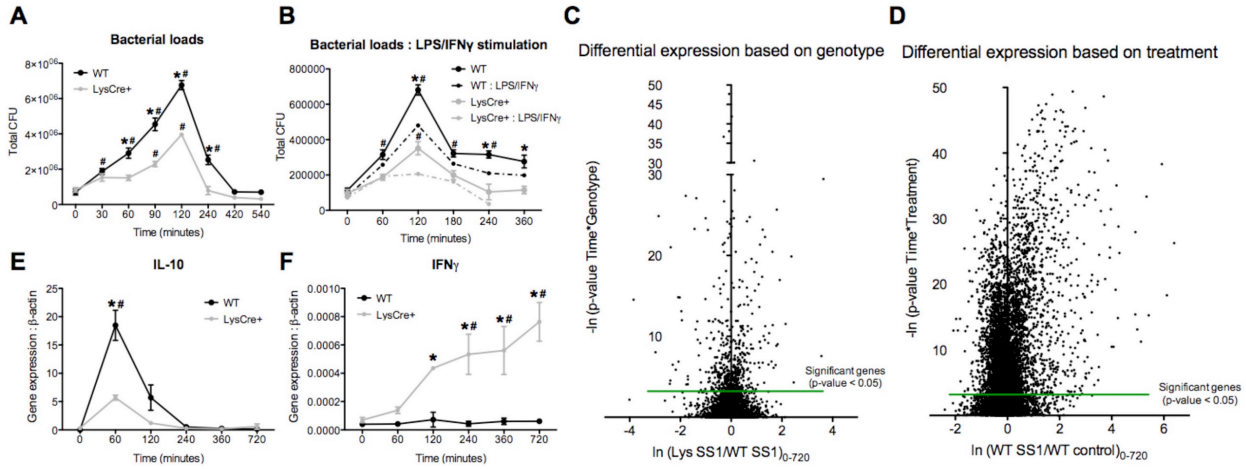

Figure 3.1. ***Helicobacter pylori*** **(*H. pylori*) co-culture strongly alters macrophage transcriptomic profile, leading to the activation of early regulatory responses and increasing bacterial persistence in WT cells.** WT and PPARγ-deficient (LysCre+) BMDM were co-cultured *ex vivo* with *H. pylori* and cells were harvested at several time-points ranging from 0 to 720 minutes after gentamycin treatment. Bacterial burden (A)

and gene expression, including IL-10 (E) and IFNγ (F) were assessed. Differential gene expression based on genotype (C) and *H. pylori* infection (D) from a whole transcriptomic analysis performed on the harvested cells were also assessed. In order to classically activate macrophages prior to *H. pylori* co-culture, cells were stimulated with LPS and IFNγ then challenged with *H. pylori* and bacterial burden was measured (B). **P*-value<0.05 between genotypes, #*P*-value<0.05 within each genotype compared to time 0.

3.4 Validation of experimental co-culture system with identification of differential expression patterns in characterized antimicrobial genes

Expression of regulatory and pro-inflammatory genes is tightly regulated and coordinated over time. Indeed, these sets of genes frequently present opposite expression kinetics under the same conditions. We selected 9 established canonical pro-inflammatory genes to initially explore and identify distinctive patterns of expression associated with pro-inflammatory and antimicrobial functions. Inflammation-related genes are characterized by an increased expression level in *H. pylori*-infected groups compared to the controls (Figure 3.2), and in the majority of genes, *H. pylori*-induced upregulation is achieved at the later time points of the co-culture (Figure 3.2B-F, H-I). As expected, lack of PPARγ results in higher gene expression of pro-inflammatory genes. We then performed a 3-way ANOVA analysis that reported the differential expression of eight genes, including *Chil1*, *Etv5*, *Iigp1*, *Ptger4*, *Sqle*, *Osm*, *Rptoros* and *Hspa2* (Figure 3.3). In fact, most of the genes revealed by the 3-way ANOVA are associated to known pro-inflammatory functions. We focused our analysis in *Chil1* (Figure 3.3A), *Iigp1* (Figure 3.3C) and *Sqle* (Figure 3.3E) due to their expression kinetics that resemble the identified inflammatory genes pattern and their well-known associated role to the host response against pathogens.

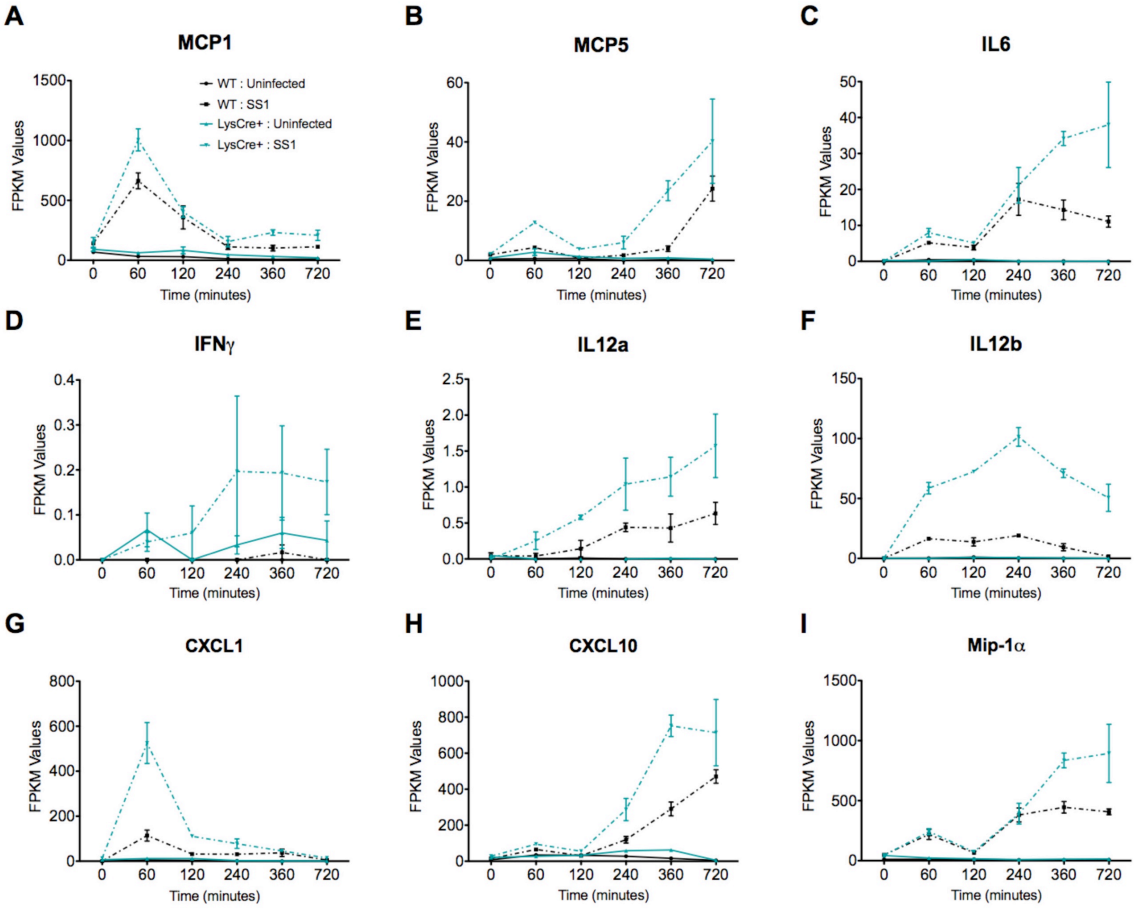

Figure 3.2. Expression kinetics of several pro-inflammatory genes during *Helicobacter pylori* co-culture. Plots represent the RNAseq reads comparing WT and LysCre+ BMDM in the distinctive time points of the gentamycin protection assay of *MCP1* (A), *MCP5* (B), *IL-6* (C), *IFNγ* (D), *IL12a* (E), *IL12b* (F), *CXCL1* (G), *CXCL10* (H), and *MIP-1α* (I).

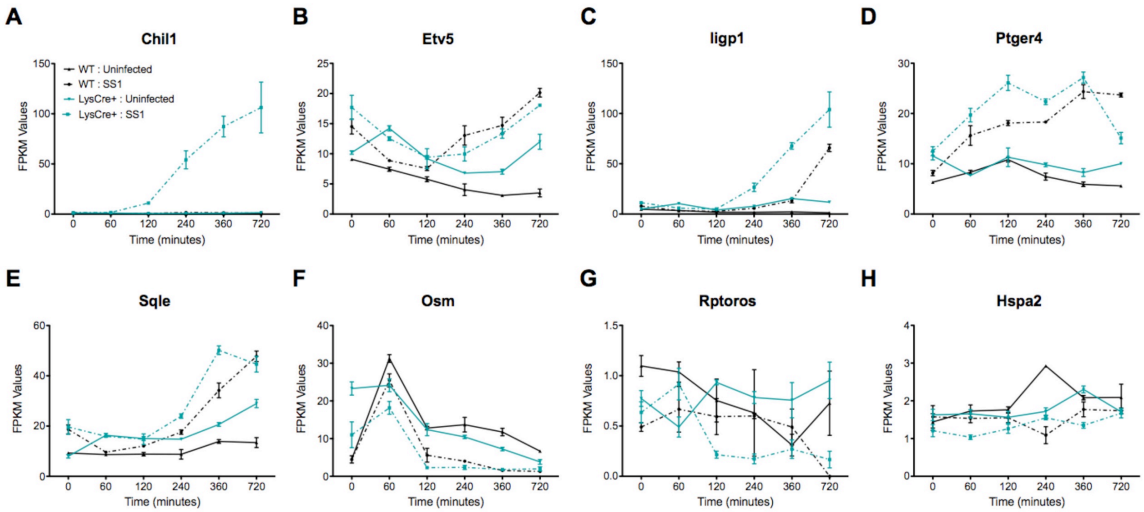

Figure 3.3. 3-way ANOVA analyses revealed 8 genes with significant differential expression pattern. Plots represent the RNAseq values of *Chil1* (A), *Etv5* (B), *Iigp1* (C), *Ptger4* (D), *Sqle* (E), *Osm* (F), *Rptoros* (G), and *Hspa2* (H). *P*-value<0.05.

RNAseq validation through qRT-PCR revealed a similar expression pattern in *Chil1* and *Iigp1*, characterized by a later upregulation due to the infection in both genotypes in case of *Iigp1* (Figure 3.4E) or only in infected LysCre+ cells in case of *Chil1* (Figure 3.4D). In contrast, the later induction of *Sqle* following *H. pylori* challenge, was undetectable in the qRT-PCR analysis (Figure 3.4F), which resulted in no differences within groups among the entire time course. In addition, *Chil1* and *Iigp1* gene silencing (Figure 3.5A-B) led to a clear increase of bacterial loads in both genotypes (Figure 3.4G). Indeed, the significant decrease of bacterial burden in LysCre+ macrophages, when compared to the WT group, was abrogated due to *Chil1* or *Iigp1* gene knock down. As expected, there were no differences in culture systems due to silencing of *Sqle*. Therefore, the initial analysis of this global transcriptomics dataset based on patterns of expression related to pro-inflammatory functions highlighted two genes, *Chil1* and *Iigp1*, with a relevant, previously established role in macrophage antimicrobial responses. Thus, it validated the potential use of this co-culture system for the identification of novel host immunoregulatory genes by means of kinetic pattern analysis within genotypes and among the time course.

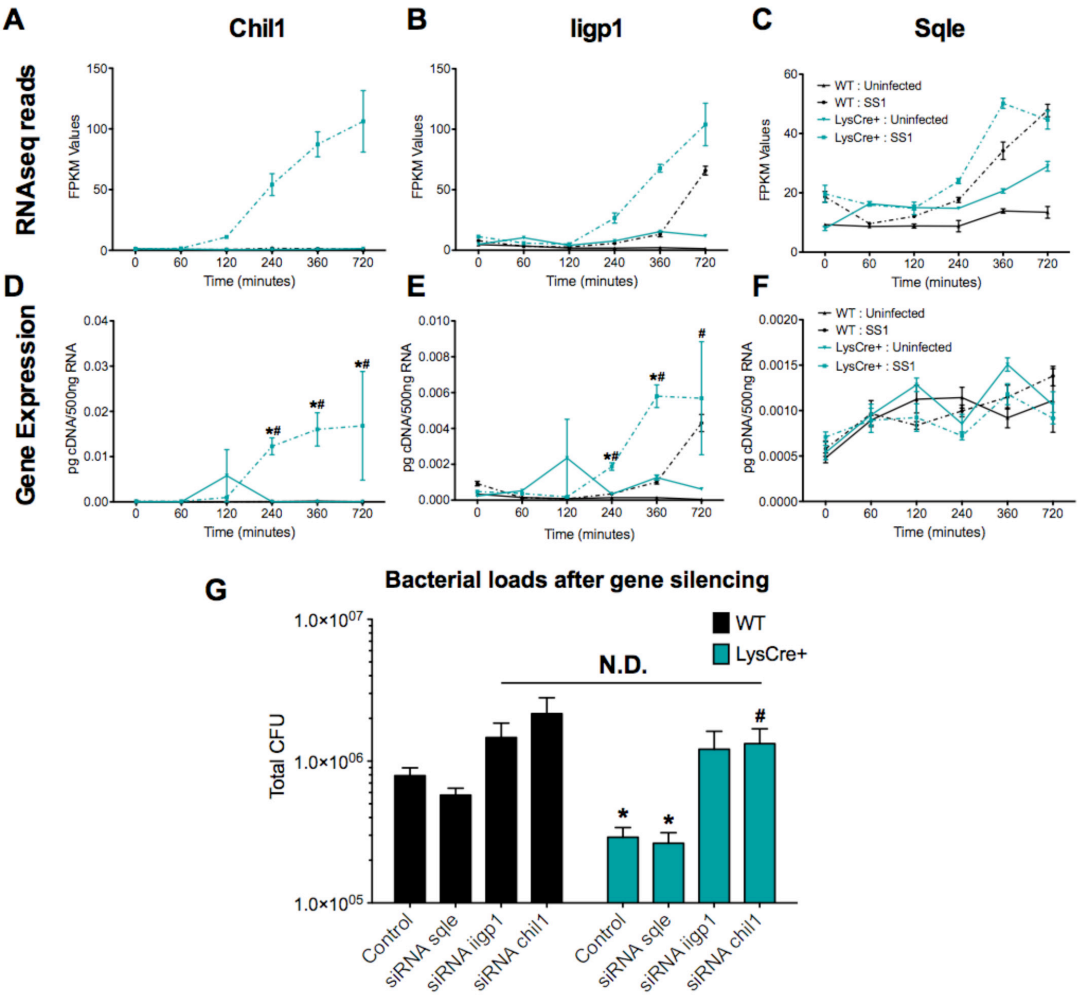

Figure 3.4. Initial analysis and validation of the whole transcriptomic analysis revealed two genes with differential expression pattern and well-defined anti-microbial functions. Plots represent RNAseq reads of *Chil1* (A), *Iigp1* (B), and *Sqle* (C) during the entire time-course comparing genotypes and treatments. *Chil1* (D), *Iigp1* (E), and *Sqle* (F) gene expression from the same co-culture was validated through qRT-PCR. Bacterial loads (G) were measured 120 minutes post-gentamycin treatment of *H. pylori* co-cultures in WT and LysCre+ macrophages transfected with *Chil1*-targeted, *Iigp1*-targeted or *Sqle*-targeted siRNA or a scrambled sequence as a negative control. **P*-value<0.05 between genotypes, #*P*-value<0.05 within each genotype compared to time 0.

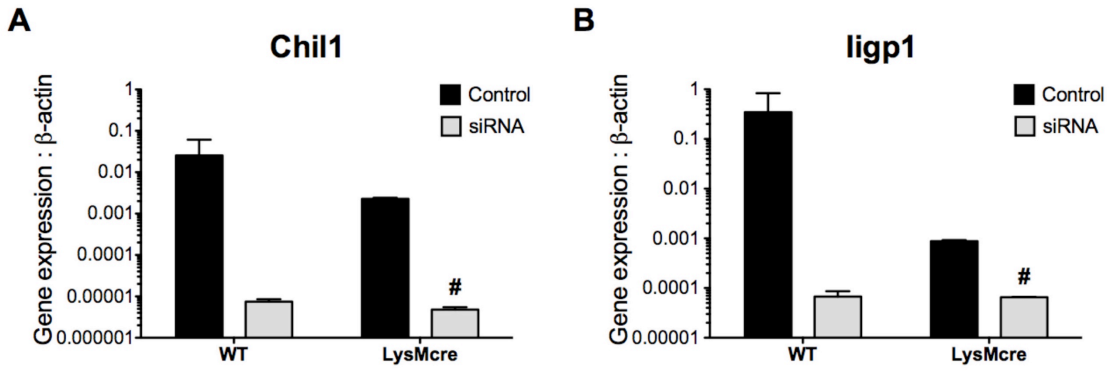

Figure 3.5. Validation of *Chil1* and *Iigp1* gene silencing by qRT-PCR. WT and LysCre+ macrophages were transfected with *Chil1*-targeted, *Iigp1*-targeted or negative scrambled siRNA prior to *H. pylori* challenge. Cells were harvested 120 minutes after *H. pylori* co-culture. *Chil1* (A) and *Iigp1* (B) gene expression was assessed. #*P*-value<0.05 within treatments.

3.5 Bioinformatics pattern-expression analysis identified five candidates as novel genes with putative regulatory functions.

Nod-like receptors (NLRs) are a subfamily of pattern recognition receptors that like PPARs, regulate innate immune responses and metabolism. Upon ligand binding, downstream activation of the NLR pathway results in the initiation and regulation of potent inflammatory mechanisms, including inflammasome formation and NF-κB activity [156, 157]. NLR and PPAR canonical immune pathways were selected to identify the opening set of expression patterns of interests. NLR and PPAR pathways encompass more than 200 genes and modulate the immune response through the activation of transcription and/or induction of metabolic changes in immune cells. Further, even the established role of the NLR pathway in innate immunity activation, and the PPAR pathway association to regulatory mechanisms, both canonical pathways in-conjunction contain a mixture of genes presenting a dominant pro-inflammatory or anti-inflammatory role, leading to a combined expression patterns in the dataset that allows the identification of regulatory patterns.

Initially, we performed an analysis based on the fold change of gene expression between genotypes for each gene of both NLR and PPAR pathways across the entire time course presented in the form of heat maps (Figure 3.6A, D) where blue represents genes downregulated in WT compared to LysCre+, while red represents upregulation of gene expression in WT related to LysCre+. We anticipated the presence of inverted patterns of regulatory and pro-inflammatory genes between both genotypes, where regulatory genes would be increased in WT compared to PPARγ-deficient, and pro-inflammatory genes overexpressed in PPARγ-deficient group. Indeed, the bioinformatics analysis revealed specific expression patterns in both signaling pathways that were clustered in groups. The NLR pathway includes two well-defined clusters based on the distinct genotype gene expression (Figure 3.6A). The orange box, at the top, contains genes upregulated in

LysCre+ macrophages, and the green box, at the bottom, contains a second class of genes with greater expression in the WT group. Interestingly, the LysCre+ upregulated genes have a delayed expression pattern, while, WT upregulated genes presented an earlier peak. The two NLR clusters are represented in the PPAR pathway, also depicted in orange and green boxes (Figure 3.6D). The analysis of genes associated with PPAR revealed an additional a third cluster, highlighted in purple, including a group of genes characterized by a dysregulated pattern. Particularly, those genes exhibited oscillating expression kinetics in each genotype among the entire time course. A plausible explanation is the existence of a strong PPARγ interaction with these genes. Therefore, the absence of the transcription factor in LysCre+ macrophages could alter the expression of the genes, due to direct activation, inhibition or even due to the upregulation of compensatory mechanisms, that result into a fluctuating expression pattern.

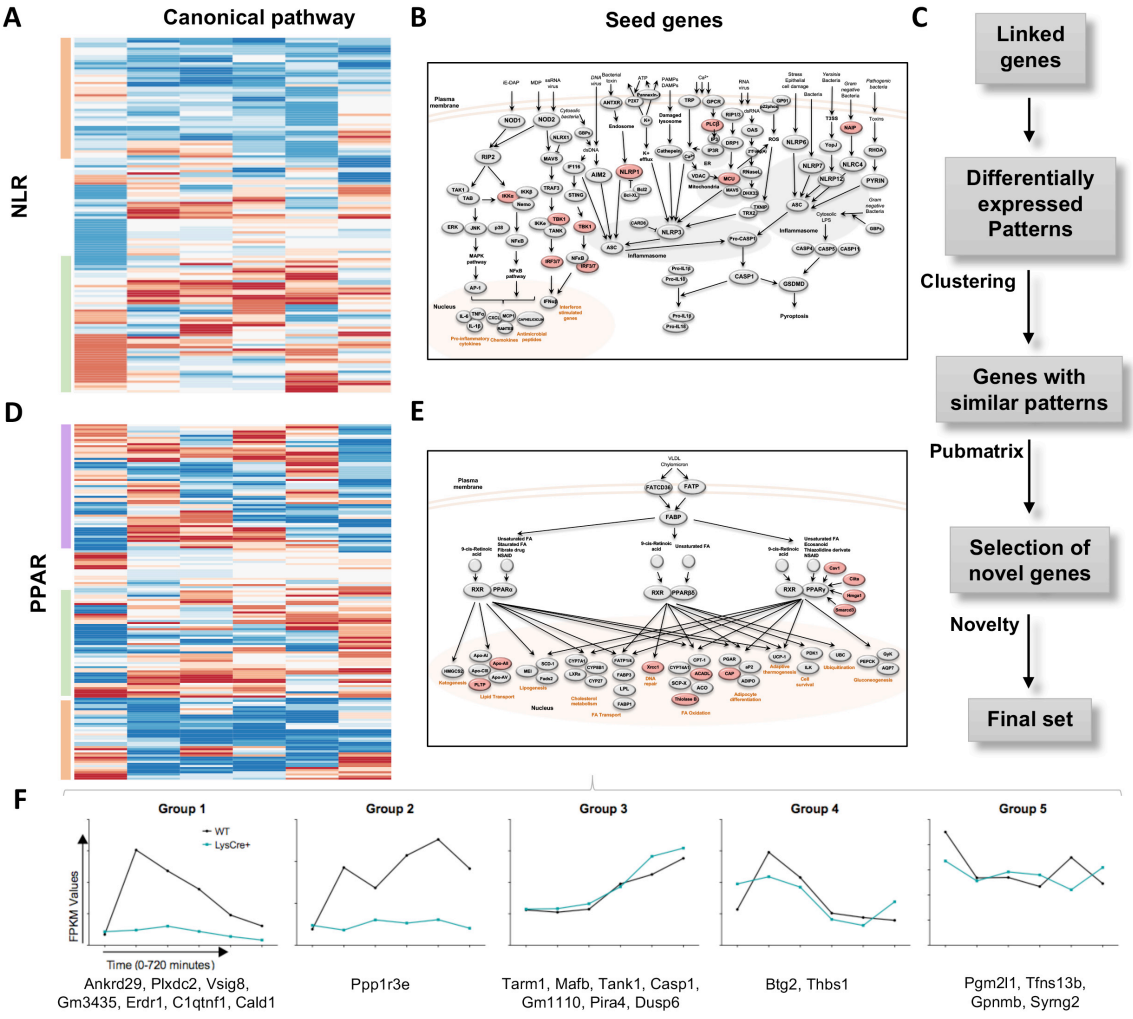

Figure 3.6. Bioinformatics pipeline utilized to analyze the RNAseq dataset and establish the differential expression patterns that lead to the identification of the potential regulatory candidates. Heatmaps represent the genotype fold-change expression from each gene in the NLR (A) and PPAR (D) pathways. Blue represents

inhibited expression in WT macrophages compared to the upregulation in LysCre+, while red indicates upregulation in WT compared to a suppressed expression in LysCre+ macrophages. NLR (B) and PPAR (E) pathways are represented in this diagram. In red are highlighted the top genes, based on the differential expression analysis represented in the heatmap, and selected as seed genes. Schematic representation of the steps performed during the bioinformatics analysis, after seed genes selection (C). The 21 genes included in the final set were classified in five groups based on their expression pattern (F).

Gene selection was narrowed to the green box cluster (i.e. genes upregulated in WT), to include genes with a positive response to *H. pylori* in WT macrophages that resembled the peak of bacterial loads reported in this genotype (Figure 3.1A). The choice included 7 NLR (Figure 3.6B) and 10 PPAR (Figure 3.6E) pathway genes highlighted in red, which were defined as seed genes. Based on the expression patterns of the seed genes, we built an initial dataset that comprised both these original genes and a group described as linked genes obtained from the global transcriptome dataset. Linked genes are characterized by their similar expression pattern and linked functions to the seed genes. Certain differentially expressed patterns were selected in this large initial dataset, and through 2 cycles of clustering within the entire global transcriptional dataset, we obtained a specific group of candidates exhibiting the defined expression kinetics. To further narrow down our search, we utilized the Pubmatrix [158] tool to select the most novel genes based on the following criteria: number of publications, cell location, and known function (Figure 3.6C). The 21 genes included in the final set were divided in 5 groups based on their expression pattern (Figure 3.7). Groups 1 and 2 exhibit a clear distinctive pattern within genotype, whereas no genotype differences were observed in groups 3, 4 and 5 (Figure 3.6F). Further, the first two groups exhibit a drastic upregulation post-*H. pylori* challenge in WT that was abrogated in PPARγ-deficient macrophages. Therefore, genes included in groups 1 and 2 displayed an expression pattern potentially associated with a regulatory function.

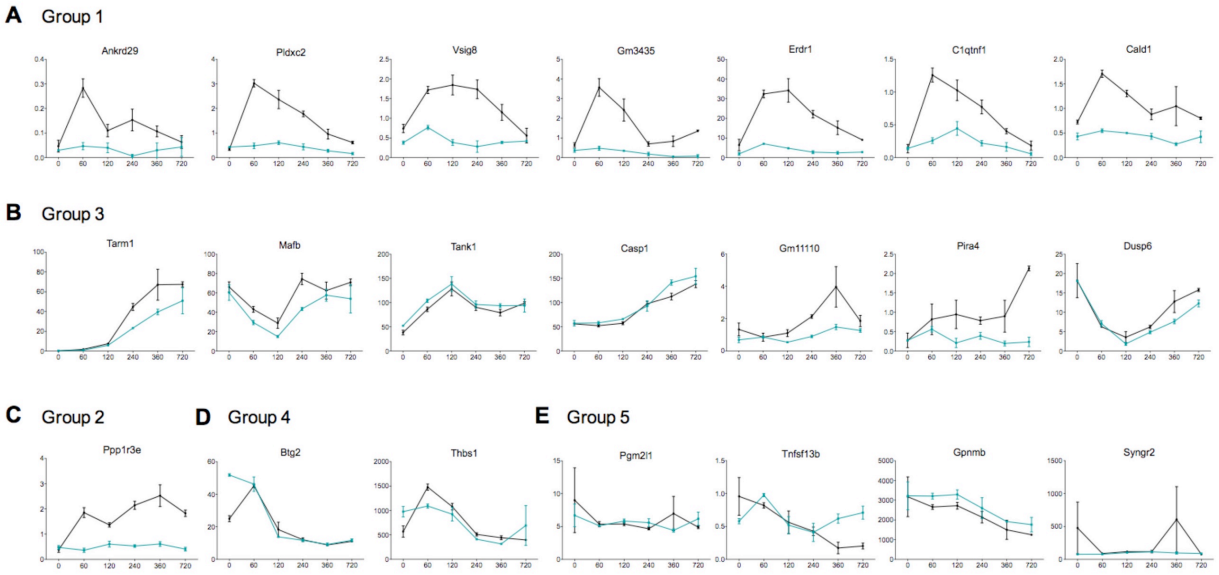

Figure 3.7. **Final set of genes from the bioinformatics analysis consists of 21 candidates classified in five groups based on the expression kinetics.** Plots represent the RNAseq reads at each time point of the experiment comparing WT and LysCre+ BMDM. Group 1 (A) includes *Ankrd29*, *Plxdc2*, *Vsig8*, *Gm3435*, *Erdr1*, *C1qtnf1*, and *Cald1*. Group 3 (B) consists of *Term1*, *Mafb*, *Tank1*, *Casp1*, *Gm11110*, *Pira4*, and *Dusp6*. Group 2 (C) only includes *Ppp1r3e*, whereas group 4 (D) includes *Btg2* and *Thbs1*. Group 5 (E) consists of *Pgm2l1*, *Tnfsf13b*, *Gpnmb,* and *Syngr2*.

Based on the pattern analysis, five genes from groups 1 and 2 of the final dataset were identified as potential new regulatory leads for further validation. Plexin domain containing 2 (*Plxdc2*, Figure 3.8A), V-set and immunoglobulin domain containing 8 (*Vsig8*, Figure 3.8C), Ankyrin repeat domain 29 (*Ankrd29*, Figure 3.8D) and C11 and tumor necrosis factor related protein 1 (*C1qtnf1*, Figure 3.8E) share an early expression peak in WT macrophages, abrogated in LysCre+, that coincides with the bacterial burden spike in the gentamycin protection assay. The kinetics of Protein phosphatase 1 regulatory subunit 3E (*Ppp1r3e*, Figure 3.8B) is slightly different since it was still upregulated in the last timepoint. However, in LysCre+ macrophages, the expression pattern of all 5 candidates was consistently downregulated and displayed as a flat line. Known properties of these five genes are described in Table 3.1. Publications linked to each of the genes reveal a large diversity of established functions; however, association with the immune system or the immune response was not reported for the majority of the genes. Interestingly, cellular location is also highly heterogeneous. Only two candidates, *Plxdc2* and *Vsig*, both plasma membrane receptors, have identified ligands. Thus, the limited number of publications together with the current established function of each gene support the novelty of their potential interaction with host immunoregulatory mechanisms.

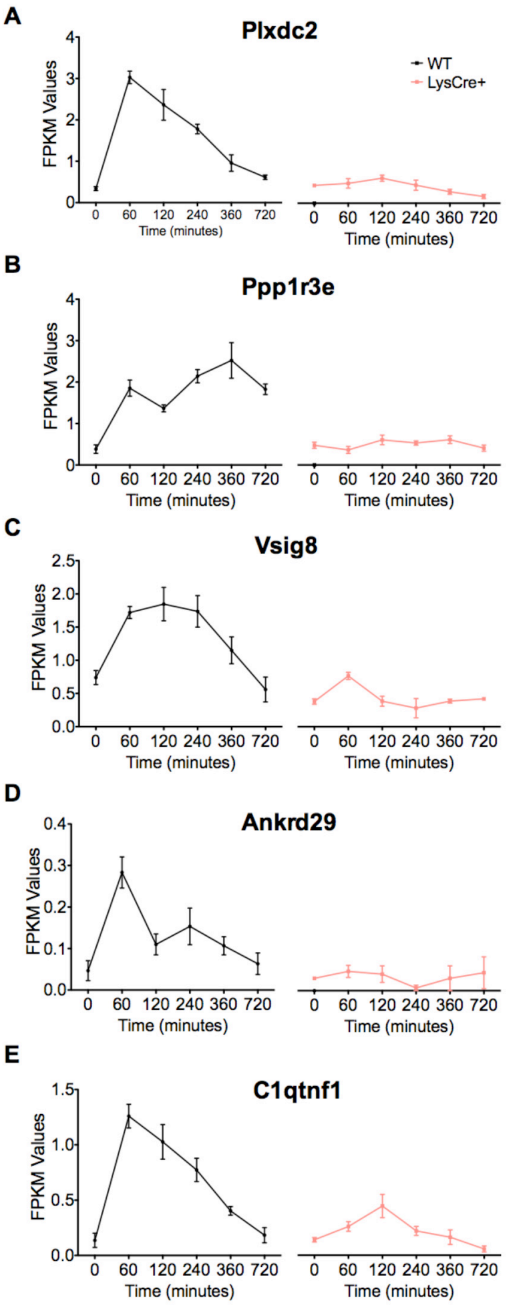

Figure 3.8. Expression kinetics of the five candidates selected from the bioinformatics analysis to undergo experimental validation. *Plxdc2* (A), *Ppp1r3e* (B), *Vsig8* (C), *Ankrd29* (D), and *C1qtnf1* (E) RNAseq reads in WT and LysCre+ macrophages expressed as FPKM values.

Gene Symbol	Gene Full Name	Number of publications	Cellular Location	Function/Role	Ligands
Plxdc2	Plexin domain containing 2	3 (22)	Plasma membrane	PEDF receptor (IL-10 expression). Nervous system development	PEDF
Ppp1r3e	Protein phosphatase 1, regulatory (inhibitor) subunit 3E	1	Cytoplasm	Glycogen metabolism (increases glycogen synthesis).	None
Vsig8	V-set and immunoglobulin domain containing 8	2	Plasma membrane	Expressed in hair shaft, follicle, nail unit, and oral cavity. VISTA receptor (potential target for cancer or infectious disease)	VISTA (not commercialized)
Ankrd29	Ankyrin repeat domain 29	1	Nucleus	Niemann-Pick Type C diseases (lipid transport)	None
C1qtnf1	C1q and tumor necrosis factor related protein 1	24 (27)	Cytoplasm, nucleus	Adipokyne related to glucose metabolism. Link to Pparγ (increased expression with rosiglitazone treatment).	None

Table 3.1. Gene information and properties of the 5 top selected candidates.

3.6 *In vivo* and *in vitro H. pylori*-induced upregulation of all five lead target candidates in WT mice is abrogated in pro-inflammatory macrophages from PPARγ null mice

To perform a validation of the five selected genes, we initially measured their expression, by qRT-PCR on samples from each time point of the gentamycin protection assay used in the global transcriptomics analysis. Similar to the observed pattern in the RNAseq dataset, *H. pylori* co-culture induces a significant early upregulation of all five candidates in WT macrophages starting at 60 minutes post co-culture. After 60 minutes, the expression of *Plxdc2* (Figure 3.9A), *Vsig8* (Figure 3.9E), *Ankrd29* (Figure 3.9G) and *C1qtnf1* (Figure 3.9I) begin to decline in cells obtained from WT mice to reach same levels as the LysCre+ BMDM at 360 or 720 minutes. Similar to the results from the RNAseq data, *Ppp1r3e* (Figure 3.9C) expression was maintained at high levels throughout the time course analysis. Cultures from LysCre+ BMDM exposed to *H. pylori* failed to upregulate expression of the selected genes. Therefore, there is an early upregulation of the five genes in WT BMDM that was suppressed in cells with a pro-inflammatory phenotype due to the loss of PPARγ.

To explore the dynamics of the selected genes *in vivo*, WT and LysCre+ mice were infected with *H. pylori.* In a previous study, we demonstrated that *H. pylori* infection *in vivo* induces strong regulatory mechanisms driven by IL-10-expressing myeloid cells starting at day 14 post infection and reaching maximum levels at day 28 post infection [104]. To evaluate whether induction of regulatory responses *in vivo* alters the kinetics of targeted genes, stomachs were collected at day 28 from infected and non-infected mice. Consistent with the *in vitro* findings, *H. pylori* infection upregulated the expression of *Plxdc2* (Figure 3.9B), *Ppp1r3e* (Figure 3.9D), *Vsig8* (Figure 3.9F), *Ankrd29* (Figure 3.9H) and *C1qtnf1* (Figure 3.9J) in WT gastric tissue. In contrast, minimal or no differences were reported upon *H. pylori* infection in PPARγ-deficient mice. Therefore, activation of regulatory responses after *H. pylori* challenge in WT mice correlate with an increased transcription of the five selected genes. However, *H. pylori* infection under pro-

inflammatory conditions, due to the lack of PPARγ, abrogates this effect on the selected lead regulatory genes.

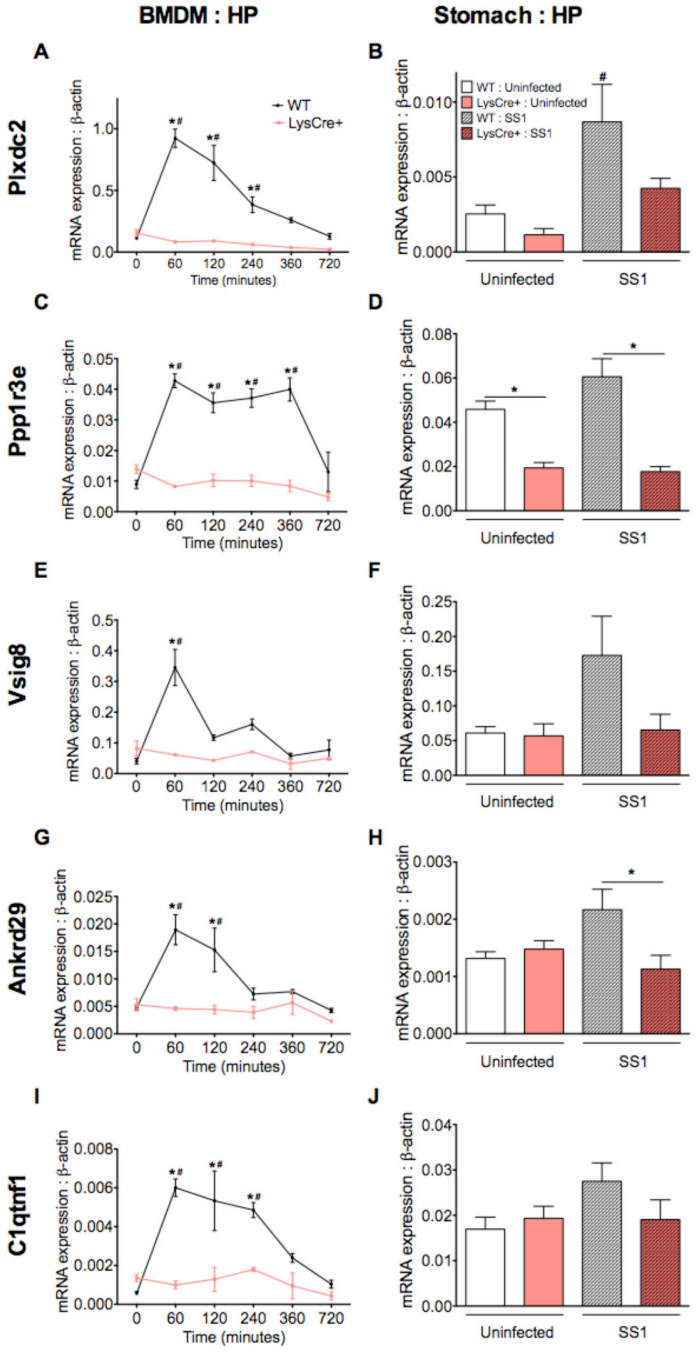

Figure 3.9. ***In vivo* and *in vitro* validation of the five selected candidates under *Helicobacter pylori*-induced regulatory conditions.** WT and LysCre+ BMDM were co-cultured *ex vivo* with *H. pylori* and harvested at several time-points ranging from 0 to 720 minutes. *Plxdc2* (A), *Ppp1r3e* (C), *Vsig8* (E), *Ankrd29* (G), and *C1qtnf1* (I) gene expression was measured by qRT-PCR. WT and LysCre+ mice were infected with *H.*

pylori SS1 strain. Non-infected mice were used as control. *Plxdc2* (B), *Ppp1r3e* (D), *Vsig8* (F), *Ankrd29* (H) and *C1qtnf1* (J) gene expression was measured by qRT-PCR. **P*-value<0.05 between genotypes, #*P*-value<0.05 within each genotype compared to time 0.

3.7 Activation of pro-inflammatory responses modulate the dynamics of the top lead regulatory target genes

To further characterize the potential regulatory functions of the selected genes, we sought to assess their behavior under inflammatory conditions in a controlled environment *in vitro*. Briefly, WT and LysCre+ BMDM were treated with 100ng/mL of LPS for 60, 120, 240, 360 and 720 minutes. LPS administration *in vitro* activates BMDM and modulates their cytokine profile. Particularly, LPS upregulates TNFα expression with a significant increment in LysCre+ macrophages (Figure 3.10F). In contrast, the IL-10-induced peak reported in WT macrophages is abrogated by the lack of PPARγ (Figure 3.10H). Additionally, LPS treatment suppressed PPARγ expression starting at 60 minutes post challenge (Figure 3.10G). The results show a slight decrease in *Plxdc2* (Figure 3.10A), *Vsig8* (Figure 3.10C) and *C1qtnf1* (Figure 3.10E) expression after LPS treatment plus a significant downregulation of *Ppp1e3r* starting at 120-minute post stimulation (Figure 3.10B) in WT compared to PPARγ-deficient macrophages. However, no differences were reported for *Ankrd29* (Figure 3.10D). As opposed to the dramatic modulation of the kinetics reported under a regulatory microenvironment *in vitro,* the effect observed upon LPS stimulation was limited and gene-specific.

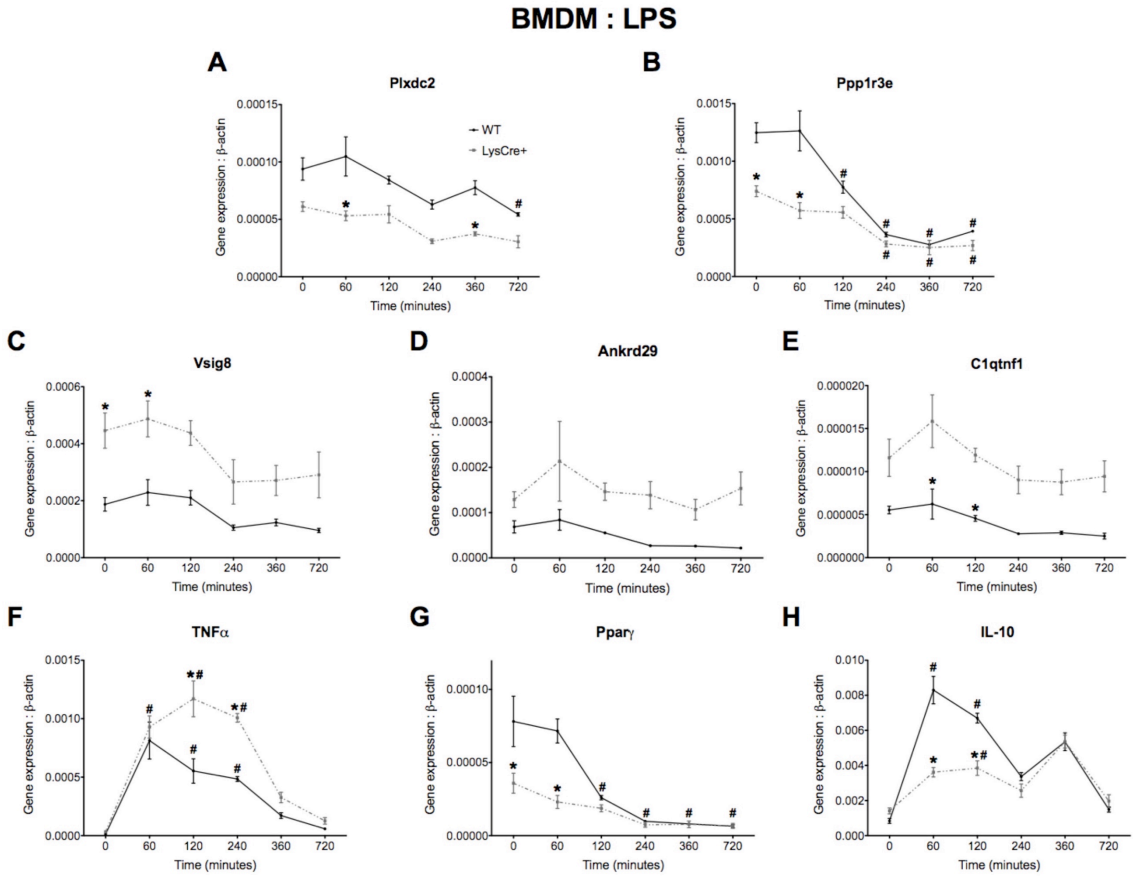

Figure 3.10. ***In vitro*** **validation of the five selected candidates under pro-inflammatory conditions.** WT and LysCre+ BMDM were stimulated with 100 ng/ml LPS and harvested at several time points ranging from 0 to 720 minutes. *Plxdc2* (A), *Ppp1r3e* (B), *Vsig8* (C), *Ankrd29* (D), *C1qtnf1* (E), *TNFα* (F), *Pparγ* (G), and *IL-10* (H) gene expression was measured through qRT-PCR. **P*-value<0.05 between genotypes, #*P*-value<0.05 within each genotype compared to time 0.

3.8 Plxdc2 silencing prevents *H. pylori*-induced regulatory phenotype in macrophages and reduces bacterial burden

Once initial screening and validation of the five lead candidates was completed, *Plxdc2* was chosen to further explore its regulatory activity. *Plxdc2* was selected based on the reported expression kinetics under regulatory and pro-inflammatory conditions, together with the fact that *Plxdc2* is a plasma receptor with a known ligand. WT and LysCre+ BMDM were transfected with 20 nM of *Plxdc2* targeted or scrambled siRNA as a negative control using Lipofectamine reagent. BMDM were subjected to the gentamycin protection assay. Cells were harvested at 0, 60, 120, 240 and 360 minutes post-challenge for gene expression analysis, and at 120 minutes for assessment of bacterial loads. Gene silencing resulted in 70% efficiency in WT macrophages, reducing *Plxdc2* expression in this group down to the levels observed in PPARγ-deficient BMDM (Figure 3.11A). At 2 hours post co-culture, *Plxdc2* silencing resulted in a 3-fold reduction of *H. pylori* burden in WT macrophages (Figure 3.11D). Additionally, a lower number of *H. pylori* colonies was isolated from both PPARγ-deficient groups in comparison to the WT. However, within LysCre+ macrophages, no differences in bacterial burden were observed after *Plxdc2* suppression via gene silencing. To assess whether the reduced bacterial replication reported in *Plxdc2*-silenced WT macrophages was due to a potential *Plxdc2* modulation of the macrophage function, we assessed the expression of Arginase 1 (Arg1) and Resistin like alpha (Retnla or fizz1) genes, associated with tissue repair and anti-inflammatory functions in these cells. Both, *Arg1* (Figure 3.11B) and *Retnla* (Figure 3.11C) reported an early response to *H. pylori,* synchronized with the *Plxdc2* expression peak at 60 minutes post-infection in WT Plxdc2-expressing macrophages. However, *Plxdc2* silencing prevented the upregulation of *Arg1* and *Retnla1* after *H. pylori* challenge, leading to a complete abrogation of the 60-minute peak. Similar to the results from bacterial loads, no differences were detected in PPARγ-deficient BMDM irrespective of the state of *Plxdc2* silencing. Indeed, in both LysCre+ groups *Arg1* and *Retnla* exhibited a constant flat expression, also previously observed in all 5 selected candidates (Figure 3.9). Therefore, *Plxdc2* silencing abrogated *H. pylori*-induced regulatory responses in macrophages, resulting into limited bacterial persistence and replication in WT BMDM.

To further validate the ability of *Plxdc2* to modulate the macrophage phenotype towards a regulatory environment, the *Plxdc2* molecular pathway was activated through the administration of pigment epithelium-derived factor (PEDF), a known Plxdc2 ligand. Interestingly, PEDF treatment slightly increased *Arg1* (Figure 3.11E) and *Retnla* (Figure 3.11F) gene expression in WT and LysCre+ macrophages compared to their respective

untreated controls. Indeed, the significant downregulation due to the loss of PPARγ in the untreated group was abrogated after PEDF treatment, exhibiting no differences in comparison to the WT control. Additionally, *Arg1* and *Retnla* expression levels were inhibited in all 4 groups transfected with *Plxdc2* siRNA, reporting no PEDF effects. Therefore, PLXDC2 activation through PEDF treatment increased the expression of anti-inflammatory genes in macrophages, and rescued the inflammatory phenotype observed in PPARγ-deficient cells.

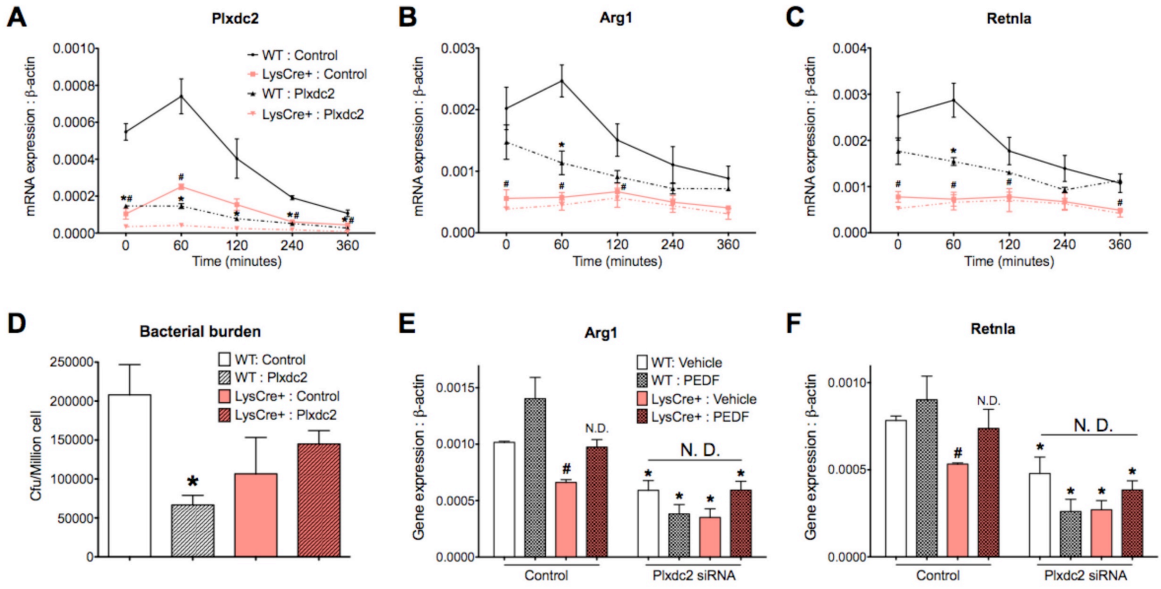

Figure 3.11. **Gene silencing and ligand-induced activation studies to confirm the regulatory role of *Plxdc2.*** WT and LysCre+ BMDM were transfected with *Plxdc2* or scrambled siRNA as a negative control prior to *H. pylori* co-culture *in vitro*. Cells were harvested at 0, 60, 120, 240 and 360 minutes post *H. pylori* challenge and *Plxdc2* (A), *Arg1* (B), and *Retna1* (C) gene expression was measured. Bacterial burden (D) was assessed 120 minutes post co-culture. WT and LysCre+ BMDM transfected with *Plxdc2* or scrambled siRNA as a negative control were treated with the Plxdc2 ligand PEDF at 10nM prior to *H. pylori* challenge. 120 minutes post co-culture cells were harvested and Arg1 (E) and Retna1 (F) gene expression was assessed.

3.9 Discussion and conclusions

We present a novel *ex vivo* co-culture system that leverages the regulatory responses induced by *H. pylori* in macrophages in combination with bioinformatics analyses to discover potential new regulatory genes with immunomodulatory properties based on expression kinetics in WT and PPARγ-deficient BMDM. This new platform was used to identify 5 genes, *Plxdc2*, *Ppp3e1r*, *Vsig8*, *Ankrd29* and *C1qtnf1* with potential regulatory functions. Induction of regulatory responses through *H. pylori* challenge *in vivo* and *in vitro,* confirmed the promising regulatory role of the selected genes. Indeed, the hypothesized regulatory pattern utilized to identify the novel genes, characterized by an

early upregulation in WT macrophages and suppression in PPARγ-deficient macrophages, coinciding with the early peak of bacterial burden, was observed in all 5 top lead candidates through *H. pylori* validation *in vitro*. Further, *H. pylori* infection *in vivo* resulted in increased gene expression of all 5 top candidates at day 28 post-infection in WT mice, coinciding with the previously identified greatest accumulation of regulatory macrophages in the gastric mucosa during this bacterial infection [104]. Therefore, functionally, the correlation between the expression of the 5 candidates and the induction of regulatory mechanisms during *H. pylori* infection, support the immunomodulatory role of the selected genes. Moreover, the validation of the co-culture system provides new insights into the application of bioinformatics screening methods for the discovery of novel molecular targets for treating inflammatory and autoimmune diseases.

H. pylori establishes life-long, chronic infections in the gastric mucosa characterized by the induction of mixed immune responses. In addition to the effector mechanisms dominated by Th1 and Th17 cells [23-28], *H. pylori* induces strong regulatory responses that suppress mucosal inflammation, contribute to tissue integrity maintenance and prevent effective bacterial clearance [29, 33, 34]. Historically, *H. pylori*-associated regulatory responses have been mainly attributed to dendritic cells by inhibition of effector T cells and promotion of regulatory T cells [30-32]. Recently, macrophages have been identified as an integral component in the generation of a regulatory gastric microenvironment during this bacterial infection [35, 104]. Applying next generation sequencing (NGS) and bioinformatics analysis, we demonstrated that in the tightly controlled environment of an *ex vivo* co-culture with BMDM, *H. pylori* challenge drastically influence macrophage gene expression profiles. The significant impact observed in macrophage transcriptomics upon bacterial challenge, resulted in the induction of regulatory genes in WT macrophages, that is inhibited by the loss of PPARγ and suppresses the effector mechanisms to promote bacterial persistence. Therefore, the synchronized *ex vivo* co-culture with macrophages, together with the utilization of NGS strategies, is a suitable approach to capture the full-spectrum of regulatory responses induced by *H. pylori* and to discover novel regulatory mechanisms with meaningful impact on the modulation of the immune response.

In addition to the combined NGS and bioinformatics analyses methods, in the current study, gene selection is based on the similarities between expression kinetics of candidate genes and known host genes with validated regulatory functions. We performed a bioinformatics pattern-based analysis utilizing genes with established regulatory functions to identify novel genes with similar characteristics. In our system, the comparison within macrophages with distinctive immunological steady states (WT versus PPARγ-deficient) was utilized to select the initial core of established genes and to validate the role of the new regulatory gene candidates. To identify the predicted regulatory patterns, we utilized the canonical immune pathways NLR and PPAR. The selection criteria were based on pathways with a dominant regulatory role or including both inflammatory and regulatory members, to allow the full-spectrum of expression kinetics and perform a suitable selection of expression patterns associated with immunomodulatory functions. PPARs are nuclear receptors that regulate lipid metabolism and exert potent immunomodulatory functions. Indeed, activation of

members in the PPAR pathway result in incremented beta-oxidation of lipid metabolism and suppression of the inflammatory response [159]. The NLR family is a main regulator of the initiation of innate immune responses in macrophages, and encompasses more than 20 members [157]. As expected, NLR pathway includes an important number of inflammation-driven genes involved in the formation of inflammasomes, such as NLRP1, NLRP3 and NLRC4 [160, 161] or associated with the activation of other inflammatory mechanisms, mainly the NF-κB or MAPK pathways, such as NOD1 and NOD2 [157]. Additionally, several genes of the NLR family hold immunoregulatory functions linked to suppression of inflammation, including NLRP10 and NLRX1 [162-165]. Therefore, NLRs constitute a highly heterogeneous and diverse family of pattern recognition receptors (PPR). Other pathways essential for the activation and maintenance of the immune response in macrophages were also considered, including the Toll-like receptors (TLR), the nuclear factor kB (NF-kB) and pathways associated to the production of reactive oxygen species (ROS). However, the strong association of such pathways with the initiation and expansion of inflammatory mechanisms with limited pro-regulatory functions in macrophages [166, 167], limited their potential value in our regulatory gene discovery pipeline. Therefore, to perform an initial screening analysis for regulatory genes, NLR and PPAR pathways were ideal candidates.

The hypothesized immunomodulatory role of the selected regulatory gene candidates was further investigated under the induction of inflammatory mechanisms. LPS stimulation *in vitro* resulted in minor alteration of the expression kinetics in both genotypes. While we observe a trend in *Plxdc2* and *Ppp1r3e* gene expression that supports the hypothesized suppression of immunoregulatory gene levels in pro-inflammatory activated macrophages, PPARγ-deficient cells exhibited slightly greater expression of *Vsig8, Ankrd29* and *C1qtnf1*. LPS stimulation induces strong pro-inflammatory cytokine production, including TNF, IL-6, and IL1β, and the generation of classically-activated macrophages [168]. Therefore, the minor LPS effect on the selected candidates suggest that they might not be associated with the induction or maintenance of pro-inflammatory responses. In conclusion, the observed results in both *in vivo* and *in vitro* experiments under the induction of regulatory and pro-inflammatory mechanisms, suggest that *Plxdc2* and *Ppp1r3e* are the two genes with greater immunomodulatory potential, and the most suitable candidates for further validation and study.

Plxdc2 encodes a 350-amino acid plasma membrane protein known to participate in cell proliferation and differentiation control during the development of the nervous system [169, 170]. Our results suggest that *Plxdc2* silencing alters the phenotype of WT macrophages *in vitro* causing a shift towards a more pro-inflammatory state, leading to a significant decrease of bacterial burden and downregulated expression of tissue healing and anti-inflammatory associated genes in comparison to the control group. *Plxdc2*, together with its homologue gene *Plxdc1*, has been identified as one of the membrane receptors of pigment epithelial-derived factor (PEDF) [171], a strong, endogenous anti-angiogenesis factor [172]. Interestingly, PEDF treatment modulates macrophage activation in Raw 264.6 cells through the increase of IL-10 production with potential association with PPARγ activation [173, 174]. Cheng et al., reported that PEDF-induced IL-10 production in Raw 264.7 macrophages is dependent on both Plxdc1 and Plxdc2

[171]. Our data suggests that *Plxdc2* can induce immunological changes independently of the presence of PEDF in addition to in response to PEDF stimulation. The changes observed in the dynamics of *Plxdc2* over the time course and after silencing of the gene suggest additional yet to be discovered signaling mechanisms with impact on anti-bacterial and overall immune responses. As a cell surface receptor, Plxdc2 is a promising therapeutic target for autoimmune diseases.

The established regulatory effect of PEDF in macrophages, together with the ability to perform ligand-induced activation in addition to loss of function analysis, triggered the selection of *Plxdc2* for further validation in this initial study. However, the kinetics of *Ppp1r3e* in the validation studies, support the regulatory role of this gene and encourage its further investigation. *Ppp1r3e* gene encodes a glycogen-targeting subunit of the protein serine/threonine phosphatase of type 1 (PP1), a phosphatase protein involved in the regulation of several cell functions, including gene expression, metabolism and cell death [175, 176]. Metabolism is an essential component of the immune response [164]. Activated cells, including macrophages and dendritic cells, undergo metabolic reprogramming, in which glucose metabolism is increased while oxygen consumption is suppressed, to produce energy at fast speed and initiate the mechanisms required for their activation [143, 144]. Glycogen-driving subunits, such as *Ppp1r3e*, increase glycogen production promoting glycogen synthase activity [175]. Moreover, *Ppp1r3e* expression levels are regulated by insulin, and are subjected to a significant suppression in diabetic liver [176]. Interestingly, glycogen also plays a role in the immunometabolic interplay of immune cells [177]. Dendritic cells have pools of stored glycogen that is catabolized during the metabolic shift to increase glucose availability and supply the energy needs during these initial steps of the immune response [177]. Moreover, deficiencies in glycogen metabolism alter the proper activation of dendritic cells [177]. Others have demonstrated that in activated macrophages with overexpression of the glucose transporter GLUT1 and increased glucose consumption, glycogen synthesis is upregulated [178]. Therefore, through the modulation of glycogen metabolism, *Ppp1r3e* might modulate the activation of immune cells, and as a consequence, exert important functions associated with the shape of the immune response.

This study has identified five candidate therapeutic targets with promising host regulatory and immunometabolic roles. Validation studies supported *Plxdc2* and *Ppp1r3e* as two genes with strong regulatory functions and great potential to modulate immune and host responses. Our screening platform can provide new insights in the identification of novel therapeutic targets for the modulation of the immune response that can drive the next wave of first-in-class therapeutics for widespread and debilitating autoimmune diseases.

3.10 Materials and methods

Animal housing and ethic statement

6 to 10 week old C57Bl/6J wild-type (WT) and PPARγ fl/fl;LysCre+ (LysCre+) mice were used for these studies. LysCre+ were generated by breeding of PPARγ fl/fl into Lys-Cre mice, to produce animals lacking PPARγ in myeloid cells. All mice were bred and housed in the same colony at Virginia Tech ventilated racks and under a 12-hour light

cycle. All experimental procedures performed were approved by the Institutional Animal Care and Use Committee (IACUC) and met or exceeded requirements of the Public Health Service/National Institutes of Health and Animal Welfare Act.

Bone marrow-derived macrophages (BMDM) isolation and culture

Bone marrow-derived macrophages (BMDM) were isolated as previously described [179]. Briefly, the femur and tibia were excised, cleaned from the attached muscle and sterilized with 70% ethanol. The distal ends of the bones were cut and the bone marrow (BM) flushed out with cold cRPMI_M, containing RPMI 1640 (Corning Incorporated, Corning, NY), 10% Fetal Bovine Serum (Corning Incorporated, Corning, NY), 2.5% Hepes (Corning Incorporated, Corning, NY), 1% Sodium pyruvate (Corning Incorporated, Corning, NY), 1% L-glutamine (Corning Incorporated, Corning, NY), 1% Penicilin/Streptamicin (Corning Incorporated, Corning, NY) and 50uM β-mercaptoethanol (Sigma Aldrich, St. Louis, MO). Osmotic lysis was used to remove red blood cells. Samples were adjusted to $7.5x10^5$ cells/mL with cold cRPMI_M supplemented with 25 ng/mL of recombinant mouse colony-stimulating factor (m-csf, Peprotech, Rocky Hill, NJ) and cultured at 37ºC, 5% CO_2 and 95% humidity to allow their differentiation. At day 3 fresh m-csf-supplemented media was added. On day 6, plates were washed to remove non-adherent cells and BMDM were harvested. Cells were re-suspended in cRPMI_M and seeded in triplicate in 12-well plates ($5x10^5$ cells per well). Cells were left to adhere overnight at 37ºC, 5% CO_2 and 95% humidity.

H. pylori culture and preparation of the inoculum

This study was performed using *H. pylori* SS1 strain. *H. pylori* was cultured at 37ºC under microaerophilic conditions in Difco Columbia blood agar (BD Biosciences, San Jose, CA) plates supplemented with 7% of Horse laked blood (Lampire Biological Laboratories, Pipersville, PA) and *H. pylori* selective supplement (5mg of Vancomycin, 2.5mg of Trimethoprim, 2.5mg of Cefsulodin and 2.5mg of Amphotericin B, Oxoid, Altrincham, England).

For *in vivo* inoculum preparation, *H. pylori* was harvested at room temperature sterile 1X PBS and adjusted to $2.5x10^8$ colony forming units (cfu) per mL. To obtain the desired concentration, *H. pylori* was adjusted to an optimal density (OD) of 1.2 at a 600-nm wavelength. The association of OD and cfu/mL was based on a previous growth curve that correlated OD with *H. pylori* colony counts. For *in vitro* inoculum preparation, *H. pylori* was harvested in antibiotic-free cRPMI and adjusted to $1x10^8$ cfu/mL as described above.

Gentamycin protection assay

BMDM cells were washed with 1X PBS and fresh antibiotic-free cRPMI was added to the plates. Cells were infected with *H. pylori* SS1 at a MOI 10 and synchronized by quick spin to ensure immediate contact. After a 15-minute incubation, non-internalized bacteria were killed by thoroughly washing the cells with PBS/5% FBS containing 100ng/ml Gentamycin (Fisher Scientific, Pittsburg, PA). Cells for time-point 0 were washed with PBS and immediately collected for downstream assays. The cells allocated for the remaining time points (30 min to 12 hours) were covered with culture media until

collection for bacterial re-isolation or assessment of differential gene expression by qRT-PCR and whole transcriptome analyses.

Bacterial Re-isolation from BMDM

BMDM cells were washed 3 times with sterile 1X PBS. 200uL of Brucella broth (BD Biosciences, San Jose, CA) were added to the well and cells were detached using a cell scraper. Cell suspensions were sonicated 5 seconds to release intracellular bacteria. Serial 10-fold dilutions of the original homogenate were plated into the *H. pylori* plates described above. After for 4 days of culture at 37ºC under microaerophilic conditions, colonies were counted.

Gene Expression

BMDM cells were collected in ice-cold RLT (supplemented with β-mercaptoethanol) and stored at -80ºC until RNA isolation was performed. Following mouse euthanasia, stomachs were excised from the animal and longitudinally opened. Collected tissues were rinsed twice in 1X PBS and stored in 350uL of RNAlater (Fisher Scientific, Pittsburg, PA) at -80ºC. Total RNA was extracted from BMDM and stomach using the RNeasy mini kit (Qiagen, Hilden, Germany) following manufacturer's instructions. RNA concentrations were quantified with a nandrop (Invitrogen, Carlsbad, CA) at 260nm. iScript cDNA synthesis kit (Bio-Rad, Hercules, CA) was utilized to generate cDNA from RNA samples. Primer-specific amplicons were produced by PCR using Taq Polymerase (Promega, Madison, WI), followed by a purification step using the Mini-Elute PCR purification kit (Qiagen, Hilden, Germany). Standard curves were generated by a series of dilutions from known concentration of the purified primer-specific amplicon, starting at $1x10^6$pg. Total gene expression levels were assessed through a quantitative real-time PCR (qRT-PCR) using a CFX96 Thermal Cycler (Bio-Rad, Hercules, CA) and SYBR Green Supermix (Bio-Rad, Hercules, CA). βeta-actin expression was utilized to normalize the expression levels of targeted genes. Primer sequences are included in Table 3.2.

Gene	Forward Primer	Reverse Primer
β-Actin	CCGAGGCATTGCTGACAGG	TGGAAGGTCGACAGTGAGGC
Chil1	GCACCCACATCATCTACA	GACTCGTCATTCCACTCC
Iigp1	ACCTGCAAATTCTGTCTCA	TGTATGTCCATGTACCATATAAAC
Sqle	CGAAGTATACAGCCACATT	CTTCTTCATTCAGCCAACT
Plxdc2	TCTCCAGAGTCCAAAGGGTTCA	TTGTGATCCGTGTCCTCCTCTATC
Ppp1r3e	AAACAGCAGGTGTGCGTAAGT	AGGCTCCTCAGTCCATAAAGGT
Vsig8	TCTCCTACAAGTGGGCCAAGAT	GGTTGATGGTGCTGTGGAATGA
Ankrd29	GCAGTGCTCAGTGGGAATGTT	GGAGCTCATTGGCCTTGTTTCT
C1qtnf1	CACCATCCTGAAAGGCGAGAAAG	CCCTGGGACCTGTAGAACCTATTT
Tnfα	CCACCACGCTCTTCTGTCTACT	ACTGATGAGAGGGAGGCCATTT
Pparγ	CAG GCT TGC TGA ACG TGA AG	GGA GCA CCT TGG CGA ACA
Il-10	GGGTTGCCAAGCCTTATCGGAAAT	TCTTCAGCTTCTCACCCAGGGAAT
Ifnγ	ATTAGCCAAGACTGTGAT	AGGTACAAGCTACAATCT
Arg1	GCCGATTCACCTGAGCTTTGAT	TCTGTAAGATAGGCCTCCCAGAAC
Retnla	GCTCTGTGGGACTCTCTCTTCTT	TGGCTGTGAGGGAAAGGACATA

Table 3.2. **qRT-PCR primers utilized in this study.**

Global Transcriptome analysis

RNA isolated from WT and LysCre+ BMDM collected at time-points 0, 30, 60, 120, 240, 360 and 720 minutes post-infection was submitted for whole transcriptome gene expression analysis using Illumina Hiseq (Biocomplexity Institute of Virginia Tech Core Lab Facilities). Once fastq files containing 100bp-long pair-end reads were received, poor quality reads (>40% of bases with PHRED score <10; percentage of N greater than 5%; and polyA reads) were excluded. Through the utilization of Bowtie [180] (version: 1.0.0) with parameters set to '-l 25 -I 1 -X 1000 -a -m 200', the remaining reads we mapped to RefSeq (mm10 from http://genome.ucsc.edu/). To calculate gene expression levels we used RSEM [181], a program based on expectation-maximization algorithm. FPKM [182] (fragments per kilobase per million sequenced reads) was used as the measurement of expression level. Data was submitted to NCBI's GEO database (Accession Number GSE67270).

Bioinformatics analysis

As described in Figure 3.6C, to analyze the RNAseq data, an initial dataset of genes linked to the selected NLR and PPAR candidates was generated. Briefly, the Genome-scale Integrated Analysis of gene Networks in Tissues (GIANT) and Gene Expression Omnibus (GEO) databases were used and integrated in the Ingenuity Pathway Analysis (IPA) software to build the initial group of genes. Hierarchical based clustering was employed to obtain differentially expressed patterns within the combined initial NLR and PPAR genes and the linked dataset generated. The *hclust* method with Ward's minimum variance method and Manhattan distance metric in R were used to cluster the data. Another clustering cycle was performed in order to obtain a larger set of genes with similar patterns of interest. The generated dataset was enhanced for novelty through an abstract searching using the Pubmatrix tool, and a final dataset of genes was obtained.

Gene silencing and BMDM treatments

For gene silencing studies, WT and LysCre+ BMDM were transfected with 20nM siRNA (27mer Dicer-substrate siRNA, DsiRNA, for the targeted gene or scrambled sequence as a negative control, Integrated Device Technology, San Jose, CA) using Lipofectamine RNAiMax Transfection Reagent (Thermo Fisher Scientific, Waltham, WA) 48 hours before the infection. Media was replaced 6 hours post-transfection. Cells were exposed to *H. pylori* following the gentamycin protection assay described above. Gene knock-down was validated by qRT-PCR.

For the induction of a pro-inflammatory environment during gentamycin protection assay, BMDM were pre-treated with LPS (100ng/mL, Sigma Aldrich, St. Louis, MO) and rIFNγ (100ng/mL) overnight. For the LPS validation, BMDM were treated with LPS (100ng/mL) for 1, 2, 4, 6 and 12 hours. For Plxdc2 activation, 48 hours post siRNA transfection, WT and LysCre+ BMDM were treated with PEDF (10nM) for 24hours. Then, BMDM were subjected to gentamycin protection assay.

In vivo H. pylori infection

8 to 10-week-old WT and LysCre+ mice were transferred to an ABSL2 room in the same colony at Virginia Tech in a ventilated rack and under a 12-hour light cycle. On days 0 and 2 of the project, mice were administered 200uL of freshly prepared $5x10^7$ cfu of *H. pylori* SS1 in 1X PBS through orogastric gavage. These studies also included a non-infected group administered with 200uL of 1X PBS without bacteria. Mice were monitored for signs of disease weekly and stomach samples were collected at 28 days post infection.

Statistics

Data are expressed as mean values and standard error of the mean represented in error bars. To calculate significance of the RNAseq dataset from the global transcriptome analysis, all genes with median expression level in all samples greater than 0 were included in a 3-way (genotype, treatment and time) ANOVA analysis. Normal quantile transformation (qqnorm from R [183]) was used to normalize the FPKM to fit the normality assumption of ANOVA (tested with Kolmogorov-Smirnov test). The 3-way ANOVA analysis was carried in R [183], FDR [184] and Bonferroni were used to calculate the adjusted *P*-values. To determine significance of the standard data, Analysis of variance (ANOVA) was performed using the general linear model procedure in SAS (SAS Institute). Significance was considered at $p \leq 0.05$ and significant differences were identified with an asterisk (genotype) or pound sign (infection or treatment).

Chapter 4

Identification of IL-1ß as Key Contributor in *Clostridium difficile*-associated Diseases and Neutrophil Recruitment

Nuria Tubau Juni, Raquel Hontecillas, Meghna Verma, and Josep Bassaganya-Riera.

4.1 Summary

Clostridium difficile is an opportunistic bacterium that infects the gastrointestinal tract upon disruption of microbiome. *Clostridium difficile* infection (CDI) is a major healthcare concern with almost half a million cases yearly in the US. *C. difficile*-associated diseases (CDAD) are currently treated with antibiotic administration, however, the high recurrence rate reported point out the need of new therapeutic strategies. CDI induces strong inflammatory processes that eventually contribute in CDAD pathogenesis. Development of host-centered therapeutics to control the initiated effector mechanisms is a promising novel therapeutic option for CDI. In this study, we analyzed the dynamics of several innate immune responses during CDI, and identified IL-1β a key inducer of inflammatory responses. Neutralization of IL-1β dramatically transform the disease outcome. Indeed, IL-1β blockage significantly improves disease severity, through reduced weight loss, symptomatology score and increased rate of survival. The beneficial effects resulted from IL-1β neutralization correlate with a 3-fold decrease in neutrophils influx, suggesting the critical role of neutrophil recruitment in CDI inflammatory mechanisms. Therefore, this study brings new insights in the complex host-pathogen interactions during *C. difficile* infection and opens new horizons for development of potential new therapeutics for CDAD.

4.2 Introduction

Clostridium difficile is a gram-positive, spore-forming, obligate anaerobic bacteria that colonizes the gastrointestinal tract. *C. difficile* infection (CDI) is considered the main cause of nosocomial antibiotic-associated diarrhea, and is frequently associated to antibiotic driven disruption of commensal bacteria in the gut [37, 38]. *C. difficile*-associated diseases (CDAD) range from asymptomatic colonization or mild diarrhea to life-threatening conditions, including pseudomembranous colitis, toxin megacolon or even death [39]. CDI is the most frequent hospital-associated infection, with an estimate of over 450,000 cases and 29,000 deaths annually in the United states [40]. Indeed, only in the US, the estimated annual healthcare expenses associated to CDI range between $1.9 and $7 billion [185]. CDI present increasing incidence and severity associated to the emergence of hyper-virulent multi-resistant strains, i.e. BI/027/NAPI [186-189]. Controversially, the standard treatment for CDAD is bacterial removal through antibiotic administration, vancomycin or metronidazole, based on the disease severity [190]. Antibiotic treatment not only targets the pathogenic bacteria, it also prevents the re-growth of the disrupted commensal microbiome that allowed the initial *C. difficile* colonization.

The recurrence rate in CDI is approximate 20-25% [48, 49]. Additionally, it is frequent to present multiple recurring episodes [191]. The average recurring time is calculated to be shorter than three weeks [50], suggesting that recurrence episodes are cause by the regrowth of remaining spores from the initial infection due to absence of competitive commensal bacteria eliminated during the antibiotic administration. Recently, alternative treatment strategies, including fecal microbiome transplantation (FMT), have been successfully utilized for the treatment of CDI recurrences with higher efficacy than antibiotic treatment [56, 57]. However, several concerns have raised regarding the safety of FMT [58-60]. The development of host-centered treatment approaches to treat CDI is an encouraging, safer alternative to FMT. Indeed, in an *in silico* platform developed to predict clinical efficacy of CDI treatment, both activation of the immunregolatory target LANCL2, and FMT would outperform the current standard regimen of antibiotics [192]. Moreover, LANCL2 activation *in vivo* resulted in an overall decrease of disease severity, and suppressed infiltration of pro-inflammatory immune subsets in lamina propria while observing an upregulation of the regulatory responses [192].

The two main virulent factors of *C. difficile* are toxin A (TdcA) and B (TcdB) [193, 194]. TcdA is an enterotoxin that stimulates fluid accumulation, tissue damage and intestinal inflammation [195, 196]. But, both TcdA and TcdB are cytotoxic, causing cell rounding at very low concentrations [194, 197]. A potential mechanism of injury in the intestinal epithelial layer is the entrance of TcdA and TcdB into epithelial cells through receptor-mediated endocytosis. Once in the cytoplasm, the N-terminal glycosyltransferase domain (GTD) of Tcda and TcdB inhibits several small GTPases from the Rho family through glucosylation [198-200]. GTPase inactivation results in: 1) disaggregation of actin filaments and disruption of the cytoskeleton, leading to cell rounding [201, 202], and 2) cytotoxic responses that result in induction of apoptosis and necrosis, accompanied with production of reactive oxygen species [199, 200, 203-206]. These factors ultimately lead to a pronounced host inflammatory response characterized by infiltration and recruitment of circulating immune cells in the gut. Following epithelial barrier disruption and infiltration to the intestinal lamina propria, TcdA and TcdB induce innate inflammatory responses by activating NF-κB and MAP kinase pathways [207-210]. As a result, monocytes, macrophages and dendritic cells (DC) become activated and several pro-inflammatory cytokines, including interleukin 1β (IL-1β), tumor necrosis factor α (TNF α), interleukin 6 (IL-6) and interleukin 8 (IL-8), are released [211, 212]. These antigen presenting cells (APCs) will then activate T cells, inducing the adaptive immune response. The initial phase of *C. difficile* infection is characterized by induction of strong inflammatory responses mostly dominant by Th17 cells and neutrophils. Indeed, upon generation of pro-inflammatory environment, from both inflamed epithelial cells or activated macrophages and dendritic cells, recruited neutrophils secrete cytotoxic granules to clear *C. difficile* infection and contain pathogenic levels, however, the released molecules will also target commensal bacteria as well as damage the epithelium barrier [213]. Additionally, neutrophil infiltration has been reported as key characteristic of CDI in both human [214] and mouse models [215-217]. Upon completion of this inflammatory phase, recovery period is initiated, when pro-inflammatory responses are suppressed and regulatory responses, mainly driven by regulatory CD4+ T cells, are

upregulated [218]. Failure in generating the regulatory response results in severe symptomatology and poor prognosis [218].

In this study, we identified IL-1ß as a key cytokine in the induction of inflammatory responses during CDI and a main contributor to disease severity. We initially performed a flow cytometry and cytokine profile analysis to evaluate the dynamics of several immune cell populations during CDI in correlation of expression of both inflammatory and regulatory markers in colonic tissue. The obtained results revealed dynamic changes in all innate immune cell population and expressed cytokines in accordance with the stage of CDI infection. Additionally, blockage of IL-1ß significantly improved the disease outcome, reporting dramatic changes in weight loss, disease activity index and rate of survival, while correlating with a suppressed influx of neutrophils in colonic lamina propria. Interestingly, no differences were reported in bacterial colonization. This study supports the paradigm that bacterial removal is a dispensable factor in the treatment of CDI. Furthermore, it supports the notion of investigating and elucidating new mechanisms induced during host-pathogen interactions, to develop novel therapeutic approaches that target host molecular targets and pathways, instead of focusing on eliminating the bacteria, to modulate effector responses and result in safer and more effective interventions.

4.3 Dynamics of innate immune cell populations during *C. difficile* infection

In order to assess the dynamics of different innate immune cell subsets during *Clostridium difficile* infection (CD), wild-type (WT) mice were infected with 10^7 cfu of *Clostridium difficile* VPI 10463. The infection course of a mouse model of CDI is divided in 3 stages. First, the initial phase, that includes day post-infection 0 to 3, and constitutes the initiation of the immune response, then, the peak of inflammation that takes place from approximately day post-infection 4 to 6, and finally the recovery phase, from day post-infection 7 to 10, that involves the activation of the regulatory component to resolve the inflammation and induce tissue healing (Figure 4.1). Here, the colonic immunophenotype was assessed through flow cytometry analysis at day post infection 0, 1, 4, 7 and 10 (Figure 4.2). The obtained results indicate that CDI induces significant alterations in the innate immune cell compartment during the different stages of the infection course. Indeed, we reported a significant recruitment of eosinophils (Figure 4.2A) and neutrophils (Figure 4.2B) that correlates with the peak of inflammation (day post-infection 4) and initiates a regression during the recovery phase, at day post-infection 7. Number of natural killer cells (Figure 4.2C) also increment at the peak of inflammation, however, this increase is maintained during the entire infection course. In a prior study, we also observed this colonic upregulation of cell numbers between day post-infection 4 or 5 in other myeloid subsets of the innate immune system, including macrophages and dendritic cells [218]. Interestingly, innate lymphoid cells (ILCs) present a distinctive response to this enteric pathogen. Indeed, our results report a slowly increase of ILC1 (Figure 4.2D) and ILC2 (Figure 4.2E) population starting at the initial time points of the infection, that achieve significance during the recovery phase. However, ILC3 (Figure 4.2F) population dynamics resembles the one reported in myeloid populations, but at a lower scale.

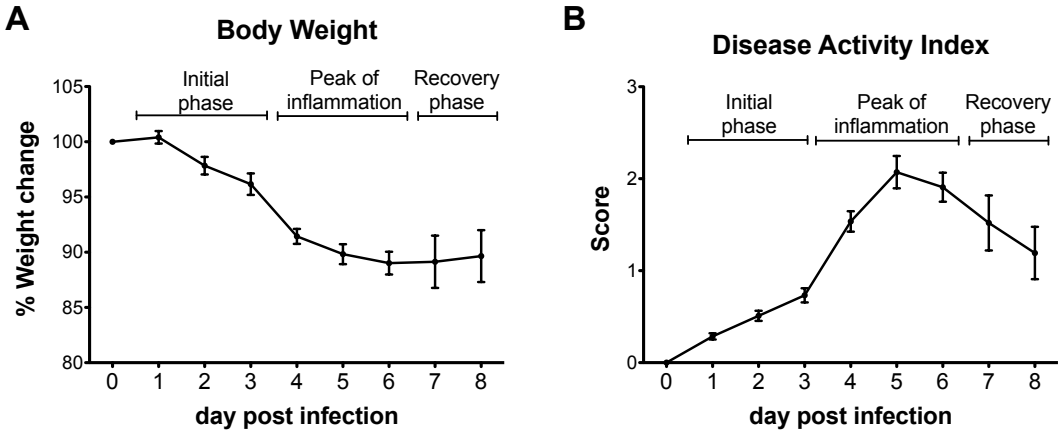

Figure 4.1. Murine model of *C. difficile* infection (CDI) presents three distinguished phases, the initiation of the immune response (initial phase), the peak of inflammation, and the resolution of the infection (recovery phase). Wild-type (WT) mice infected with *C. difficile* VPI 10463 were monitored daily to assess diseases severity. Changes in initial body weight (A) and disease activity index (B) were assessed. Data represent means ± SEM.

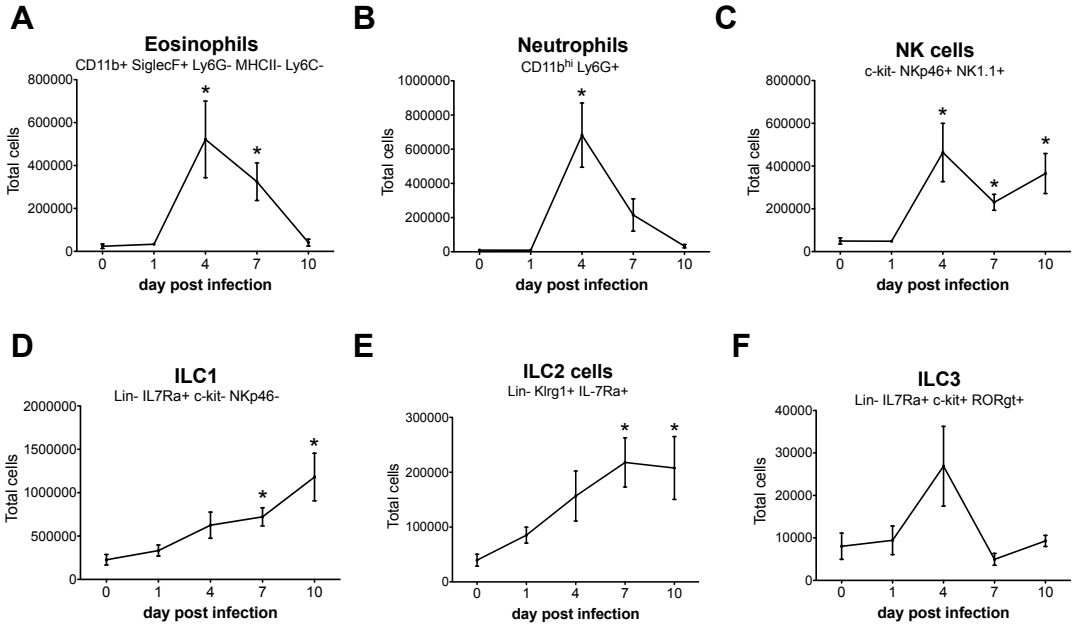

Figure 4.2. Flow cytometry time-course analysis of several innate immune cell subsets in colonic lamina propria (LP) during CDI. WT mice were infected with *C. difficile* VPI 10463 and euthanized at different timepoints (0, 1, 4, 7, and 10 days post-infection). Presence of eosinophils (A), neutrophils (B), natural killer cells (C), innate lymphoid cell type 1 (D), innate lymphoid cell type 2 (E) and innate lymphoid cell type 3 (F) were analyzed. Data represent means ± SEM of 5-6 mice per group. *Represent $P \leq 0.05$ compared to the non-infected group at day 0.

4.4 Pro-inflammatory and regulatory cytokine profile in *C. difficile*-infected colonic tissue

Expression of pro-inflammatory and anti-inflammatory cytokines and markers was assessed at colonic tissue during the time course of the infection. WT mice were infected with *C. difficile* VPI 10463 and euthanized at day post-infection 0, 1, 3, 4, 5, 7, 8 and 10. Total RNA was extracted from colon and gene expression assessed through qRT-PCR. Our results indicate an upregulated gene expression of the majority of the pro-inflammatory cytokines and markers analyzed, including, TNFα (Figure 4.3A), IL-1ß (Figure 4.3B), iNOS (Figure 4.3C), IFNγ (Figure 4.3D) and IL-17 (Figure 4.3 E) starting approximately at day post-infection 3 and maintaining high levels until the initiation of the recovery phase. In contrast, the anti-inflammatory cytokine IL-10 (Figure 4.3F) as well as IL-25 (Figure 4.3G), present downregulated gene expression during the inflammatory stages and are upregulated, specially IL-10, during the recovery phase. Gene expression of IL-22 (Figure 4.3H) was not affected by CDI. Additionally, IL-1ß presented the higher increase in gene expression during the peak of inflammation in comparison to the non-infected group (Figure 4.3I).

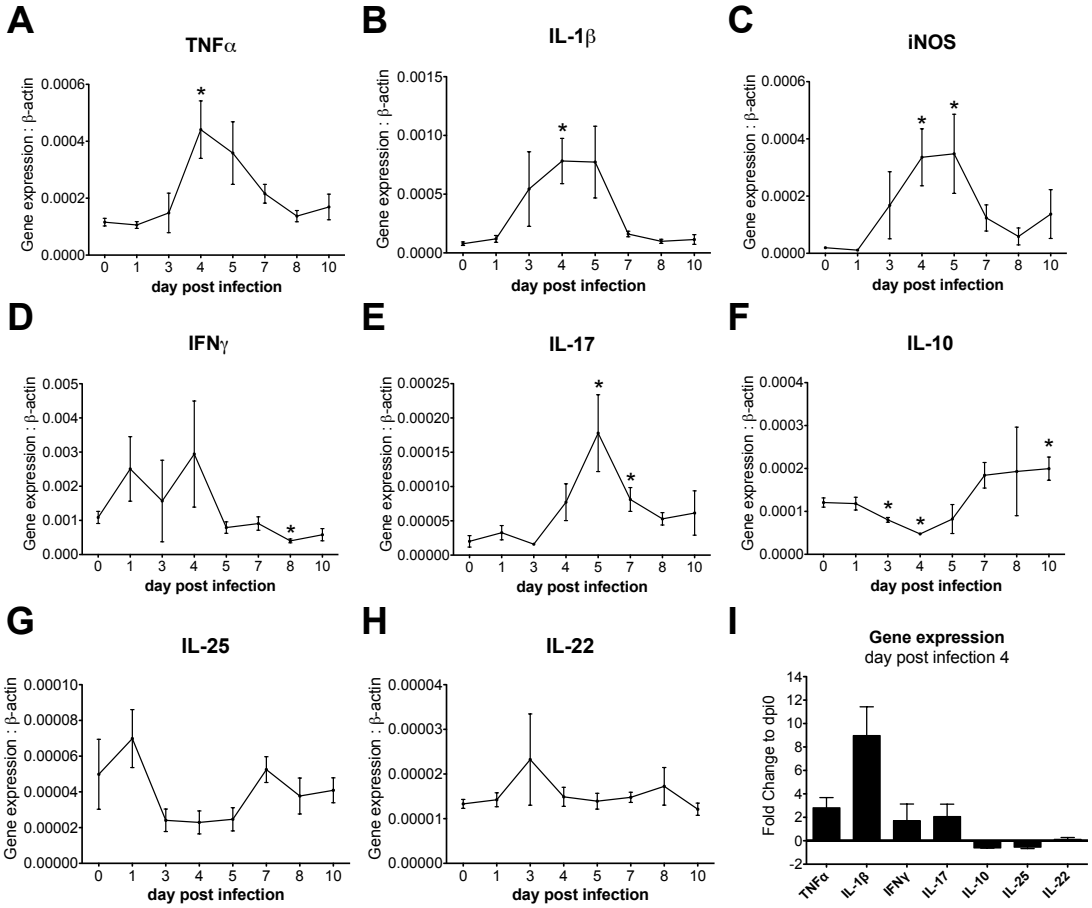

Figure 4.3. Analysis of colonic gene expression inflammatory profile during CDI infection. WT mice were infected with *C. difficile* VPI 10463 and euthanized on day post infection 0, 1, 3, 4, 5, 7, 8 and 10. Gene expression of TNFα (A), IL-1ß (B), inducible NO synthase (iNOS, C), interferon γ (IFNγ, D), IL-17 (E), IL-10 (F), IL-25 (G), and IL-22 (H) was assessed through quantitative real-time PCR (qRT-PCR). Results are expressed as total gene expression levels of each target gene normalized to ß-actin. Gene expression fold change at day post-infection 4 relative to day post-infection 0 of all seven cytokines analyzed (I). Data represent means ± SEM of 5-6 mice per group. *Represent $P \leq 0.05$ compared to the non-infected group at day 0.

4.5 IL-1ß neutralization significantly improves disease symptomatology in a murine model of CDI

Based on the results obtained in the gene expression analysis, that identified IL-1ß as a the most *C. difficile*-responsive cytokine from our analyzed group, we selected this cytokine to perform a neutralization study. WT mice were infected with *C. difficile* VPI 10463. Mice received two doses of anti-mouse IL-1ß antibody intraperitoneally starting at day post-infection 3 to achieve a maintained suppression of this cytokine during the peak of inflammation and the initial stages of the recovery phase. A control group was also included and received the same doses of an isotype control. Upon antibody administration, IL-1ß-neutralized group presented a significant improvement in both percentage of weight change (Figure 4.4A) and diseases activity index (Figure 4.4B) as early as one day post treatment administration. These differences in disease severity were maintained through the entire study until day post-infection 8. Additionally, blocking of IL-1ß also affected the mortality rate (Figure 4.4C) of the infected mice. Indeed, survival rate in the IL-1ß-neutralized group at the end of the experiment was over 10% higher than the one calculated in the control group. Interestingly, no statistical significant differences were reported in bacterial burden between the two experimental groups (Figure 4.4D).

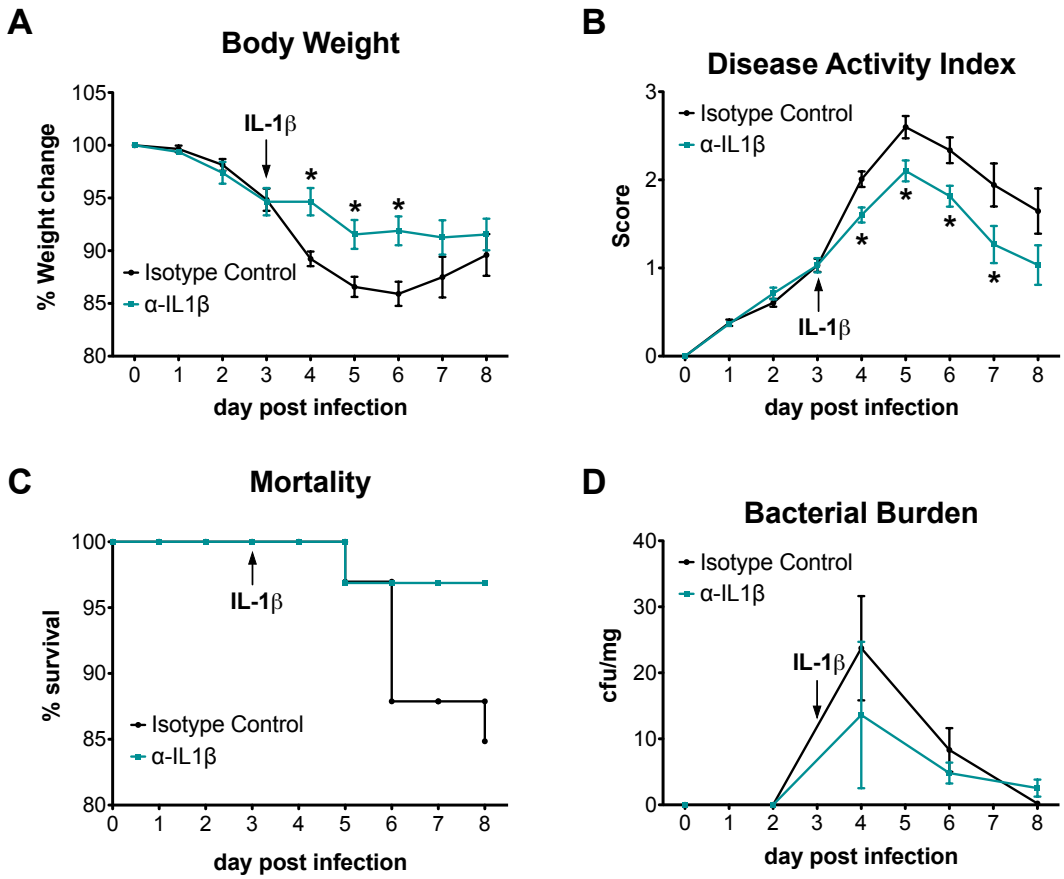

Figure 4.4. Neutralization of IL-1ß during CDI reduces disease severity and mortality rate with no effects on bacterial colonization. *C. difficile*-infected WT mice received two doses of anti-IL-1ß starting at day post-infection 3. A control group receiving isotype control was also included. Mice were monitored daily to assess changes in body weight (A), disease activity index (B) and survival (C). Bacterial burden (D) was assessed on day post-infection 0, 2, 4, 6 and 8. Data represent means ± SEM of 15 mice per group. *Represent $P \leq 0.05$ compared to the control (isotype control) group in each timepoint.

4.6 IL-1ß neutralization inhibits *C. difficile*-induced neutrophil recruitment in colonic lamina propia

C. difficile-infected WT mice challenged with anti-IL-1ß or isotype control were euthanized at day post-infection 7 to assess recruitment of immune cell population in colonic lamina propria. Immunophenotype analysis reported that IL-1ß-neutralization results into a 3-fold decrease of *C. difficile*-induced neutrophil recruitment in colonic lamina propria 7 days post bacterial challenge (Figure 4.5A). Additionally, this flow cytometry analysis indicated an overall slight decrease of immune cell infiltration, especially in the myeloid compartment (Figure 4.5), due to IL-1ß blocking. However, besides the mentioned differences in neutrophil infiltration, no statistically significant

differences were observed in myeloid cells (Figure 4.5), CD4+ T cells (Figure 4.6A-C) or ILCs (Figure 4.6D, E) due blockage of IL-1ß functions.

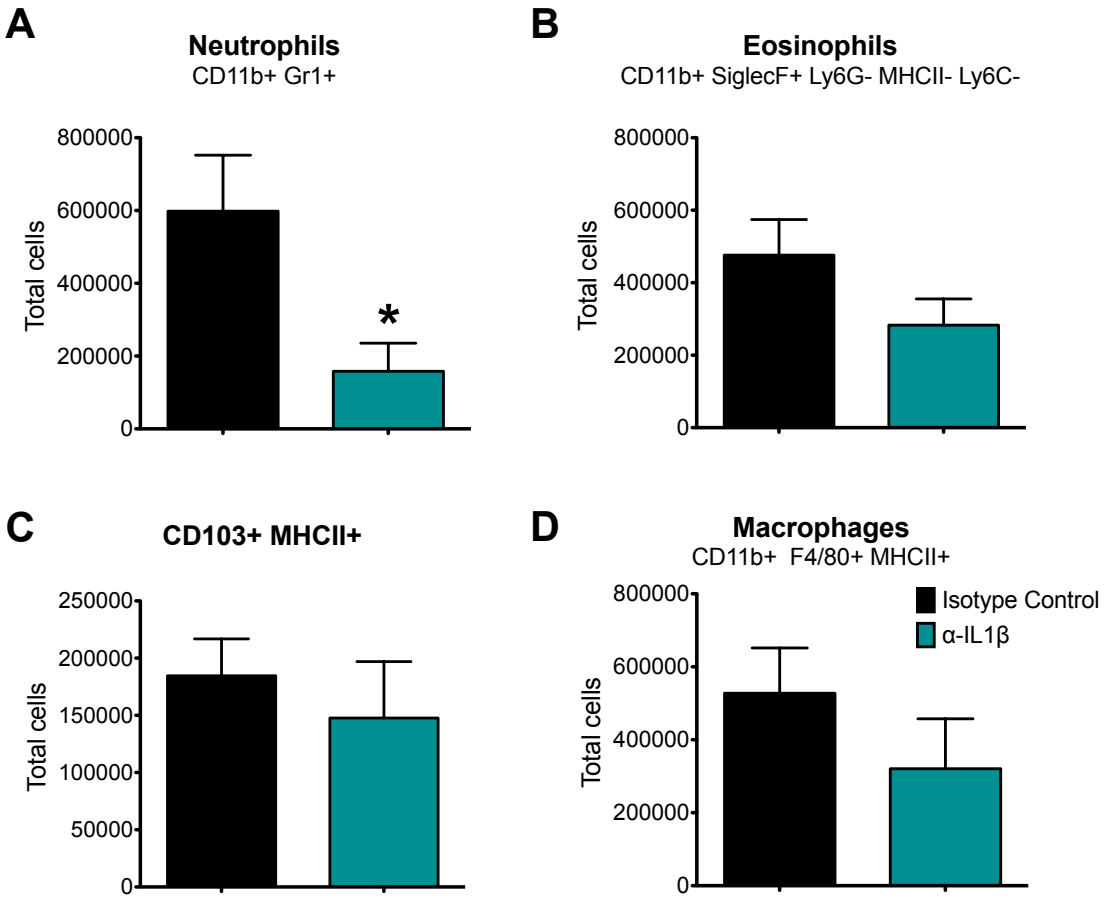

Figure 4.5. Neutralization of IL-1ß inhibits neutrophil infiltration in colonic lamina propria of *C. difficile*-infected mice. *C. difficile*-infected WT mice challenged with anti-IL-1ß or isotype control were euthanized at day post-infection 7 for immunophenotypic analysis of the myeloid compartment in colonic lamina propria using flow cytometry. Total number of Neutrophils (A), eosinophils (B), CD103+MHCII+ cells (C), and macrophages (D). Data represent means ± SEM of 15 mice per group. *Represent $P \leq 0.05$ compared to the control (isotype control) group.

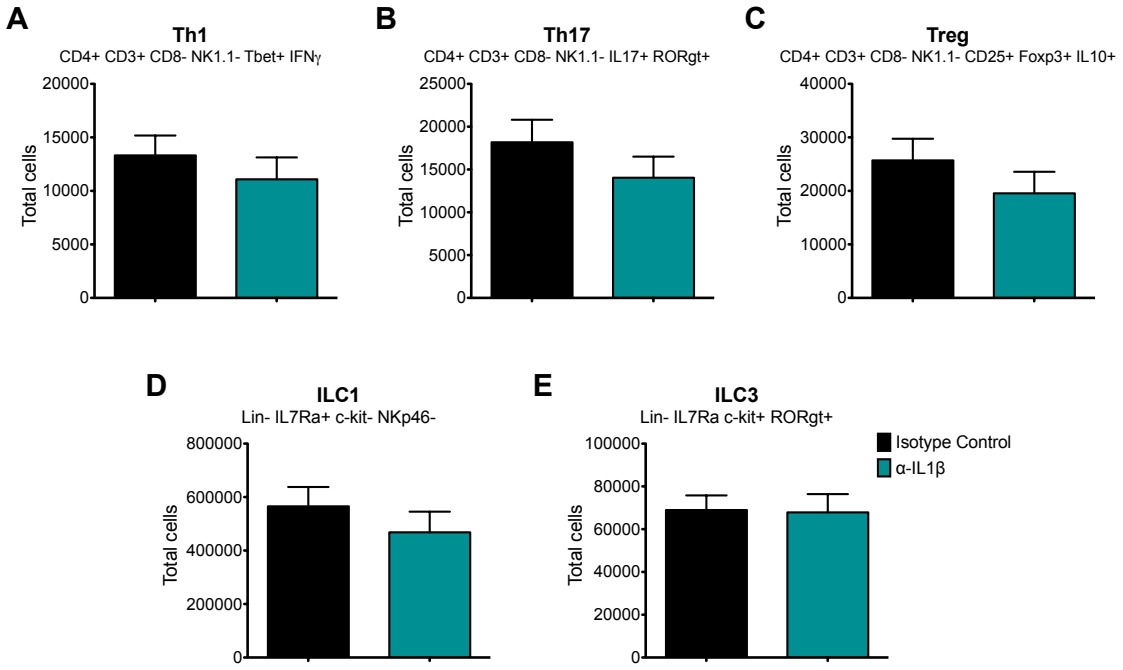

Figure 4.6. IL-1ß neutralization produced no differences in the lamina propria lymphoid compartment in *C. difficile*-infected mice. *C. difficile*-infected WT mice challenged with anti-IL-1ß or isotype control were euthanized at day post-infection 7 for immunophenotypic analysis of CD4+ T cells and innate-lymphoid cells. Total number of Type 1 T helper cells (Th1, A), Type 17 T helper cells (Th17, B), CD4+ regulatory T cell (Treg, C), ILC1 (D) and ILC3 (D) were analyzed employing flow cytometry. Data represent means ± SEM of 15 mice per group. *Represent $P \leq 0.05$ compared to the control (isotype control) group.

4.7 Discussion and conclusions

Clostridium difficile is an opportunistic bacterium that causes the induction of strong inflammatory responses when colonizing the gastrointestinal tract upon disruption of gut microbiome [37, 38]. Antibiotic regimen is the primary treatment for CDI [190], however, the associated high recurrence rates, due to the close association with removal of commensal bacteria, and the emergence of new hypervirulent, multi-resistant strains, point out the urgent need of new, safer and more effective therapeutic strategies. Upon initiation of the immune response, the activated effector mechanisms, together with *C. difficile* virulent factors, are the main cause for the destruction of the epithelial barrier [199, 213, 219], that will eventually result in the clinical symptomatology described in CDAD. Moreover, in addition to antibiotic treatment, host effector immune responses against *C. difficile* are responsible for the removal of commensal species. Indeed, secretion of antimicrobial peptides as well as release of neutrophilic granules target both the pathogenic bacteria and the beneficial bacteria. Thus, modulation of the immune responses towards a regulatory environment, is a promising pathway to develop host-targeted therapeutic strategies, that will control the induction of inflammatory processes, in order to decrease tissue destruction and allow commensal bacterial regrowth, to

prevent *C. difficile* pathogenesis. Indeed, in previous studies, pharmacological activation of two immunoregulatory targets decreased disease severity, reduced inflammatory lesions and suppressed proinflamamtory immune cell infiltration [150, 192]. Of note, the improve in disease severity was not correlated to higher bacterial clearance [192], supporting that the targeted elimination of *C, difficile* bacteria is not a requirement to achieve CDAD resolution.

In this study, we identified IL-1ß as a key player in the induction of inflammatory responses during CDI. Indeed, neutralization of this cytokine resulted into a dramatic improvement in both disease symptomatology and survival rate, that correlated with a significant inhibition of neutrophil recruitment in colonic lamina propria at day post infection 7. The initial analysis of several innate immune cell populations, already revealed the relevance of neutrophil population during *C. difficile*-induced effector responses, reporting a dramatic increase of this population together with eosinophils and natural killer cells during the peak of inflammation. Neutrophil recruitment in CDI has been associated to several cytokines and chemokines, including IL-23 [220], IL-8 [221], and IL1ß [222, 223]. IL1ß is a pro-inflammatory cytokine upregulated during CDI [215, 217], that triggers neutrophil recruitment in several inflammatory processes [224-226]. Our results indicate that in CDI, IL-1ß is a crucial inducer of neutrophil infiltration, since neutralization of this cytokine results into a 3-fold reduced number of neutrophils in colonic lamina propria.

Neutrophil influx has previously been reported as one of the main features of CDI in both human and murine models [214-217], however, the role of this innate subset as a host protector or main contributor of CDAD symptomatology remains unclear. Even though neutrophils have been associated to severe symptomatology and poor prognosis [227-230], a protector role has also been reported [216, 222, 223, 231]. Jarchum et al. observed increased mortality in neutrophil-depleted *C. difficile* infected mice in comparison to the control group [216]. In consistency with these results, Hasegawa et al. also reported higher mortality in IL-1ß-deficient mice associated to impaired neutrophil infiltration and increased translocation of commensal species [222, 223]. The correlation between a significantly improved disease severity and a decreased neutrophil influx in the IL-1ß-neutralized group, with no effects in any other immune cell subset analyzed, observed in our data, suggest that neutrophils are one of the main contributors of C. *difficile*-induced inflammation and CDAD. Therefore, our data does not support the published protective role of IL-1ß-induced neutrophil recruitment, indeed, the absence of this mechanism dramatically improved the disease outcome. On a site note, the significant differences in weight loss and disease activity during the peak of inflammation, suggest that other effector mechanisms associated to IL-1ß, in addition to neutrophil infiltration, may also be effected and might also be relevant contributors in CDAD. However, these responses might have already been resolved by day post-infection 7, and therefore were not reported in our analysis.

In any case, this study demonstrates that IL-1ß is a master inducer of inflammatory responses during CDI, and bring new insight in the regulation of this cytokine as a potential therapeutic approach for CDAD. Additionally, it also postulates the modulation

of neutrophil influx as a potential mechanism to treat CDAD. However, the reported protector role reported for both IL-1ß and neutrophil influx, even that no validated with our data, points out the need of deeper elucidation the host-pathogen interaction during CDI, to allow the discovery of mechanisms, that can modulate the immune response in a therapeutic manner.

4.8 Materials and methods

Animal housing and ethic statement

16 to 20-week-old C57Bl/6J wild-type male mice were employed in this study. Mice were housed with a maximum of 5 mice per cage, in ventilated racks and 12h ligh-dark cycle. All mice were bred and maintained in the same room in Virginia Tech's animal facilities. All experimental procedures performed in this study were approved by the Institutional Animal Care and Use Committee (IACUC) and met or exceeded requirements of the Public Health Service/National Institutes of Health and Animal Welfare Act. Upon bacterial challenge, mice were monitored daily to assess weight loss and disease symptomatology. Score of 3 triggered 4 hour checks. Mice were euthanized prior to scheduled end point if severe signs of diseases were present, i.e. loss of mobility, large weight loss. Mice were euthanized through carbon dioxide (CO_2) narcosis and cervical dislocation as secondary method of euthanasia.

Clostridium difficile infection

C. difficile infection was performed as described in [232]. Briefly, five days prior to bacterial challenge, mice were administered a mixture of antibiotics containing Colistin (4.2mg/kg, Cayman Chemicals, Ann Arbor, MI), Gentamicin (3.5mg/kg, FisherScientific, Hampton, NH), Metronidazole (21.5mg/kg, Cayman Chemicals, Ann Arbor, MI) and Vancomycin (4.5mg/kg, Cayman Chemicals, Ann Arbor, MI) in sterile drinking water. Three days of antibiotic pretreatment is sufficient to disrupt the intestinal microbiome and allow *C. difficile* infection. After three days of pretreatment, antibiotic mixture was removed and replaced by sterile drinking water. One day prior bacterial challenge, mice received a single dose of clindamycin (32mg/kg, Santa Cruz Biotechnology, Dallas, TX) in sterile 1X PBS through intraperitoneal injection. Non-infected control mice received the same antibiotic regimen. At day 0, mice were infected with 10^7cfu of *C. difficile* VPI 10463 (ATTC 43255, Manassas, VA) in 100 µL of Brucella Broth (FisherScientific, Hampton, NH) through intragastric gavage. Mice were initially monitored daily, and after achieving higher diseases scores every 4 hours, to assess weight loss and signs of disease, including, diarrhea, hunchback position, altered activity piloerection, etc. Mice were euthanized at day post infection 0, 1, 3, 4, 5, 7, 8, 9 and 10 through CO_2 narcosis and cervical dislocation.

Cell isolation from colonic lamina propria

Colons were collected, opened and rinsed twice with 1X PBS. Tissues were digested in RPMI (RPMI 1640, Corning Incorporated, Corning, NY, 10% FBS, Corning Incorporated, Corning, NY, 2.5% Hepes, Corning Incorporated, Corning, NY, and 1% Sodium pyruvate, Corning Incorporated, Corning, NY) supplemented with 300U/mL of collagenase (Sigma Aldrich, St. Louis, MO) and 50U/mL of DNase I (Sigma Aldrich, St.

Louis, MO) during 1 hour at 37ºC and under stirring conditions. Samples were filtered and purified through Percoll gradient of density (44/67%). Enriched immune cells, present in the interphase layer, were collected, washed and counted prior to staining.

Flow cytometry

Between $3x10^5$ and $5x10^5$ cells were plated in 96-well plates for immunphenotype staining. Samples were initially incubated 10 min at 4ºC with Fc block (BD Biosciences, San Jose, CA), following by an incubation with fluorochrome-conjugated antibodies against extracellular molecules 20 min at 4ºC. Antibody mixtures included, anti-CD45 APC-cy7, anti-CD64 PE, anti-Cd11b AF700, anti-CD4 BV605, anti-CD3 BV421, anti-CD8 BV786, anti-SiglecF PE, anti-IL-7Ra BV421, anti-NKp46 PerCpCy5.5, anti-CD25 Biotin (BD Biosciences, San Jose, CA), anti-F4/80 PeCy5, anti-MHC II Biotin, anti-Gr1 PeCy7, anti-CD103 FITC, Anti-CD4 AF700, anti-CD8 PerCPCy5.5, anti-Ly6C PerCpCy5.5, anti-linage FITC, anti-IL-7Ra PerCPy5.5, anti-ckit PeCy7, anti-Klrg1 Biotin, and anti-NK1.1 PeCy7 (ThermoFisher Scientific, Waltham, MA). Then, samples were incubated for secondary staining with the Streptavidin-Texas Red (BD Biosciences, San Jose, CA). Samples requiring intracellular staining, were then fixed and permeabilized using the eBiosciences reagent kit and then incubated with mixture containing the fluorochrome-conjugated antibodies against intracellular markers anti-IL10 APC, anti-Tbet PerCPCy5.5, anti-IFNγ PE (BD Biosciences, San Jose, CA), anti-IL17 APC, anti-Foxp3 FITC, and anti-RORγt (ThermoFisher Scientific, Waltham, MA). Data was acquired using a BD LSRII flow cytometer (BD Biosciences, San Jose, CA). instrument and the FACSDiva software (BD Biosciences, San Jose, CA).

Gene Expression

Colonic tissue was excised, rinsed with 1X PBS and stored in RNAlater (Fisher Scientific, Pittsburg, PA) at -80ºC. Total RNA extraction was performed using the RNAeasy kit (Qiagen, Hilden, Germani) following manufacturer's instructions. RNA was quantified using a nanodrop (Invitrogen, Carlsbad, CA). cDNA from RNA samples was generated using the iScript cDNA synthesis kit (Biorad, Hercules, CA). For gene-specific standards, primer-specific amplicons were produced by Polymerase chain reaction (PCR) using Taq Polymerase (Promega, Madison, WI) and purified with the Mini-elute PCR purification kit (Qiagen, Hilden, Germany). Purified product was utilized to perform a series of dilutions starting at $1x10^6$ pg. For gene expression assessment, the SYBR Green supermix (Biorad, Hercules, CA) was utilized in a quantitative real-time PCR (RT-PCR) using a CFX96 Thermal Cycler (Bio-Rad, Hercules, CA). Data was represented as total gene expression normalized to ß-actin.

IL-1ß neutralization

To neutralize IL-1ß, *C. difficile*-infected mice received two doses of 250 µg of inVivoMAb anti-mouse/rat IL-1β (BioXcell, West Lebanon, NH) in 100 µL of 1X Sterile PBS through intraperitoneal injection starting at day post infection 3. A control group received 250 µg of InVivoMAb polyclonal Armenian hamster IgG (BioXcell, West Lebanon, NH) in 100 µL of 1X Sterile PBS through intraperitoneal injection was also included. Mice were euthanized at day post infection 7.

Bacterial reisolation from colonic contents

Weighed colonic contents were homogenized in *Brucella Broth* using a grinder. Homogenates were then incubated at 68ºC for 2h. Samples were centrifuged and serial dilutions performed (10^{-1}, 10^{-2}, 10^{-3}, 10^{-4}, 10^{-5}). Homogenates and diluted samples were plated in Oxoid *Clostridium difficile* agar plates (Oxoid, Altrincham, England) supplemented with 7% Horse Laked blood (Lampire Biological Laboratories, Pipersville, PA) and the *Clostridium difficile* antibiotic supplement (Dent, Oxoid, Altrincham, England). Plates were incubated 4 days at 37ºC in anaerobic conditions using a BD EZ anaerobic kit (BD Biosciences, San Jose, CA). Colonies were counted and numbers normalized to original weights.

Statistical analysis

Data are expressed as means ± standard error of the mean represented in error bars. Analysis of variance (ANOVA) was performed in SAS (SAS Institute) using the general linear model procedure to determine significance. $P \leq 0.05$ was considered significant and was identified with an asterisk.

Chapter 5

Concluding remarks

Nuria Tubau Juni, Raquel Hontecillas, and Josep Bassaganya-Riera.

Mucosal immunity of the gastrointestinal tract constitutes an extremely complex and dynamic network of immune components that act in precise coordination for the generation of specialized responses. In this study, we aimed to characterize new regulatory mechanisms in the interphase of host-pathogen interactions during *Helicobacter pylori* and *Clostridium difficile* infection.

In Chapter 2, a novel regulatory mechanism induced during *H. pylori* colonization was discovered. We identified a new population of $CD11b^{+}F4/80^{hi}CD64^{+}CX_3CR1^{+}$ tissue resident macrophages that accumulate in gastric tissue upon bacterial infection. Indeed, our phenotypic analysis revealed the presence of a complex and heterogeneous network of mononuclear phagocytes in gastric mucosa. In the context of *H. pylori* infection, $CD11b^{+}F4/80^{hi}CD64^{+}CX_3CR1^{+}$ cells mediate an IL-10-driven generation of regulatory environment in coordination with regulatory lymphocytes. In this context, effector processes, mostly Th17-dominated response, are inhibited, resulting in higher bacterial colonization.

In Chapter 3, we developed a novel integrated bioinformatics analysis and experimental validation platform to identify genes with novel regulatory functions. The platform employs an *ex vivo H. pylori* co-culture system using WT and PPARγ-deficient bone marrow-derived macrophages (BMDM) together with a global transcriptomics analysis, to discover regulatory genes based on their expression kinetics. We initially identified 5 lead candidates and then validated their regulatory pattern of expression performing *in vitro* and *in vivo* studies, under both pro-inflammatory and regulatory-induced conditions. From this initial pool, the top lead candidate *Plxdc2* was selected for addition validation through gene-silencing and ligand-specific activation studies. In summary, the developed pipeline provides a new screening method for the identification of genes with promising host regulatory functions and identification of new regulatory targets for the potential development of new host-targeted therapeutic approaches for infectious diseases.

Chapter 4 investigates the dynamics of several innate immune responses during the different phases of *C. difficile* infection (CDI). Using a mouse model of CDI, we identified the pro-inflammatory cytokine IL-1ß as a crucial mediator of the host inflammatory responses against *C. difficile*. IL-1ß neutralization results in dramatic changes in CDI outcome, reporting a significant decrease of both weight loss and disease activity index, as well as, improving the overall survival. In addition, blockage of IL-1ß correlated with a 3-fold decrease of neutrophils in lamina propria, suggesting that this cytokine is a main inducer of *C. difficile*-induced neutrophil recruitment during CDI. These results also suggest that IL-1ß and neutrophil recruitment are relevant contributors of severity of CDAD due to the activation excessive effector responses. Furthermore, our

data support that development of novel therapeutics that target the modulation of pro-inflammatory are a promising path for the treatment of CDI.

In summary, this dissertation presents an integrative-model approach for the characterization of novel mechanisms involved in the host immune response against enteric pathogens. Additionally, it leverages the potential of novel regulatory mechanisms and molecular targets to drive the development of host-centered therapeutic approaches for infectious diseases.

References

1. Helander, H.F. and L. Fandriks, *Surface area of the digestive tract - revisited.* Scand J Gastroenterol, 2014. **49**(6): p. 681-9.
2. Tokuhara, D., et al., *A comprehensive understanding of the gut mucosal immune system in allergic inflammation.* Allergol Int, 2019. **68**(1): p. 17-25.
3. Murphy, K. and C. Weaver, *Janeway's immunobiology*. Ninth edition. ed. 2017, New York, NY, USA: Garland Science, Taylor & Francis Group, LLC.
4. Allaire, J.M., et al., *The Intestinal Epithelium: Central Coordinator of Mucosal Immunity.* Trends Immunol, 2018. **39**(9): p. 677-696.
5. Shi, N., et al., *Interaction between the gut microbiome and mucosal immune system.* Mil Med Res, 2017. **4**: p. 14.
6. Murphy K., W.C., *Janeway's Immunobiology*. 9th ed. 2017.
7. Collaborators, G.B.D.D.D., *Estimates of global, regional, and national morbidity, mortality, and aetiologies of diarrhoeal diseases: a systematic analysis for the Global Burden of Disease Study 2015.* Lancet Infect Dis, 2017. **17**(9): p. 909-948.
8. Perez-Lopez, A., et al., *Mucosal immunity to pathogenic intestinal bacteria.* Nat Rev Immunol, 2016. **16**(3): p. 135-48.
9. Warren, J.R. and B. Marshall, *Unidentified curved bacilli on gastric epithelium in active chronic gastritis.* Lancet, 1983. **1**(8336): p. 1273-5.
10. Marshall, B.J. and J.R. Warren, *Unidentified curved bacilli in the stomach of patients with gastritis and peptic ulceration.* Lancet, 1984. **1**(8390): p. 1311-5.
11. Goodwin, C.S. and J.A. Armstrong, *Microbiological aspects of Helicobacter pylori (Campylobacter pylori).* Eur J Clin Microbiol Infect Dis, 1990. **9**(1): p. 1-13.
12. O'Rourke, J. and G. Bode, *Morphology and Ultrastructure*, in *Helicobacter pylori: Physiology and Genetics*, H.L.T. Mobley, G.L. Mendz, and S.L. Hazell, Editors. 2001: Washington (DC).
13. Linz, B., et al., *An African origin for the intimate association between humans and Helicobacter pylori.* Nature, 2007. **445**(7130): p. 915-918.
14. Bik, E.M., et al., *Molecular analysis of the bacterial microbiota in the human stomach.* Proc Natl Acad Sci U S A, 2006. **103**(3): p. 732-7.
15. Reibman, J., et al., *Asthma is inversely associated with Helicobacter pylori status in an urban population.* PLoS One, 2008. **3**(12): p. e4060.
16. van Wijck, Y., et al., *Therapeutic Application of an Extract of Helicobacter pylori Ameliorates the Development of Allergic Airway Disease.* J Immunol, 2018. **200**(5): p. 1570-1579.
17. Xie, F.J., et al., *Helicobacter pylori infection and esophageal cancer risk: an updated meta-analysis.* World J Gastroenterol, 2013. **19**(36): p. 6098-107.
18. de Martel, C., et al., *Helicobacter pylori infection and the risk of development of esophageal adenocarcinoma.* J Infect Dis, 2005. **191**(5): p. 761-7.
19. Bassaganya-Riera, J., et al., *Helicobacter pylori colonization ameliorates glucose homeostasis in mice through a PPAR gamma-dependent mechanism.* PLoS One, 2012. **7**(11): p. e50069.

20. *Schistosomes, liver flukes and Helicobacter pylori. IARC Working Group on the Evaluation of Carcinogenic Risks to Humans. Lyon, 7-14 June 1994.* IARC Monogr Eval Carcinog Risks Hum, 1994. **61**: p. 1-241.
21. Marshall, B.J., *The pathogenesis of non-ulcer dyspepsia.* Med J Aust, 1985. **143**(7): p. 319.
22. Wroblewski, L.E., R.M. Peek, Jr., and K.T. Wilson, *Helicobacter pylori and gastric cancer: factors that modulate disease risk.* Clin Microbiol Rev, 2010. **23**(4): p. 713-39.
23. Smythies, L.E., et al., *Helicobacter pylori-induced mucosal inflammation is Th1 mediated and exacerbated in IL-4, but not IFN-gamma, gene-deficient mice.* J Immunol, 2000. **165**(2): p. 1022-9.
24. D'Elios, M.M., et al., *T helper 1 effector cells specific for Helicobacter pylori in the gastric antrum of patients with peptic ulcer disease.* J Immunol, 1997. **158**(2): p. 962-7.
25. Bhuiyan, T.R., et al., *Th1 and Th17 responses to Helicobacter pylori in Bangladeshi infants, children and adults.* PLoS One, 2014. **9**(4): p. e93943.
26. Caruso, R., et al., *IL-23-mediated regulation of IL-17 production in Helicobacter pylori-infected gastric mucosa.* Eur J Immunol, 2008. **38**(2): p. 470-8.
27. Shi, Y., et al., *Helicobacter pylori-induced Th17 responses modulate Th1 cell responses, benefit bacterial growth, and contribute to pathology in mice.* J Immunol, 2010. **184**(9): p. 5121-9.
28. Carbo, A., et al., *Predictive computational modeling of the mucosal immune responses during Helicobacter pylori infection.* PLoS One, 2013. **8**(9): p. e73365.
29. Raghavan, S. and M. Quiding-Jarbrink, *Immune modulation by regulatory T cells in Helicobacter pylori-associated diseases.* Endocr Metab Immune Disord Drug Targets, 2012. **12**(1): p. 71-85.
30. Kabisch, R., et al., *Helicobacter pylori gamma-Glutamyltranspeptidase Induces Tolerogenic Human Dendritic Cells by Activation of Glutamate Receptors.* J Immunol, 2016. **196**(10): p. 4246-52.
31. Kaebisch, R., et al., *Helicobacter pylori cytotoxin-associated gene A impairs human dendritic cell maturation and function through IL-10-mediated activation of STAT3.* J Immunol, 2014. **192**(1): p. 316-23.
32. Tanaka, H., et al., *The CagA protein of Helicobacter pylori suppresses the functions of dendritic cell in mice.* Arch Biochem Biophys, 2010. **498**(1): p. 35-42.
33. Lundgren, A., et al., *Helicobacter pylori-specific CD4+ CD25high regulatory T cells suppress memory T-cell responses to H. pylori in infected individuals.* Infect Immun, 2003. **71**(4): p. 1755-62.
34. Raghavan, S., et al., *Absence of CD4+CD25+ regulatory T cells is associated with a loss of regulation leading to increased pathology in Helicobacter pylori-infected mice.* Clin Exp Immunol, 2003. **132**(3): p. 393-400.
35. Leber, A., et al., *Modeling the Role of Lanthionine Synthetase C-Like 2 (LANCL2) in the Modulation of Immune Responses to Helicobacter pylori Infection.* PLoS One, 2016. **11**(12): p. e0167440.
36. Romano, M. and A. Cuomo, *Eradication of Helicobacter pylori: a clinical update.* MedGenMed, 2004. **6**(1): p. 19.

37. Lo Vecchio, A. and G.M. Zacur, *Clostridium difficile infection: an update on epidemiology, risk factors, and therapeutic options.* Curr Opin Gastroenterol, 2012. **28**(1): p. 1-9.
38. Alyousef, A.A., *Clostridium difficile: Epidemiology, Pathogenicity, and an Update on the Limitations of and Challenges in Its Diagnosis.* J AOAC Int, 2018. **101**(4): p. 1119-1126.
39. Rupnik, M., M.H. Wilcox, and D.N. Gerding, *Clostridium difficile infection: new developments in epidemiology and pathogenesis.* Nat Rev Microbiol, 2009. **7**(7): p. 526-36.
40. Lessa, F.C., et al., *Burden of Clostridium difficile infection in the United States.* N Engl J Med, 2015. **372**(9): p. 825-34.
41. Ricciardi, R., et al., *Increasing prevalence and severity of Clostridium difficile colitis in hospitalized patients in the United States.* Arch Surg, 2007. **142**(7): p. 624-31; discussion 631.
42. Pepin, J., et al., *Clostridium difficile-associated diarrhea in a region of Quebec from 1991 to 2003: a changing pattern of disease severity.* CMAJ, 2004. **171**(5): p. 466-72.
43. Loo, V.G., et al., *A predominantly clonal multi-institutional outbreak of Clostridium difficile-associated diarrhea with high morbidity and mortality.* N Engl J Med, 2005. **353**(23): p. 2442-9.
44. O'Connor, J.R., S. Johnson, and D.N. Gerding, *Clostridium difficile infection caused by the epidemic BI/NAP1/027 strain.* Gastroenterology, 2009. **136**(6): p. 1913-24.
45. Kuijper, E.J., et al., *Emergence of Clostridium difficile-associated disease in North America and Europe.* Clin Microbiol Infect, 2006. **12 Suppl 6**: p. 2-18.
46. Kyne, L., et al., *Health care costs and mortality associated with nosocomial diarrhea due to Clostridium difficile.* Clin Infect Dis, 2002. **34**(3): p. 346-53.
47. Debast, S.B., et al., *European Society of Clinical Microbiology and Infectious Diseases: update of the treatment guidance document for Clostridium difficile infection.* Clin Microbiol Infect, 2014. **20 Suppl 2**: p. 1-26.
48. Cornely, O.A., et al., *Treatment of first recurrence of Clostridium difficile infection: fidaxomicin versus vancomycin.* Clin Infect Dis, 2012. **55 Suppl 2**: p. S154-61.
49. Pepin, J., et al., *Increasing risk of relapse after treatment of Clostridium difficile colitis in Quebec, Canada.* Clin Infect Dis, 2005. **40**(11): p. 1591-7.
50. Hu, M.Y., et al., *Prospective derivation and validation of a clinical prediction rule for recurrent Clostridium difficile infection.* Gastroenterology, 2009. **136**(4): p. 1206-14.
51. Reveles, K.R., et al., *National epidemiology of initial and recurrent Clostridium difficile infection in the Veterans Health Administration from 2003 to 2014.* PLoS One, 2017. **12**(12): p. e0189227.
52. Song, J.H. and Y.S. Kim, *Recurrent Clostridium difficile Infection: Risk Factors, Treatment, and Prevention.* Gut Liver, 2019. **13**(1): p. 16-24.
53. Kyne, L., et al., *Association between antibody response to toxin A and protection against recurrent Clostridium difficile diarrhoea.* Lancet, 2001. **357**(9251): p. 189-93.

54. Bakken, J.S., et al., *Treatment approaches including fecal microbiota transplantation for recurrent Clostridium difficile infection (RCDI) among infectious disease physicians.* Anaerobe, 2013. **24**: p. 20-4.
55. Fekety, R., et al., *Recurrent Clostridium difficile diarrhea: characteristics of and risk factors for patients enrolled in a prospective, randomized, double-blinded trial.* Clin Infect Dis, 1997. **24**(3): p. 324-33.
56. Hvas, C.L., et al., *Fecal Microbiota Transplantation Is Superior to Fidaxomicin for Treatment of Recurrent Clostridium difficile Infection.* Gastroenterology, 2019. **156**(5): p. 1324-1332 e3.
57. van Nood, E., et al., *Duodenal infusion of donor feces for recurrent Clostridium difficile.* N Engl J Med, 2013. **368**(5): p. 407-15.
58. Quera, R., et al., *Bacteremia as an adverse event of fecal microbiota transplantation in a patient with Crohn's disease and recurrent Clostridium difficile infection.* J Crohns Colitis, 2014. **8**(3): p. 252-3.
59. Schwartz, M., M. Gluck, and S. Koon, *Norovirus gastroenteritis after fecal microbiota transplantation for treatment of Clostridium difficile infection despite asymptomatic donors and lack of sick contacts.* Am J Gastroenterol, 2013. **108**(8): p. 1367.
60. Kootte, R.S., et al., *The therapeutic potential of manipulating gut microbiota in obesity and type 2 diabetes mellitus.* Diabetes Obes Metab, 2012. **14**(2): p. 112-20.
61. Xu, Z., et al., *Fecal Microbiota Transplantation from Healthy Donors Reduced Alcohol-induced Anxiety and Depression in an Animal Model of Chronic Alcohol Exposure.* Chin J Physiol, 2018. **61**(6): p. 360-371.
62. Stolte, M., *Helicobacter pylori gastritis and gastric MALT-lymphoma.* Lancet, 1992. **339**(8795): p. 745-6.
63. Pernitzsch, S.R. and C.M. Sharma, *Transcriptome complexity and riboregulation in the human pathogen Helicobacter pylori.* Front Cell Infect Microbiol, 2012. **2**: p. 14.
64. Suerbaum, S. and P. Michetti, *Helicobacter pylori infection.* N Engl J Med, 2002. **347**(15): p. 1175-86.
65. Amieva, M.R. and E.M. El-Omar, *Host-bacterial interactions in Helicobacter pylori infection.* Gastroenterology, 2008. **134**(1): p. 306-23.
66. Pacifico, L., et al., *Consequences of Helicobacter pylori infection in children.* World J Gastroenterol, 2010. **16**(41): p. 5181-94.
67. Arnold, I.C., et al., *Helicobacter pylori infection prevents allergic asthma in mouse models through the induction of regulatory T cells.* J Clin Invest, 2011. **121**(8): p. 3088-93.
68. Qing, Y., et al., *Correlation between Helicobacter pylori-associated gastric diseases and colorectal neoplasia.* World J Gastroenterol, 2016. **22**(18): p. 4576-84.
69. Cook, K.W., et al., *Helicobacter pylori infection reduces disease severity in an experimental model of multiple sclerosis.* Front Microbiol, 2015. **6**: p. 52.
70. Engler, D.B., et al., *Effective treatment of allergic airway inflammation with Helicobacter pylori immunomodulators requires BATF3-dependent dendritic cells and IL-10.* Proc Natl Acad Sci U S A, 2014. **111**(32): p. 11810-5.

71. Cherdantseva, L.A., et al., *Association of Helicobacter pylori and iNOS production by macrophages and lymphocytes in the gastric mucosa in chronic gastritis.* J Immunol Res, 2014. **2014**: p. 762514.
72. Ji, J., et al., *CD4+CD25+ regulatory T cells restrain pathogenic responses during Leishmania amazonensis infection.* J Immunol, 2005. **174**(11): p. 7147-53.
73. Rad, R., et al., *CD25+/Foxp3+ T cells regulate gastric inflammation and Helicobacter pylori colonization in vivo.* Gastroenterology, 2006. **131**(2): p. 525-37.
74. Lundgren, A., et al., *Mucosal FOXP3-expressing CD4+ CD25high regulatory T cells in Helicobacter pylori-infected patients.* Infect Immun, 2005. **73**(1): p. 523-31.
75. Kandulski, A., et al., *Naturally occurring regulatory T cells (CD4+, CD25high, FOXP3+) in the antrum and cardia are associated with higher H. pylori colonization and increased gene expression of TGF-beta1.* Helicobacter, 2008. **13**(4): p. 295-303.
76. Altobelli, A., et al., *Helicobacter pylori VacA Targets Myeloid Cells in the Gastric Lamina Propria To Promote Peripherally Induced Regulatory T-Cell Differentiation and Persistent Infection.* MBio, 2019. **10**(2).
77. Kao, J.Y., et al., *Helicobacter pylori immune escape is mediated by dendritic cell-induced Treg skewing and Th17 suppression in mice.* Gastroenterology, 2010. **138**(3): p. 1046-54.
78. Kao, J.Y., et al., *Helicobacter pylori-secreted factors inhibit dendritic cell IL-12 secretion: a mechanism of ineffective host defense.* Am J Physiol Gastrointest Liver Physiol, 2006. **291**(1): p. G73-81.
79. Bimczok, D., et al., *Human primary gastric dendritic cells induce a Th1 response to H. pylori.* Mucosal Immunol, 2010. **3**(3): p. 260-9.
80. Carbo, A., et al., *Systems modeling of the role of interleukin-21 in the maintenance of effector CD4+ T cell responses during chronic Helicobacter pylori infection.* MBio, 2014. **5**(4): p. e01243-14.
81. Carbo, A., et al., *Computational modeling of heterogeneity and function of CD4+ T cells.* Front Cell Dev Biol, 2014. **2**: p. 31.
82. Hitkova, I., et al., *Caveolin-1 protects B6129 mice against Helicobacter pylori gastritis.* PLoS Pathog, 2013. **9**(4): p. e1003251.
83. Li, S.L., et al., *Increased expression of matrix metalloproteinase-9 associated with gastric ulcer recurrence.* World J Gastroenterol, 2013. **19**(28): p. 4590-5.
84. Barton, S.G., et al., *Expression of heat shock protein 32 (hemoxygenase-1) in the normal and inflamed human stomach and colon: an immunohistochemical study.* Cell Stress Chaperones, 2003. **8**(4): p. 329-34.
85. Varol, C., A. Mildner, and S. Jung, *Macrophages: development and tissue specialization.* Annu Rev Immunol, 2015. **33**: p. 643-75.
86. Yona, S., et al., *Fate mapping reveals origins and dynamics of monocytes and tissue macrophages under homeostasis.* Immunity, 2013. **38**(1): p. 79-91.
87. Jakubzick, C., et al., *Minimal differentiation of classical monocytes as they survey steady-state tissues and transport antigen to lymph nodes.* Immunity, 2013. **39**(3): p. 599-610.

88. Gautier, E.L., et al., *Gene-expression profiles and transcriptional regulatory pathways that underlie the identity and diversity of mouse tissue macrophages.* Nat Immunol, 2012. **13**(11): p. 1118-28.
89. Rivollier, A., et al., *Inflammation switches the differentiation program of Ly6Chi monocytes from antiinflammatory macrophages to inflammatory dendritic cells in the colon.* J Exp Med, 2012. **209**(1): p. 139-55.
90. Hoeffel, G. and F. Ginhoux, *Fetal monocytes and the origins of tissue-resident macrophages.* Cell Immunol, 2018. **330**: p. 5-15.
91. Zhao, Y., et al., *The origins and homeostasis of monocytes and tissue-resident macrophages in physiological situation.* J Cell Physiol, 2018. **233**(10): p. 6425-6439.
92. Ginhoux, F., et al., *Fate mapping analysis reveals that adult microglia derive from primitive macrophages.* Science, 2010. **330**(6005): p. 841-5.
93. Hashimoto, D., et al., *Tissue-resident macrophages self-maintain locally throughout adult life with minimal contribution from circulating monocytes.* Immunity, 2013. **38**(4): p. 792-804.
94. Waqas, S.F.H., et al., *Neuropeptide FF increases M2 activation and self-renewal of adipose tissue macrophages.* J Clin Invest, 2017. **127**(7): p. 2842-2854.
95. Hume, D.A., V.H. Perry, and S. Gordon, *The mononuclear phagocyte system of the mouse defined by immunohistochemical localisation of antigen F4/80: macrophages associated with epithelia.* Anat Rec, 1984. **210**(3): p. 503-12.
96. Lee, S.H., P.M. Starkey, and S. Gordon, *Quantitative analysis of total macrophage content in adult mouse tissues. Immunochemical studies with monoclonal antibody F4/80.* J Exp Med, 1985. **161**(3): p. 475-89.
97. Bain, C.C., et al., *Constant replenishment from circulating monocytes maintains the macrophage pool in the intestine of adult mice.* Nat Immunol, 2014. **15**(10): p. 929-937.
98. Serbina, N.V. and E.G. Pamer, *Monocyte emigration from bone marrow during bacterial infection requires signals mediated by chemokine receptor CCR2.* Nat Immunol, 2006. **7**(3): p. 311-7.
99. De Schepper, S., et al., *Self-Maintaining Gut Macrophages Are Essential for Intestinal Homeostasis.* Cell, 2018. **175**(2): p. 400-415 e13.
100. Shaw, T.N., et al., *Tissue-resident macrophages in the intestine are long lived and defined by Tim-4 and CD4 expression.* J Exp Med, 2018. **215**(6): p. 1507-1518.
101. Guirado, E., et al., *Deletion of PPARgamma in lung macrophages provides an immunoprotective response against M. tuberculosis infection in mice.* Tuberculosis (Edinb), 2018. **111**: p. 170-177.
102. Malur, A., et al., *Deletion of PPAR gamma in alveolar macrophages is associated with a Th-1 pulmonary inflammatory response.* J Immunol, 2009. **182**(9): p. 5816-22.
103. Szanto, A., et al., *STAT6 transcription factor is a facilitator of the nuclear receptor PPARgamma-regulated gene expression in macrophages and dendritic cells.* Immunity, 2010. **33**(5): p. 699-712.
104. Viladomiu, M., et al., *Cooperation of Gastric Mononuclear Phagocytes with Helicobacter pylori during Colonization.* J Immunol, 2017. **198**(8): p. 3195-3204.

105. Jung, S., et al., *In vivo depletion of CD11c+ dendritic cells abrogates priming of CD8+ T cells by exogenous cell-associated antigens.* Immunity, 2002. **17**(2): p. 211-20.
106. Hochweller, K., et al., *A novel CD11c.DTR transgenic mouse for depletion of dendritic cells reveals their requirement for homeostatic proliferation of natural killer cells.* Eur J Immunol, 2008. **38**(10): p. 2776-83.
107. Rahman, S., et al., *Depletion of dendritic cells enhances susceptibility to cell-free infection of human T cell leukemia virus type 1 in CD11c-diphtheria toxin receptor transgenic mice.* J Immunol, 2010. **184**(10): p. 5553-61.
108. Isaksson, M., et al., *Conditional DC depletion does not affect priming of encephalitogenic Th cells in EAE.* Eur J Immunol, 2012. **42**(10): p. 2555-63.
109. Wirth, T., et al., *Distinguishing human ethnic groups by means of sequences from Helicobacter pylori: lessons from Ladakh.* Proc Natl Acad Sci U S A, 2004. **101**(14): p. 4746-51.
110. Falush, D., et al., *Traces of human migrations in Helicobacter pylori populations.* Science, 2003. **299**(5612): p. 1582-5.
111. Mane, S.P., et al., *Host-interactive genes in Amerindian Helicobacter pylori diverge from their Old World homologs and mediate inflammatory responses.* J Bacteriol, 2010. **192**(12): p. 3078-92.
112. Fonseca-Nunes, A., et al., *Body iron status and gastric cancer risk in the EURGAST study.* Int J Cancer, 2015.
113. Hu, N., et al., *Genome-wide association study of gastric adenocarcinoma in Asia: a comparison of associations between cardia and non-cardia tumours.* Gut, 2015.
114. Schulfer, A. and M.J. Blaser, *Risks of Antibiotic Exposures Early in Life on the Developing Microbiome.* PLoS Pathog, 2015. **11**(7): p. e1004903.
115. von Hertzen, L., et al., *Helsinki alert of biodiversity and health.* Ann Med, 2015. **47**(3): p. 218-25.
116. Shiu, J. and T.G. Blanchard, *Dendritic cell function in the host response to Helicobacter pylori infection of the gastric mucosa.* Pathog Dis, 2013. **67**(1): p. 46-53.
117. Shiu, J., et al., *IRAK-M expression limits dendritic cell activation and proinflammatory cytokine production in response to Helicobacter pylori.* PLoS One, 2013. **8**(6): p. e66914.
118. Kronsteiner, B., et al., *Systems-wide analyses of mucosal immune responses to Helicobacter pylori.* World Journal of Gastroenterology, 2015.
119. Zhang, M., et al., *Helicobacter pylori directs tolerogenic programming of dendritic cells.* Gut Microbes, 2010. **1**(5): p. 325-329.
120. Engler, D.B., et al., *Helicobacter pylori-specific protection against inflammatory bowel disease requires the NLRP3 inflammasome and IL-18.* Inflamm Bowel Dis, 2015. **21**(4): p. 854-61.
121. Gobert, A.P., et al., *Heme oxygenase-1 dysregulates macrophage polarization and the immune response to Helicobacter pylori.* J Immunol, 2014. **193**(6): p. 3013-22.
122. Krakowiak, M.S., et al., *Matrix metalloproteinase 7 restrains Helicobacter pylori-induced gastric inflammation and premalignant lesions in the stomach by altering macrophage polarization.* Oncogene, 2015. **34**(14): p. 1865-71.

123. Wee, J.L., et al., *Protease-activated receptor-1 down-regulates the murine inflammatory and humoral response to Helicobacter pylori.* Gastroenterology, 2010. **138**(2): p. 573-82.
124. Welch, J.S., et al., *PPARgamma and PPARdelta negatively regulate specific subsets of lipopolysaccharide and IFN-gamma target genes in macrophages.* Proc Natl Acad Sci U S A, 2003. **100**(11): p. 6712-7.
125. Quiding-Jarbrink, M., S. Raghavan, and M. Sundquist, *Enhanced M1 macrophage polarization in human helicobacter pylori-associated atrophic gastritis and in vaccinated mice.* PLoS One, 2010. **5**(11): p. e15018.
126. Lee, J.M., S.S. Kim, and Y.S. Cho, *The Role of PPARgamma in Helicobacter pylori Infection and Gastric Carcinogenesis.* PPAR Res, 2012. **2012**: p. 687570.
127. Barlic, J., et al., *Oxidized lipid-driven chemokine receptor switch, CCR2 to CX3CR1, mediates adhesion of human macrophages to coronary artery smooth muscle cells through a peroxisome proliferator-activated receptor gamma-dependent pathway.* Circulation, 2006. **114**(8): p. 807-19.
128. Huang, B., et al., *CagA-positive Helicobacter pylori strains enhanced coronary atherosclerosis by increasing serum OxLDL and HsCRP in patients with coronary heart disease.* Dig Dis Sci, 2011. **56**(1): p. 109-14.
129. Kawakami, T., et al., *Resident renal mononuclear phagocytes comprise five discrete populations with distinct phenotypes and functions.* J Immunol, 2013. **191**(6): p. 3358-72.
130. Longman, R.S., et al., *CX(3)CR1(+) mononuclear phagocytes support colitis-associated innate lymphoid cell production of IL-22.* J Exp Med, 2014. **211**(8): p. 1571-83.
131. Tsou, C.L., et al., *Critical roles for CCR2 and MCP-3 in monocyte mobilization from bone marrow and recruitment to inflammatory sites.* J Clin Invest, 2007. **117**(4): p. 902-9.
132. Boring, L., et al., *Impaired monocyte migration and reduced type 1 (Th1) cytokine responses in C-C chemokine receptor 2 knockout mice.* J Clin Invest, 1997. **100**(10): p. 2552-61.
133. Moreira-Teixeira, L., et al., *T Cell-Derived IL-10 Impairs Host Resistance to Mycobacterium tuberculosis Infection.* J Immunol, 2017. **199**(2): p. 613-623.
134. Redford, P.S., P.J. Murray, and A. O'Garra, *The role of IL-10 in immune regulation during M. tuberculosis infection.* Mucosal Immunol, 2011. **4**(3): p. 261-70.
135. Gong, J.H., et al., *Interleukin-10 downregulates Mycobacterium tuberculosis-induced Th1 responses and CTLA-4 expression.* Infect Immun, 1996. **64**(3): p. 913-8.
136. O'Leary, S., M.P. O'Sullivan, and J. Keane, *IL-10 blocks phagosome maturation in mycobacterium tuberculosis-infected human macrophages.* Am J Respir Cell Mol Biol, 2011. **45**(1): p. 172-80.
137. Kusters, J.G., A.H. van Vliet, and E.J. Kuipers, *Pathogenesis of Helicobacter pylori infection.* Clin Microbiol Rev, 2006. **19**(3): p. 449-90.
138. Noto, J.M. and R.M. Peek, Jr., *The gastric microbiome, its interaction with Helicobacter pylori, and its potential role in the progression to stomach cancer.* PLoS Pathog, 2017. **13**(10): p. e1006573.

139. Sheh, A. and J.G. Fox, *The role of the gastrointestinal microbiome in Helicobacter pylori pathogenesis.* Gut Microbes, 2013. **4**(6): p. 505-31.
140. Hooi, J.K.Y., et al., *Global Prevalence of Helicobacter pylori Infection: Systematic Review and Meta-Analysis.* Gastroenterology, 2017. **153**(2): p. 420-429.
141. Ernst, P.B. and B.D. Gold, *The disease spectrum of Helicobacter pylori: the immunopathogenesis of gastroduodenal ulcer and gastric cancer.* Annu Rev Microbiol, 2000. **54**: p. 615-40.
142. Chionh, Y.T., et al., *Protease-activated receptor 1 suppresses Helicobacter pylori gastritis via the inhibition of macrophage cytokine secretion and interferon regulatory factor 5.* Mucosal Immunol, 2015. **8**(1): p. 68-79.
143. Rodriguez-Prados, J.C., et al., *Substrate fate in activated macrophages: a comparison between innate, classic, and alternative activation.* J Immunol, 2010. **185**(1): p. 605-14.
144. Kelly, B. and L.A. O'Neill, *Metabolic reprogramming in macrophages and dendritic cells in innate immunity.* Cell Res, 2015. **25**(7): p. 771-84.
145. Jha, A.K., et al., *Network integration of parallel metabolic and transcriptional data reveals metabolic modules that regulate macrophage polarization.* Immunity, 2015. **42**(3): p. 419-30.
146. Vats, D., et al., *Oxidative metabolism and PGC-1beta attenuate macrophage-mediated inflammation.* Cell Metab, 2006. **4**(1): p. 13-24.
147. Ip, W.K.E., et al., *Anti-inflammatory effect of IL-10 mediated by metabolic reprogramming of macrophages.* Science, 2017. **356**(6337): p. 513-519.
148. Odegaard, J.I., et al., *Macrophage-specific PPARgamma controls alternative activation and improves insulin resistance.* Nature, 2007. **447**(7148): p. 1116-20.
149. Namgaladze, D., et al., *Inhibition of macrophage fatty acid beta-oxidation exacerbates palmitate-induced inflammatory and endoplasmic reticulum stress responses.* Diabetologia, 2014. **57**(5): p. 1067-77.
150. Viladomiu, M., et al., *Modeling the role of peroxisome proliferator-activated receptor gamma and microRNA-146 in mucosal immune responses to Clostridium difficile.* PLoS One, 2012. **7**(10): p. e47525.
151. Hontecillas, R., et al., *Immunoregulatory mechanisms of macrophage PPAR-gamma in mice with experimental inflammatory bowel disease.* Mucosal Immunol, 2011. **4**(3): p. 304-13.
152. Chu, Y.T., et al., *Invasion and multiplication of Helicobacter pylori in gastric epithelial cells and implications for antibiotic resistance.* Infect Immun, 2010. **78**(10): p. 4157-65.
153. Oh, J.D., S.M. Karam, and J.I. Gordon, *Intracellular Helicobacter pylori in gastric epithelial progenitors.* Proc Natl Acad Sci U S A, 2005. **102**(14): p. 5186-91.
154. Tang, B., et al., *Compromised autophagy by MIR30B benefits the intracellular survival of Helicobacter pylori.* Autophagy, 2012. **8**(7): p. 1045-57.
155. Wang, Y.H., J.J. Wu, and H.Y. Lei, *The autophagic induction in Helicobacter pylori-infected macrophage.* Exp Biol Med (Maywood), 2009. **234**(2): p. 171-80.
156. Kim, Y.K., J.S. Shin, and M.H. Nahm, *NOD-Like Receptors in Infection, Immunity, and Diseases.* Yonsei Med J, 2016. **57**(1): p. 5-14.

157. Zhong, Y., A. Kinio, and M. Saleh, *Functions of NOD-Like Receptors in Human Diseases.* Front Immunol, 2013. **4**: p. 333.
158. Becker, K.G., et al., *PubMatrix: a tool for multiplex literature mining.* BMC Bioinformatics, 2003. **4**: p. 61.
159. Varga, T., Z. Czimmerer, and L. Nagy, *PPARs are a unique set of fatty acid regulated transcription factors controlling both lipid metabolism and inflammation.* Biochim Biophys Acta, 2011. **1812**(8): p. 1007-22.
160. He, Y., H. Hara, and G. Nunez, *Mechanism and Regulation of NLRP3 Inflammasome Activation.* Trends Biochem Sci, 2016. **41**(12): p. 1012-1021.
161. Masters, S.L., et al., *NLRP1 inflammasome activation induces pyroptosis of hematopoietic progenitor cells.* Immunity, 2012. **37**(6): p. 1009-23.
162. Imamura, R., et al., *Anti-inflammatory activity of PYNOD and its mechanism in humans and mice.* J Immunol, 2010. **184**(10): p. 5874-84.
163. Leber, A., et al., *NLRX1 Modulates Immunometabolic Mechanisms Controlling the Host-Gut Microbiota Interactions during Inflammatory Bowel Disease.* Front Immunol, 2018. **9**: p. 363.
164. Leber, A., et al., *NLRX1 Regulates Effector and Metabolic Functions of CD4(+) T Cells.* J Immunol, 2017. **198**(6): p. 2260-2268.
165. Xia, X., et al., *NLRX1 negatively regulates TLR-induced NF-kappaB signaling by targeting TRAF6 and IKK.* Immunity, 2011. **34**(6): p. 843-53.
166. Liu, T., et al., *NF-kappaB signaling in inflammation.* Signal Transduct Target Ther, 2017. **2**.
167. Kawai, T. and S. Akira, *TLR signaling.* Cell Death Differ, 2006. **13**(5): p. 816-25.
168. Arango Duque, G. and A. Descoteaux, *Macrophage cytokines: involvement in immunity and infectious diseases.* Front Immunol, 2014. **5**: p. 491.
169. Miller, S.F., et al., *Expression of Plxdc2/TEM7R in the developing nervous system of the mouse.* Gene Expr Patterns, 2007. **7**(5): p. 635-44.
170. Miller-Delaney, S.F., et al., *Plxdc2 is a mitogen for neural progenitors.* PLoS One, 2011. **6**(1): p. e14565.
171. Cheng, G., et al., *Identification of PLXDC1 and PLXDC2 as the transmembrane receptors for the multifunctional factor PEDF.* Elife, 2014. **3**: p. e05401.
172. Dawson, D.W., et al., *Pigment epithelium-derived factor: a potent inhibitor of angiogenesis.* Science, 1999. **285**(5425): p. 245-8.
173. Zamiri, P., et al., *Pigment epithelial growth factor suppresses inflammation by modulating macrophage activation.* Invest Ophthalmol Vis Sci, 2006. **47**(9): p. 3912-8.
174. Yang, S.L., et al., *Pigment epithelium-derived factor induces interleukin-10 expression in human macrophages by induction of PPAR gamma.* Life Sci, 2010. **87**(1-2): p. 26-35.
175. Ceulemans, H., W. Stalmans, and M. Bollen, *Regulator-driven functional diversification of protein phosphatase-1 in eukaryotic evolution.* Bioessays, 2002. **24**(4): p. 371-81.
176. Munro, S., et al., *A novel glycogen-targeting subunit of protein phosphatase 1 that is regulated by insulin and shows differential tissue distribution in humans and rodents.* FEBS J, 2005. **272**(6): p. 1478-89.

177. Thwe, P.M., et al., *Cell-Intrinsic Glycogen Metabolism Supports Early Glycolytic Reprogramming Required for Dendritic Cell Immune Responses.* Cell Metab, 2017. **26**(3): p. 558-567 e5.
178. Freemerman, A.J., et al., *Metabolic reprogramming of macrophages: glucose transporter 1 (GLUT1)-mediated glucose metabolism drives a proinflammatory phenotype.* J Biol Chem, 2014. **289**(11): p. 7884-96.
179. Zhang, X., R. Goncalves, and D.M. Mosser, *The isolation and characterization of murine macrophages.* Curr Protoc Immunol, 2008. **Chapter 14**: p. Unit 14 1.
180. Langmead, B., et al., *Ultrafast and memory-efficient alignment of short DNA sequences to the human genome.* Genome Biol, 2009. **10**(3): p. R25.
181. Li, B. and C.N. Dewey, *RSEM: accurate transcript quantification from RNA-Seq data with or without a reference genome.* BMC Bioinformatics, 2011. **12**: p. 323.
182. Trapnell, C., et al., *Transcript assembly and quantification by RNA-Seq reveals unannotated transcripts and isoform switching during cell differentiation.* Nat Biotechnol, 2010. **28**(5): p. 511-5.
183. Ihaka, R. and R. Gentleman, *R: A Language for Data Analysis and Graphics.* Journal of Computational and Graphical Statistics, 1996. **5**(3): p. 299-314.
184. Benjamini, Y. and Y. Hochberg, *Controlling the False Discovery Rate: A Practical and Powerful Approach to Multiple Testing.* Journal of the Royal Statistical Society. Series B (Methodological), 1995. **57**(1): p. 289-300.
185. Zhang, S., et al., *Cost of hospital management of Clostridium difficile infection in United States-a meta-analysis and modelling study.* BMC Infect Dis, 2016. **16**(1): p. 447.
186. Owens, R.C., *Clostridium difficile-associated disease: changing epidemiology and implications for management.* Drugs, 2007. **67**(4): p. 487-502.
187. Gould, C.V., T.M. File, Jr., and L.C. McDonald, *Causes, Burden, and Prevention of Clostridium difficile Infection.* Infect Dis Clin Pract (Baltim Md), 2015. **23**(6): p. 281-288.
188. Stabler, R.A., et al., *Comparative analysis of BI/NAP1/027 hypervirulent strains reveals novel toxin B-encoding gene (tcdB) sequences.* J Med Microbiol, 2008. **57**(Pt 6): p. 771-5.
189. McDonald, L.C., et al., *An epidemic, toxin gene-variant strain of Clostridium difficile.* N Engl J Med, 2005. **353**(23): p. 2433-41.
190. Gerding, D.N., T.M. File, Jr., and L.C. McDonald, *Diagnosis and Treatment of Clostridium difficile Infection (CDI).* Infect Dis Clin Pract (Baltim Md), 2016. **24**(1): p. 3-10.
191. Johnson, S., *Recurrent Clostridium difficile infection: a review of risk factors, treatments, and outcomes.* J Infect, 2009. **58**(6): p. 403-10.
192. Leber, A., et al., *Modeling new immunoregulatory therapeutics as antimicrobial alternatives for treating Clostridium difficile infection.* Artif Intell Med, 2017. **78**: p. 1-13.
193. Lyras, D., et al., *Toxin B is essential for virulence of Clostridium difficile.* Nature, 2009. **458**(7242): p. 1176-9.
194. Awad, M.M., et al., *Clostridium difficile virulence factors: Insights into an anaerobic spore-forming pathogen.* Gut Microbes, 2014. **5**(5): p. 579-93.

195. Lyerly, D.M., H.C. Krivan, and T.D. Wilkins, *Clostridium difficile: its disease and toxins.* Clin Microbiol Rev, 1988. **1**(1): p. 1-18.
196. Borriello, S.P., et al., *Virulence factors of Clostridium difficile.* Rev Infect Dis, 1990. **12 Suppl 2**: p. S185-91.
197. Lawrence, J.P., et al., *Effects of epidermal growth factor and Clostridium difficile toxin B in a model of mucosal injury.* J Pediatr Surg, 1997. **32**(3): p. 430-3.
198. Just, I., et al., *The low molecular mass GTP-binding protein Rho is affected by toxin A from Clostridium difficile.* J Clin Invest, 1995. **95**(3): p. 1026-31.
199. Brito, G.A., et al., *Mechanism of Clostridium difficile toxin A-induced apoptosis in T84 cells.* J Infect Dis, 2002. **186**(10): p. 1438-47.
200. Fiorentini, C., et al., *Clostridium difficile toxin B induces apoptosis in intestinal cultured cells.* Infect Immun, 1998. **66**(6): p. 2660-5.
201. Just, I., et al., *Glucosylation of Rho proteins by Clostridium difficile toxin B.* Nature, 1995. **375**(6531): p. 500-3.
202. Just, I., et al., *The enterotoxin from Clostridium difficile (ToxA) monoglucosylates the Rho proteins.* J Biol Chem, 1995. **270**(23): p. 13932-6.
203. Chumbler, N.M., et al., *Clostridium difficile Toxins TcdA and TcdB Cause Colonic Tissue Damage by Distinct Mechanisms.* Infect Immun, 2016. **84**(10): p. 2871-7.
204. Brito, G.A., et al., *Clostridium difficile toxin A induces intestinal epithelial cell apoptosis and damage: role of Gln and Ala-Gln in toxin A effects.* Dig Dis Sci, 2005. **50**(7): p. 1271-8.
205. Gerhard, R., et al., *Glucosylation of Rho GTPases by Clostridium difficile toxin A triggers apoptosis in intestinal epithelial cells.* J Med Microbiol, 2008. **57**(Pt 6): p. 765-70.
206. Qa'Dan, M., et al., *Clostridium difficile toxin B activates dual caspase-dependent and caspase-independent apoptosis in intoxicated cells.* Cell Microbiol, 2002. **4**(7): p. 425-34.
207. Chae, S., et al., *Epithelial cell I kappa B-kinase beta has an important protective role in Clostridium difficile toxin A-induced mucosal injury.* J Immunol, 2006. **177**(2): p. 1214-20.
208. Chen, X., et al., *Saccharomyces boulardii inhibits ERK1/2 mitogen-activated protein kinase activation both in vitro and in vivo and protects against Clostridium difficile toxin A-induced enteritis.* J Biol Chem, 2006. **281**(34): p. 24449-54.
209. Jefferson, K.K., M.F. Smith, Jr., and D.A. Bobak, *Roles of intracellular calcium and NF-kappa B in the Clostridium difficile toxin A-induced up-regulation and secretion of IL-8 from human monocytes.* J Immunol, 1999. **163**(10): p. 5183-91.
210. Warny, M., et al., *p38 MAP kinase activation by Clostridium difficile toxin A mediates monocyte necrosis, IL-8 production, and enteritis.* J Clin Invest, 2000. **105**(8): p. 1147-56.
211. Linevsky, J.K., et al., *IL-8 release and neutrophil activation by Clostridium difficile toxin-exposed human monocytes.* Am J Physiol, 1997. **273**(6 Pt 1): p. G1333-40.

212. Sun, X., et al., *Essential role of the glucosyltransferase activity in Clostridium difficile toxin-induced secretion of TNF-alpha by macrophages.* Microb Pathog, 2009. **46**(6): p. 298-305.
213. Jose, S. and R. Madan, *Neutrophil-mediated inflammation in the pathogenesis of Clostridium difficile infections.* Anaerobe, 2016. **41**: p. 85-90.
214. Price, A.B. and D.R. Davies, *Pseudomembranous colitis.* J Clin Pathol, 1977. **30**(1): p. 1-12.
215. McDermott, A.J., et al., *The role of Gr-1(+) cells and tumour necrosis factor-alpha signalling during Clostridium difficile colitis in mice.* Immunology, 2015. **144**(4): p. 704-16.
216. Jarchum, I., et al., *Critical role for MyD88-mediated neutrophil recruitment during Clostridium difficile colitis.* Infect Immun, 2012. **80**(9): p. 2989-96.
217. Sadighi Akha, A.A., et al., *Acute infection of mice with Clostridium difficile leads to eIF2alpha phosphorylation and pro-survival signalling as part of the mucosal inflammatory response.* Immunology, 2013. **140**(1): p. 111-22.
218. Leber, A., et al., *Systems Modeling of Interactions between Mucosal Immunity and the Gut Microbiome during Clostridium difficile Infection.* PLoS One, 2015. **10**(7): p. e0134849.
219. Nusrat, A., et al., *Clostridium difficile toxins disrupt epithelial barrier function by altering membrane microdomain localization of tight junction proteins.* Infect Immun, 2001. **69**(3): p. 1329-36.
220. McDermott, A.J., et al., *Interleukin-23 (IL-23), independent of IL-17 and IL-22, drives neutrophil recruitment and innate inflammation during Clostridium difficile colitis in mice.* Immunology, 2016. **147**(1): p. 114-24.
221. Liu, F., J. Poursine-Laurent, and D.C. Link, *The granulocyte colony-stimulating factor receptor is required for the mobilization of murine hematopoietic progenitors into peripheral blood by cyclophosphamide or interleukin-8 but not flt-3 ligand.* Blood, 1997. **90**(7): p. 2522-8.
222. Hasegawa, M., et al., *Nucleotide-binding oligomerization domain 1 mediates recognition of Clostridium difficile and induces neutrophil recruitment and protection against the pathogen.* J Immunol, 2011. **186**(8): p. 4872-80.
223. Hasegawa, M., et al., *Protective role of commensals against Clostridium difficile infection via an IL-1beta-mediated positive-feedback loop.* J Immunol, 2012. **189**(6): p. 3085-91.
224. Miller, L.S., et al., *Inflammasome-mediated production of IL-1beta is required for neutrophil recruitment against Staphylococcus aureus in vivo.* J Immunol, 2007. **179**(10): p. 6933-42.
225. Charmoy, M., et al., *The Nlrp3 inflammasome, IL-1beta, and neutrophil recruitment are required for susceptibility to a nonhealing strain of Leishmania major in C57BL/6 mice.* Eur J Immunol, 2016. **46**(4): p. 897-911.
226. Lee, D.J., et al., *Integrated pathways for neutrophil recruitment and inflammation in leprosy.* J Infect Dis, 2010. **201**(4): p. 558-69.
227. Walker, A.S., et al., *Relationship between bacterial strain type, host biomarkers, and mortality in Clostridium difficile infection.* Clin Infect Dis, 2013. **56**(11): p. 1589-600.

228. Solomon, K., et al., *Mortality in patients with Clostridium difficile infection correlates with host pro-inflammatory and humoral immune responses.* J Med Microbiol, 2013. **62**(Pt 9): p. 1453-60.
229. Kelly, C.P., et al., *Neutrophil recruitment in Clostridium difficile toxin A enteritis in the rabbit.* J Clin Invest, 1994. **93**(3): p. 1257-65.
230. Castagliuolo, I., et al., *Clostridium difficile toxin A stimulates macrophage-inflammatory protein-2 production in rat intestinal epithelial cells.* J Immunol, 1998. **160**(12): p. 6039-45.
231. Huang, A.M., et al., *Risk factors for recurrent Clostridium difficile infection in hematopoietic stem cell transplant recipients.* Transpl Infect Dis, 2014. **16**(5): p. 744-50.
232. Chen, X., et al., *A mouse model of Clostridium difficile-associated disease.* Gastroenterology, 2008. **135**(6): p. 1984-92.